UiT The Arctic University of Norway

Faculty of Biosciences, Fisheries and Economics

Design and construction of a cellular biosensor for detection of autoinducer-2 quorum sensing inhibitors using a genetic toggle switch

Johan Bjerg

Master’s thesis in Marine Biotechnology FSK-3860 January 2022

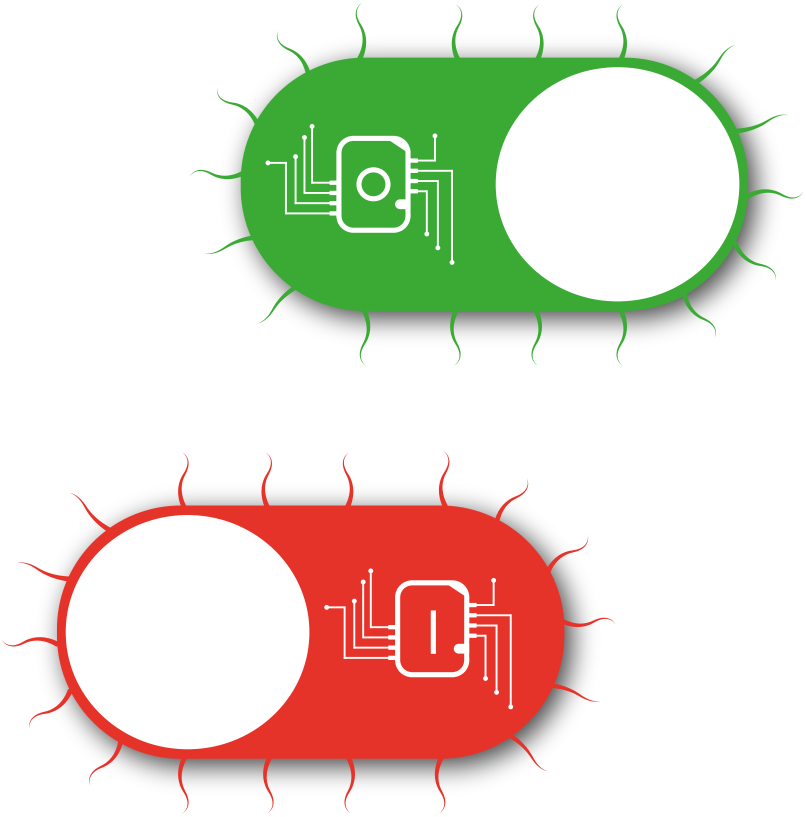

Preface

This master's thesis was conducted at the Faculty of Biosciences, Fisheries and Economics at UiT The Arctic University of Norway in collaboration with the Marine Bioprospecting Research Group. The 60 ECTS thesis constitutes a 12-month exchange study programme between the University of Copenhagen and UiT. The work was commenced in January 2021 and finalized in January 2022.

Firstly, I would like to thank my main supervisor, Hans-Matti Blencke for being open-minded and forthcoming when I sent an e-mail from Copenhagen to Tromsø about a master's project back in August 2019. Thank you for trusting me to pursue my own ideas on how this project should be tackled and for the generous amount of feedback throughout the last 12 months.

I am also sending a big thank you at my co-supervisors, Céline Sarah Marine Richard, Andrea Iselin Elvheim and Dennis Tin Chat Chan for welcoming me and taking the time to answer numerous question. A special thanks to Dennis for being patient, for introducing me to the world of synthetic biology and for letting me plunder your -20 freezer for precious reagents.

I would also like to thank my friends and family for love and support, and, especially, my beloved girlfriend and number-one travel companion, Juni, for going on this master's thesis voyage with me.

I knew writing a master's thesis would be hard work. And writing a master thesis in combination with an ongoing pandemic, a jaw surgery, a lack of proper ryebread, expensive beers and the constant urge to go fishing did not make it easier. But it has all been part of an unforgettable journey above the Arctic Circle.

Table of contents

Abstract *1*

Abbreviations *2*

List of tables *3*

List of figures *3*

1 Introduction *9*

1.1 Quorum sensing **10**

1.1.1 Bacteria communicate with various quorum sensing systems 11

1.1.2 Autoinducer-2: A universal signaling molecule 13

1.2 Jamming the signal: Quenching of quorum sensing **16**

1.2.1 Criteria for quorum quenching molecules 17

1.2.2 Quorum quenching strategies 17

1.3 Using biosensors to find quorum quenching compounds **18**

1.3.1 Examples of quorum quenching detecting biosensors 19

1.4 A synthetic biology approach via the BASIC DNA assembly system **20**

1.4.1 The principles of BASIC 21

1.4.2 Tuneability and adaptation is achieved by BASIC linkers 21

1.5 Aim of this study **21**

2 Materials and methods *22*

2.1 Bacterial strains and plasmids used in this study **22**

2.2 Growth medium, supplements and conditions **22**

2.3 Cloning of genetic constructs **23**

2.3.1 Adaptation of parts into BASIC format 23

2.3.2 Storage of parts 24

2.3.3 Assembly of constructs with more than 4 parts 24

2.3.4 Transformation of *in vitro* assembled constructs 24

2.3.5 Assembly confirmation and sanger-sequencing 24

2.4 Induction and biosensor assays **25**

2.4.1 Addition of solutions to assays 26

2.4.2 Specific fluorescence calculations and statistics 26

2.5 Data visualization and figure design **26**

2.6 LB-sAI2 plates and fluorescent imaging **27**

3 Results *27*

3.1 Genetic circuit of the biosensor and its mode of operation 27

3.2 Building a library of parts and cloning genetic constructs 30

3.3 Induction of P_{lsr} 31

3.3.1 Strategy 1: Induction of P_{lsr} with supernatant from AI-2 producing cells 31
3.3.2 Strategy 2: Induction of P_{lsr} by transformation of *E. coli* M4100 with sensor plasmid 32
3.3.3 Strategy 3: Induction of P_{lsr} using a synthetic form of AI-2 33
3.3.4 Troubleshooting: Testing sfGFP as a reporter gene 34
3.3.5 Induction of P_{lsr} on LB-sAI2 plates 35

3.4 Tuning the expression of *sfGFP* from P_{tet} 36

3.5 Simulating quorum quenching by artificially triggering the switch 37

3.6 Proof of concept biosensor 39

4 Discussion 40

4.1 Second signal output decreases risk of false-positives 40

4.2 P_{lsr} remains unaffected by all three induction strategies 41

4.2.1 Methods for induction of P_{lsr} 42
4.2.2 Different versions of P_{lsr} have previously been used successfully 43

4.3 mRFP1 provides little or no fluorescence 44

4.4 One module of the genetic switch functions under a quorum quenching simulation 46

4.4.1 Considerations on the proof of concept circuit 47

4.5 Modularity via BASIC and alternative cloning strategy 48

4.6 Optimization and future prospects 49

5 Concluding remarks 50

6 References 51

7 Appendix 60

7.1 Primers used in this study 60

7.2 Example of verification of assembly by PCR 61

7.3 Induction with MC4100 supernatant in LB medium 62

7.4 Induction with 100 mM sAI-2 in LB medium 63

7.5 Induction with 50 mM sAI-2 in M9 medium 64

7.6 Green fluorescence from pJB32 on LB agar plate 65

7.7 QQ simulation: Testing biosensor construct in high copy number vector backbone 66

7.8 Colony PCR of proof of concept circuit assembly attempt 67

Abstract

Bacteria employ molecular communication systems termed quorum sensing (QS) to sense cell density and organize collective behavior. Many of these behaviors have implications on modern society and human health. As the antimicrobial toolbox of classic antibiotics shrinks due to extensive spread of resistance in pathogenic bacteria, interfering with bacterial communication by ‘quenching’ the QS signals poses a promising strategy for novel antimicrobial drugs. Many bacterial biosensors have been used in the search of natural compounds interfering with QS. However, the majority of these detect compounds quenching autoinducer-1 QS and only a few detects compounds which quench other types of QS. Additionally, simple quorum quenching (QQ) biosensors are prone to bias and false-positive results. This thesis aims to employ synthetic biology tools to construct a modular and tunable cellular biosensor based on a bistable genetic circuit with two signal outputs for detecting compounds capable of quenching autoinducer-2 (AI-2) QS. In order to maintain tunability and modularity of the biosensor, the BASIC DNA Assembly system was used. A library of modular bioparts was generated and assembled into the biosensor plasmids. *Escherichia coli* DH5α, which is unable to produce AI-2, was used as primary sensor chassis. The promoter of the AI-2-regulated *lsr*-operon, P_{lsr}, was employed as the sensing entity to control expression of a repressor, TetR, and a red fluorescent protein, mRFP1. The expression of sfGFP, a green fluorescent protein, was controlled by the TetR-repressed promoter P_{tet}. The biosensor plasmid therefore switches fluorescence color of DH5α depending on whether AI-2 QS is active or quenched. Different strategies were used to induce P_{lsr}, but these proved unsuccessful. Leaky expression occurring through P_{lsr} and lack of fluorescence by mRFP1 in the genetic construct were instead identified as possible reasons for the non-functional sensor. Further experiments revealed that one sensor module was functional, and that the inherent modularity of the BASIC DNA Assembly system allows for straightforward tuning of different parts. Future studies can therefore rely on the module containing P_{tet} and sfGFP and focus on tuning the P_{lsr}- module.

Keywords: quorum quenching, quorum sensing inhibition, synthetic biology, biosensor, genetic toggle switch

Abbreviations

QS	Quorum Sensing
QQ	Quorum Quenching
AI-1	Autoinducer-1
AI-2	Autoinducer-2
AI-3	Autoinducer-3
sAI-2	Synthetic autoinducer-2 (5-methyl-4-hydroxy-3-furanone
aTC	Anhydrotetracycline
DPD	4,5-dihydroxi-2,3-pentanedione
AMC	Activated methyl cycle
SAM	S-adenosylmethionine
SAH	S-adenosylhomocysteine
SRH	S-ribosylhomocysteine
R or S-THMF	R- or S-2-methyl-2,3,3,4-tetrahydroxytetrahydrofuran (AI-2)

List of tables

Table 1 | Overview of quorum sensing mediated implications to modern society. 12

Table 2 | Overview of genetic parts used this study. $^{(*)}$ Standard European Vector Architecture [70]. 29

Table 3 | Primers used in this study. 60

List of figures

Figure 1 | The activated methyl cycle (AMC) with the relevant steps highlighted in color. **(A)** Coming from the other half of the AMC, a methyl group is removed from SAM which converts it to SAH (a toxic intermediate). **(B)** Organisms with sahH convert this directly to homocysteine. **(C)** Organisms with luxS convert it to homocysteine in two steps: SAH is converted by MTAN to SRH before LuxS converts it to homocysteine and DPD (the linear form of AI-2). **(D)** DPD rapidly rearranges into S-THMF or R-THMF, which to bacteria is the recognizable form of AI-2. Adapted and modified from Pereira, Thompson and Xavier, 2013 [37]. 14

Figure 2. Model for AI-2 secretion, uptake and signalling by the lsr system. (A) In low cell densities, i.e. lag phase, the extracellular concentration of AI-2 is low, and the lsr operon is repressed by LsrR. **(B)** In the exponential growth phase, AI-2 accumulates extracellularly, and initial uptake occurs through PTS-dependent transporters. Imported AI-2 is phosphorylated by LsrK to P-AI-2 which upon binding and removal of LsrR derepresses the lsr operon. **(C)** Activation of lsr operon leads to increased uptake by the LsrACDB-transporter-complex. A positive feedback loop occurs, and the extracellular concentration of AI-2 decreases rapidly. P-AI-2 is eventually degraded by LsrG and LsrF. Adapted and modified from Pereira et al. [37] 16

Figure 3 | BASIC standardization and workflow. **(A)** The BASIC DNA part is flanked by a prefix (iP) and a suffix (iS) sequence, each containing an inward facing BsaI site. Upon digestion with BsaI, a specific 4 bp overhang is generated to which DNA-linkers will ligate with its own 4 bp overhang. **(B)** The workflow of BASIC assembly. Step 1: Simultaneous digestion and ligation of linkers, separate for each part. Step 2: Purification, removal of unligated linkers. Step 3: Linker-adapted parts are mixed together and assembled into one construct. Figure adapted and modified from Storch et al. 2015. 20

Figure 4 | Genetic circuit of the biosensor and its operational principle. **(A)** Signal output when quorum sensing (QS) is active (i.e. not inhibited). **A1-A2.** Addition of autoinducer-2 (AI-2) induces the P_{lsr} promoter, which enables expression of downstream genes. **A3.** The expressed TetR repressor protein binds to and represses P_{tet} which blocks transcription of sfGFP. **A4.** Expression of mRFP1 results in a red fluorescent signal output. **(B)** Signal output when quorum sensing is inhibited. **B1.** A given mechanism inhibits AI-2, and P_{lsr} remains uninduced. **B2.** Transcription of sfGFP is initiated through P_{tet}, generating a green fluorescent signal output. λtl3 terminator prevents further downstream transcription. 28

Figure 5 | Overview of genetic constructs cloned in this study. The figure illustrates the order of the different parts from Table 2 and linkers. Note that the representation of the constructs in this figure is linear, opposed to the circular structure of the plasmids in their natural state. 30

Figure 6 | Induction with MC4100 supernatant in LB medium. **(A)** Genetic overview of constructs tested in this experiment. **(B-F)** Test constructs in DH5α (pJB12, pJB17, pJB18, negative control without plasmid) were grown in culture tubes, and 80 µl culture were transferred upon reaching early exponential phase to a 96 well plate. Test constructs were supplied with 20 µl supernatant from E. coli MC4100 in exponential growth phase, and controls (uninduced) were supplied with 20 uL LB medium. Fluorescence (excitation: 580 and emission: 615) and OD_{600} were monitored every 15 minutes for 8 hours. Graphs only depict 2-8 hours. Results are displayed as specific fluorescence (normalized with OD_{600} value and background fluorescence from medium subtracted). The displayed specific fluorescence values are the mean of three technical replicates, and the shaded area depicts the standard error of the mean. 32

Figure 7 | Self-inducing pJB18 in E. coli MC4100. **(A)** Genetic overview of construct tested in this experiment. **(B-C)** The test construct in MC4100 and control (MC4100 without plasmid) were grown in culture tubes, and 100 µl culture were transferred upon reaching exponential phase to a 96 well plate. Fluorescence (excitation: 580 and emission: 615) and OD_{600} were monitored every 15 minutes for 8 hours. Graphs only depicts 2-8 hours. Results are displayed as specific fluorescence (normalized with OD_{600} value and background fluorescence from medium subtracted). The displayed specific fluorescence values are the mean of three technical replicates, and shaded area depict standard error of the mean. **(B)**

Experiment conducted in LB medium. **(C)** Similar experiment conducted with M9 glucose medium instead of LB medium... 33

Figure 8 | Induction with 50 mM 5-methyl-4-hydroxy-3-furanone in LB medium. **(A)** Genetic overview of constructs tested in this experiment. **(B-F)** Test constructs in DH5α (pJB12, pJB17, pJB18, negative control without plasmid) were grown in culture tubes, and 90 µl culture were transferred upon reaching early exponential phase to a 96 well plate. Test constructs were supplied with 10 uL 5-methyl-4-hydroxy-3-furanone (sAI2) solution reaching a final concentration of 50 mM sAI2. Controls (uninduced) were supplied with H_2O. Fluorescence (excitation: 580 and emission: 615) and OD_{600} were monitored every 15 minutes for 8 hours. Graphs only depicts 2-8 hours. Results are displayed as specific fluorescence (normalized with OD_{600} value and background fluorescence from medium subtracted). The displayed specific fluorescence values are the mean of three technical replicates, and shaded area depict standard error of the mean... 34

Figure 9 | Induction with 50 mM 5-methyl-4-hydroxy-3-furanone in LB medium. **(A)** Genetic overview of the construct tested in this experiment. **(B-C)** Test constructs in DH5α (pJB25, negative control without plasmid) were grown in culture tubes, and 90 µl culture were transferred upon reaching exponential phase to a 96 well plate. pJB25 were supplied with 10 uL 5-methyl-4-hydroxy-3-furanone (sAI2) solution reaching a final concentration of 50 mM sAI2. Controls (uninduced) were supplied with H_2O. Fluorescence (excitation: 480 and emission: 515) and OD_{600} were monitored every 15 minutes for 8 hours. Graphs only depict 2-8 hours. Results are displayed as specific fluorescence (normalized with OD_{600} value and background fluorescence from medium subtracted). The displayed specific fluorescence values are the mean of three technical replicates, and shaded area depict standard error of the mean... 35

Figure 10 | P_{lsr} induction on LB agar plates containing 50 mM sAI-2. (A) Overview of the genetic construct in each strain tested. **(B)** Pictures of LB agar plates. Exponentially growing cultures of each strain were spread evenly on the plates in the evening and pictures were taken the following morning. LB agar plates contained ampicillin (100 µg/ml) to maintain plasmid stability.. 36

Figure 11 | Tuning the green signal output from sfGFP. **(A)** Genetic overview of the constructs tested in this experiment. **(B-C)** The test constructs and controls were grown in culture tubes, and 90 µl culture were transferred upon reaching early exponential phase to a 96 well plate and thereafter supplemented with 10 µl LB medium. Fluorescence (excitation:

480 and emission: 515) and OD_{600} were monitored every 15 minutes for 8 hours. Graphs only depict 2-8 hours. Results are displayed as specific fluorescence (normalized with OD_{600} value and background fluorescence from medium subtracted). The displayed specific fluorescence values are the mean of three technical replicates, and shaded area depict standard error of the mean. 37

Figure 12 | Simulation of QQ: Artificially triggering the signal switch. **(A)** Genetic overview of the construct tested in this experiment. **(B-C)** The test constructs and controls were grown in culture tubes in LB and were transferred upon reaching early exponential phase to a 96 well plate. Thereafter, they were supplemented with either a final concentration of 100 mM 5-methyl-4-hydroxy-3-furanone (sAI2), both 100 mM sAI2 and 0.96 µM aTC, only 0.96 µM aTC or dH2O. Fluorescence (excitation: 480 and emission: 515) and OD_{600} were monitored every 15 minutes for 8 hours. Graphs only depicts 2-8 hours. Results are displayed as specific fluorescence (normalized with OD_{600} value and background fluorescence from medium subtracted). The displayed specific fluorescence values are the mean of three technical replicates, and shaded area depict standard error of the mean. 38

Figure 13 | Genetic design of proof of concept circuit. Note that the representation of the construct in this figure is linear, opposed to the circular structure of the plasmid in their natural state. 39

Figure 14 | Lengths of the lsr (P_{lsr}) regulatory region of selected studies. (A) Overview of E. coli lsr operon. **(B)** The genomic area around the lsr regulatory region (P_{lsr}) is singled out and an overview is shown of the different regions used by Tsao et al. [92], Weiland-Bräuer et al. [60], this study, Zhou et al. [99] and Xavier et al. [100]. Sequence and annotations were retrieved from Benchling (2021), https://benchling.com, and graphical elements for explanations are subsequently added. 44

Figure 15 | Proposed alternative cloning strategy. Abbreviations: RBS, ribosomal binding site. QS, quorum sensing. POC, proof of concept. 48

Figure 16 | PCR verification of biosensor and test constructs. Example of part-wise PCR verification using primers binding to linkers for amplification of each part. All bands are from separate reactions with an inward-facing primer pair binding to the two linkers flanking the part of interest. Part sizes can be found in Table 2. DNA ladder used is 1 Kb Plus DNA Ladder from Invitrogen, Thermo Fisher Scientific (catalog number 10787018). 61

Figure 17 | Induction with MC4100 supernatant in LB medium. **(A)** Genetic overview of constructs tested in this experiment. **(B-F)** Test constructs in DH5α (pJB12, pJB17, pJB18, negative control without plasmid) were grown in culture tubes, and 80 µl culture were transferred upon reaching early exponential phase to a 96 well plate. Test constructs were supplied with 20 µl supernatant from E. coli MC4100 in exponential growth phase, and controls (uninduced) were supplied with 20 uL LB medium. Fluorescence (excitation: 580 and emission: 615) and OD_{600} were monitored every 15 minutes for 8 hours. Graphs only depicts 2-8 hours. Results are displayed as specific fluorescence (normalized with OD_{600} value and background fluorescence from medium subtracted). The displayed specific fluorescence values are the mean of three technical replicates, and shaded area depict standard error of the mean. 62

Figure 18. | Induction with 100 mM 5-methyl-4-hydroxy-3-furanone in LB medium. **(A)** Genetic overview of constructs tested in this experiment. **(B-F)** Test constructs in DH5α (pJB12, pJB17, pJB18, negative control without plasmid) were grown in culture tubes, and 90 µl culture were transferred upon reaching exponential phase to a 96 well plate. Test constructs were supplied with 10 uL 5-methyl-4-hydroxy-3-furanone (sAI2) solution reaching a final concentration of 100 mM sAI2. Controls (uninduced) were supplied with H_2O. Fluorescence (excitation: 580 and emission: 615) and OD_{600} were monitored every 15 minutes for 8 hours. Graphs only depicts 2-8 hours. Results are displayed as specific fluorescence (normalized with OD_{600} value and background fluorescence from medium subtracted). The displayed specific fluorescence values are the mean of three technical replicates, and shaded area depict standard error of the mean. 63

Figure 19. | Induction with 50 mM 5-methyl-4-hydroxy-3-furanone in M9 medium. **(A)** Genetic overview of constructs tested in this experiment. **(B-F)** Test constructs in DH5α (pJB12, pJB17, pJB18, negative control without plasmid) were grown in culture tubes, and 90 µL culture were transferred upon reaching early exponential phase to a 96 well plate. Test constructs were supplied with 10 µL 5-methyl-4-hydroxy-3-furanone (sAI2) solution reaching a final concentration of 50 mM sAI2. Controls (uninduced) were supplied with 10 µL H_2O. Fluorescence (excitation: 580 and emission: 615) and OD_{600} were monitored every 15 minutes for 8 hours. Graphs only depicts 2-8 hours. Results are displayed as specific fluorescence (normalized with OD_{600} value and background fluorescence from medium subtracted). The displayed specific fluorescence values are the mean of three technical replicates, and shaded area depict standard error of the mean. 64

Figure 20 | Fluorescent image of LB agar plates with negative control and pJB32. (A) Overview of pJB32 genetic composition. **(B)** Pictures of LB agar plates. Exponentially growing cultures of each strain were spread evenly on the plates in the evening and pictures were taken the following morning. The LB agar plate which pJB32 were spread on also contained ampicillin (100 µg/mL) to maintain plasmid stability. This is an cropped image taken with a cell phone of the screen image generated by the Kodak Image Station 4000 MM Pro. 65

Figure 21 | Simulation of QQ: Testing the signal switch in high copy number backbone. **(A)** Genetic overview of the construct tested in this experiment. **(B-C)** The test constructs and controls were grown in culture tubes in LB, and 90 µl culture were transferred upon reaching early exponential phase to a 96 well plate (if stated anhydrotetracycline (aTC) was also added). Thereafter, they were supplemented with 5-methyl-4-hydroxy-3-furanone (sAI2) reaching a final concentration of 100 mM. Fluorescence (excitation: 480 and emission: 515) and OD_{600} were monitored every 15 minutes for 8 hours. Graphs only depicts 2-8 hours. Results are displayed as specific fluorescence (normalized with OD_{600} value and background fluorescence from medium subtracted). The displayed specific fluorescence values are the mean of three technical replicates, and shaded area depict standard error of the mean. 66

Figure 22 | Colony PCR of POC assembly attempt. The eight bands above pJB30 are the products 8 colony PCR (cPCR) reactions of pJB33 transformants (excluding the vector backbone) using insert-specific primers. Predicted size is 3110 bp. The 10 bands in the middle are the products of 10 cPCR reactions of the proof-of-concept construct transformatns using insert-specific primers. Predicted size was 3325 bp. The rightmost band is an control PCR reaction of the pJB30 biosensor construct using the same insert-specific primers and settings as the other bands (predicted size 3110 bp). DNA ladder used is 1 Kb Plus DNA Ladder from Invitrogen, Thermo Fisher Scientific (catalog number 10787018). 67

1 Introduction

Bacteria, once believed to be unicellular life forms living as self-sufficient individuals, have been shown to reside in organized, complex communities [1]. This previous perception of bacteria as being solely unicellular organisms living solitarily stems from the era of Robert Koch and the "pure-culture paradigm". Although these ideas played a significant role in both the identification of many bacterial pathogens and the development of antibiotics for treatment of bacterial infections, it was later discovered that bacteria rarely grow in planktonic pure-cultures outside of the laboratory [1], [2]. This was understood four decades ago after great advances in the research fields of biofilm development and quorum sensing (QS). A biofilm is defined as a self-produced matrix of extracellular polymeric substances in which the cells reside [3], and quorum sensing as a communication strategy based on chemical signal molecules [4]. These advances clearly showed that not only do bacteria form complex communities in which they are interdependent, but they are also able to communicate and coordinate activities [1], [5]. Put together, bacterial communities exhibit equally complex behavior as larger multicellular organisms [4].

To coordinate these community-wide activities, bacteria use quorum sensing. While many quorum sensing coordinated activities are beneficial to mankind, such as their role in biogeochemical cycling [6], interspecies communication within symbiotic gut microbiota [7], [8], and enhanced crop protection [9], there is a wide range of implications affecting human health and modern society. The most impactful examples are bacterial virulence, biofilm formation and antibiotic resistance development [10]. Perhaps one of the greatest threats to mankind is the increasing spread of antibiotic resistant bacteria. Humanity is now marching into the so-called 'post-antibiotic era', where multi-resistant strains emerge quicker than the development of antimicrobial drugs [11]. The World Health Organization (WHO) estimates that this will cause 10 million deaths annually in 2050, deeming it one of the biggest threats to global health [12], [13]. In addition, the few newly developed drugs have the same chemical motifs as the existing ones, which means that bacteria ultimately will develop resistance to these [14]. This rapid emergence of antibiotic resistance is mainly caused by the very widespread use of antibiotics and the 'life-or-death' selection pressure innate to their modes-of-action [11], [15].

It is evident that development of new types of antimicrobial intervention strategies are needed. Interference with the bacterial QS system, also called quorum quenching (QQ), has in the past decade emerged as a promising strategy for combating bacteria. ‘Silencing’ bacteria by jamming their QS-based communication has several advantages, for instance [16]: (1) a single molecule can simultaneously interfere with multiple functions like biofilm formation, expression of virulence factors etc., (2) if used in combination, QQ molecules could enhance the effect of existing antibiotics, e.g. by limiting biofilm formation, (3) in theory, QQ molecules should not exert an evolutionary pressure for resistance development if growth remains unaffected [17]. Hence, being able to disrupt QS would be a valuable element in the antimicrobial toolbox. This study aims to develop a modular biosensor system for the detection of QQ compounds specific for the interspecies AI-2-based QS (described in Section 1.5). The system is based on a genetic circuit employed in a bacterial host, and such a biosensor can be used to screen natural product libraries. A more detailed aim of this study is described in Section 1.5.

1.1 Quorum sensing

In most societies in nature, communication is key for cooperation. Being unicellular organisms with limited motility, bacteria have evolved QS to allow for communication-based coordination within communities. In short, QS is chemical communication by collective production, release and detection of extracellular signaling molecules (called autoinducers, AI), which enable synchronized genetic regulation [1], [18]. This cross-talk enables bacterial communities to react to environmental changes by regulating physiological processes in a cell density dependent manner, only carrying out specific activities when they are most productive and beneficial [1], [19]. Typically, the formation of autoinducer-receptor complexes induces expression of the gene(s) responsible for autoinducer production, quickly increasing the extracellular concentration of the respective autoinducers. This creates a feed forward loop, synchronizing behaviors across a given population of bacteria [18]. From a human perspective, perhaps one of the most relevant scenarios of QS is the regulation of virulence factors upon bacterial invasion of a host organism: For pathogenic bacteria, it can be vital to reach a certain number of invading bacteria before initiating virulence in order to resist defense mechanisms of the host. [1]. The opportunistic pathogen *Pseudomonas aeruginosa* will, for example, induce genes encoding virulence factors responsible for host tissue destruction (mainly *lasB* and *lasA*, an elastase and a protease) when reaching a given cell density threshold [5], [20]. Conversely, as shown in a study by Hammer & Bassler, 2003, *Vibrio cholerae* carries out an oppositely regulated pattern, where virulence factors and especially biofilm formation are expressed at low cell density and repressed during high cell densities. This is due to the nature of the *V. cholerae* infection process: Upon early infection at low cell densities, typically via contaminated water entering the host, *V. cholerae* form biofilm in order to colonize the intestinal epithelia, where they secrete toxins causing severe diarrhea. As the cell density rises, biofilm production is repressed and bacteria now freed from the biofilm will be flushed and returned to the environment, allowing population dispersal to new hosts [21].

The implications of QS to mankind are widespread and not only limited to human pathogens. These are summarized in Table 1. Put together, there is a wide array of mechanisms regulated by quorum sensing, and it is now widely accepted that bacteria are able to communicate not only within a species but also on an interspecies and even interkingdom level [22]. This capability is the result of the evolution of different types of QS systems.

1.1.1 Bacteria communicate with various quorum sensing systems

Traditionally, QS has been divided into three overall systems [1], [23]: (1) an acyl-homoserine lactone (AHL) based species-specific system in Gram-negative bacteria, also known as autoinducer-1 (AI-1) QS, (2) the *luxS*-based autoinducer-2 (AI-2) system used by both Gram-negative and Gram-positive bacteria, and (3) a two-component system in Gram-positive bacteria using small autoinducing peptides (known as AIP-QS). Other types of QS which go beyond these classes have later been discovered, with examples like the *Pseudomonas* quinolone signal [24], the diffusible signal factor (DSF) [25], and an autoinducer-3 (AI-3) [26]. All known QS systems but one are species-specific. The exception is the AI-2 system [14] which is prevalent within the domains of Bacteria. It has been shown that more than 100 species of both Gram-negative and Gram-positive bacteria are able to recognize and produce AI-2 [22].

Table 1 | Overview of quorum sensing mediated implications to modern society.

QS regulated mechanism	**Industry**	**Consequence**	**Reference**
Biofilm formation			
	Transport	Bacterial biofilm formation on ship hulls leads to colonization by marine invertebrates and algae (also known as biofouling), which increases fuel usage as a consequence of additional drag	[27]
	Medicine, food industry	Due to reduced permeation of the biofilm, bacteria embedded in biofilm will acquire increased resistance to antibiotics, host immune defense mechanisms and cleaning agents	[28], [29]
	Food industry	Biofilm formation on processing utensils causes increased contamination of food with bacterial pathogens, resulting in food waste	[28]
	Water treatment, transport	QS induced biofilm formation has been shown in sulfate-reducing bacteria, which are key-contributors to microbial biocorrosion of metal surfaces	[30]
Efflux pumps			
	Medicine	QS has been shown to regulate efflux pumps, which are able to extrude antibiotics from within the bacterial cell	[15]
Antibiotic resistance development			
	Medicine	Induction of competence has been shown to be regulated by QS, enabling bacteria to take up exogenous DNA and thereby possibly share genes encoding antibiotic resistance horizontally	[31]
Virulence			
	Medicine	A wide array of human and veterinary pathogens, e.g. *S. aureus, P. aeruginosa, V. cholerae*, collectively induce virulence genes (causing disease in host) by QS	[32]
	Aquaculture	Aquatic pathogens rely heavily on QS for host colonization and virulence induction, especially among members of the ubiquitous *Vibrio* genus, which is a major constraint within the aquacultural industry	[33]
Microbial degradation	Food industry	Proteolytic, pectinolytic, chitinolytic and lipolytic mechanisms associated with spoilage of food are regulated by QS	[29]

1.1.2 Autoinducer-2: A universal signaling molecule

The first indications of a second QS system came when Bassler *et al*. 1993 discovered that *V. harveyi* mutants incapable of AHL synthesis (AI-1) still remained capable of QS-dependent gene activation, and only a few years later, it was shown that this system could be induced with cell-free culture fluids from other bacterial species [34], [35]. Researchers then identified the gene responsible for AI-2 production, designated *luxS*. Homologs of *luxS* were found in several other sequenced genomes [36]. Fast forward one and a half decade, and many hundred genomes with *luxS* homologues have been discovered, establishing the fact that AI-2 indeed is a universal signaling molecule [37]. It has also been found to influence the transcription of more than hundred genes in some species [38]. Here, the path of AI-2, from production to export, import and response, will be described.

1.1.2.1 LuxS: AI-2 synthase and part of central metabolism

In all species capable of AI-2 production, the enzyme LuxS is responsible for synthesizing 4,5-dihydroxy-2,3-pentanedione (DPD), a precursor of the AI-2 signaling molecule. LuxS is a part of the pathway called the activated methyl cycle (AMC), which is responsible for the recycling of a major cellular methyl donor, the S-adenosylmethionine (SAM) [39]. As shown in Figure 1, SAM is metabolized to S-adenosylhomocysteine (SAH). SAH can be converted directly to homocysteine if the organism has genes encoding the S-adenosylhomocysteine hydrolase (SahH). AI-2 producing bacteria instead convert SAH in a two-step reaction: 5'-methylthioadenosine/S-adenosylhomocysteine nucleosidase (MTAN, encoded by *pfs*) converts SAH to S-ribosylhomocysteine (SRH), and S-ribosylhomocysteine lyase (LuxS, encoded by *luxS*) converts SRH to homocysteine and DPD, being the linear form of AI-2 [37]. As DPD is highly unstable, it readily rearranges into R- or S-2-methyl-2,3,3,4-tetrahydroxytetrahydrofuran (R- or S-THMF). Both of these isomers are better known as AI-2 [40]. Although the explained biosynthetic pathway and chemical byproducts are similar in all bacteria capable of producing AI-2, the isomer of the AI-2 signaling molecule (R- or S-THMF) detected by the bacteria was later shown to differ. However, because R- or S-THMF are capable of interconversion and the fact that they are in equilibrium when in solution, AI-2-based QS still works across species regardless of the isomer a species detects [37].

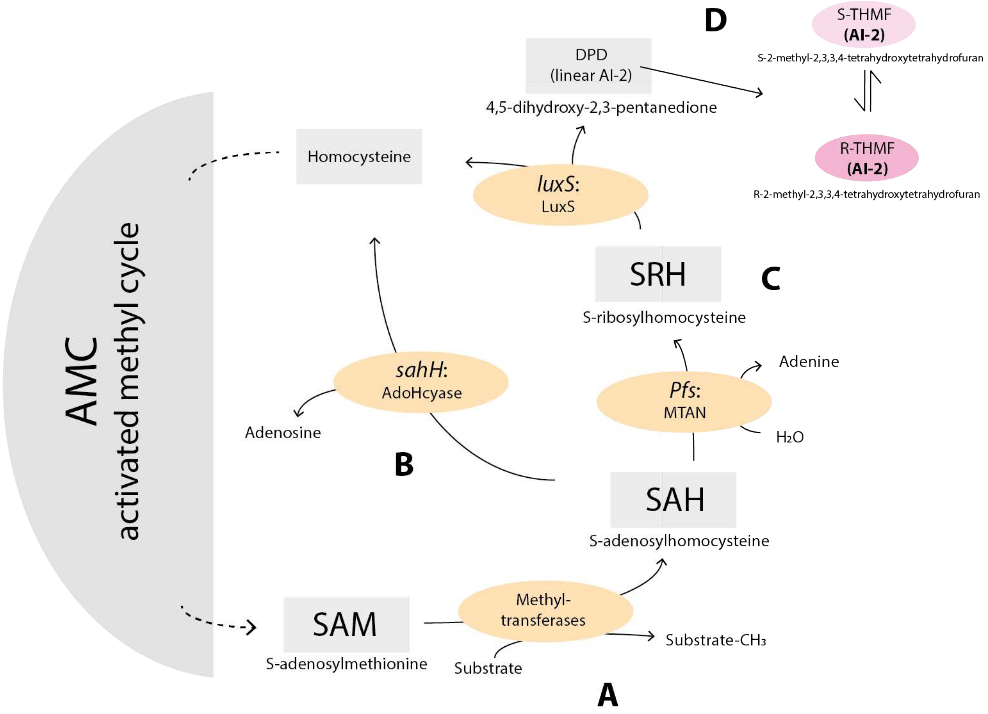
D
S-THMF
(AI-2)
S-2-methyl-2,3,3,4-tetrahydroxytetrahydrofuran
R-THMF
(AI-2)
R-2-methyl-2,3,3,4-tetrahydroxytetrahydrofuran
DPD
(linear AI-2)
4,5-dihydroxy-2,3-pentanedione
Homocysteine
luxS:
LuxS
SRH
S-ribosylhomocysteine
C
AMC
activated methyl cycle
sahH:
AdoHcyase
Adenosine
B
Pfs:
MTAN
Adenine
H₂O
SAH
S-adenosylhomocysteine
SAM
S-adenosylmethionine
Methyl-
transferases
Substrate
Substrate-CH₃
A

Figure 1 | **The activated methyl cycle (AMC) with the relevant steps highlighted in color**. **(A)** Coming from the other half of the AMC, a methyl group is removed from SAM which converts it to SAH (a toxic intermediate). **(B)** Organisms with *sahH* convert this directly to homocysteine. **(C)** Organisms with *luxS* convert it to homocysteine in two steps: SAH is converted by MTAN to SRH before LuxS converts it to homocysteine and DPD (the linear form of AI-2). **(D)** DPD rapidly rearranges into S-THMF or R-THMF, which to bacteria is the recognizable form of AI-2. Adapted and modified from Pereira, Thompson and Xavier, 2013 [37].

1.1.2.2 Sending a signal: Export of AI-2

Because of the fact that AI-2 is hydrophilic with low affinity to lipids in nature, the cell membrane acts as a permeability barrier [37]. The cellular export mechanism of AI-2 remained unknown until Herzberg *et al*., 2010 showed that deleting the gene *tqsA* (previously known as *ydgG*), which encodes a previously uncharacterized membrane-spanning protein TqsA (YdgG), resulted in decreased extracellular and increased intracellular concentrations of AI-2, increased cell motility and increased biofilm formation. However, these phenotypes were restored when expressing *tqsA* in *trans* [41]. Nevertheless, as stated by Pereira *et al.* 2013, since the extracellular accumulation of AI-2 in TqsA deficient strains, in conditions where AI-2 uptake is inhibited, is only twofold lower compared to wild type, TqsA is not the sole exporter of AI-2. Hence, other export mechanisms must exist [37].

1.1.2.3 Various types of AI-2 perception

AI-2 detecting bacteria use different genetic systems to relay, interpret and process the actual signaling molecules. The systems are named after their receptor. Three types of receptors specific to AI-2 have been characterized to this date, being the LsrB protein in *Salmonella typhimurium* and *E. coli*, the LuxP protein in *Vibrio* species, and the RbsB protein in *Aggregatibacter actinomycetemcomitans* [42]. In addition, bacteria lacking the above mentioned receptors have been shown to respond to AI-2, indicating that other unidentified receptors exist [37]. The LsrB receptor and the Lsr system, which is of most relevance to this study and therefore will be focused on, is a part of the LsrACDB-transporter [14]. The initial uptake of AI-2 happens through a secondary, promiscuous PTS transporter [43], and as elaborated below, when the QS feedback loop has been activated, the LsrB protein binds the R-THMF isomer of AI-2 and initiates internalization of AI-2 via the LsrACD part of the transporter. [42].

1.1.2.4 Modification and termination of AI-2 by the *lsr* system

Upon transportation into the cell, the AI-2 molecule is phosphorylated by a kinase, LsrK, into P-AI-2. Inside the cell, the P-AI-2 binds to LsrR, a repressor. In the absence of P-AI-2, LsrR binds to a regulatory region (in this study, the whole region is denoted P_{lsr}) and represses the divergently transcribed *lsrRK-ACDBFG* operon. This operon contains genes regulating its own expression (*lsrRK*), genes for transporters responsible for uptake of AI-2 (*lsrACDB*), and genes for downstream processing and termination (*lsrFG*). High P-AI-2 concentrations promote transcription of the operon by removing LsrR from P_{lsr}, which in turn creates a positive feedback loop, increasing both the uptake and phosphorylation and, eventually, depletion of AI-2 from the extracellular medium[14], [37]. This process, from export to termination, is depicted and elaborated in Figure 2.

Bacteria with this *lsr* system and the depletion of AI-2 from the extracellular medium towards the stationary phase seem to contradict the paradigm of QS, being that autoinducers accumulate with increasing cell density [37]. This has led to the hypothesis that species harboring the *lsr* system not only use AI-2 molecules to perceive the surrounding cell density but also remove AI-2 to deceive and confuse other nearby species to gain an advantage [43].

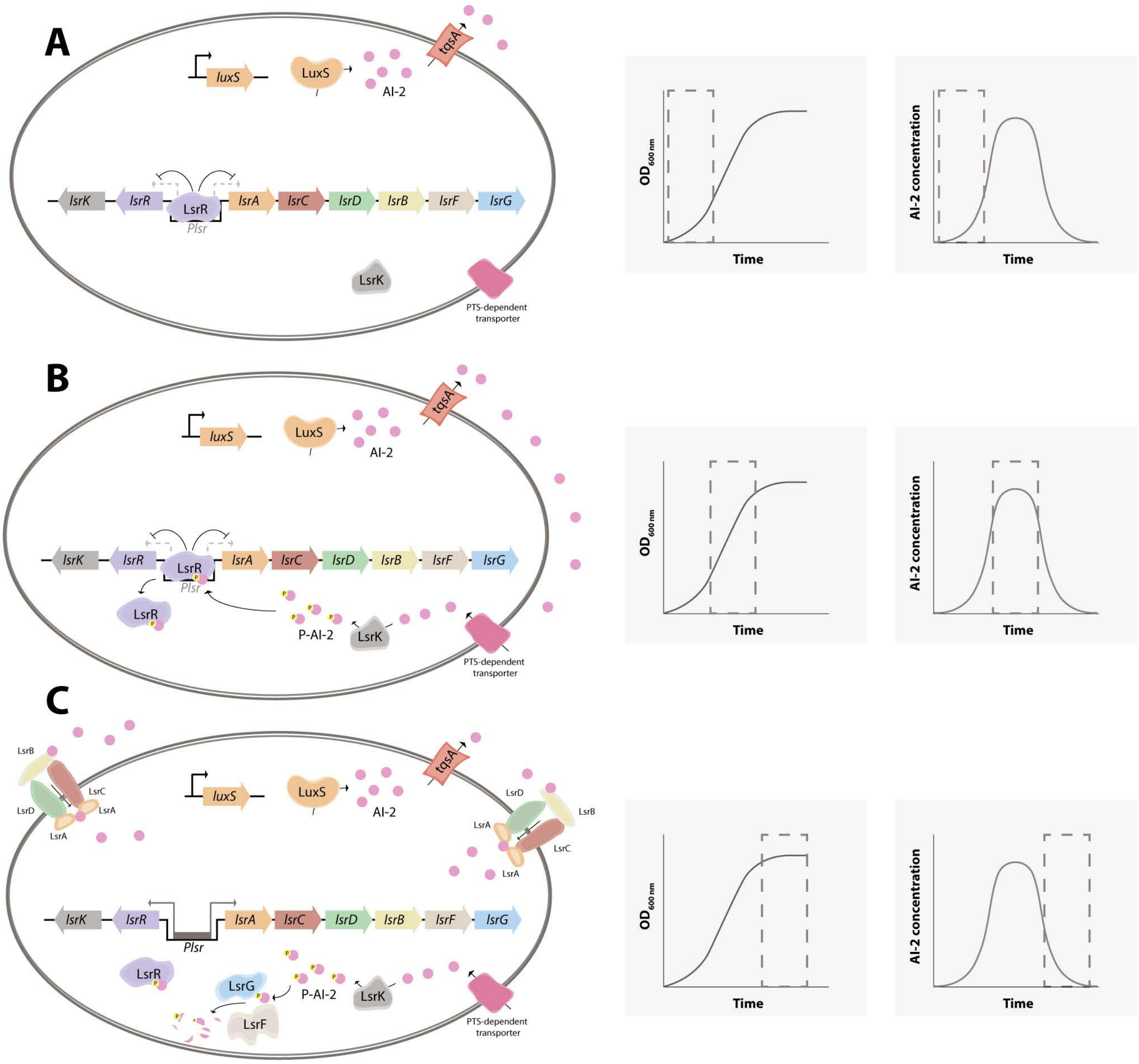
A
luxS
LuxS
AI-2
tqsA
lsrK
lsrR
LsrR
Plsr
lsrA
lsrC
lsrD
lsrB
lsrF
lsrG
LsrK
PTS-dependent transporter
OD600 nm
Time
AI-2 concentration
Time
B
luxS
LuxS
AI-2
tqsA
lsrK
lsrR
LsrR
Plsr
lsrA
lsrC
lsrD
lsrB
lsrF
lsrG
LsrR
P-AI-2
LsrK
PTS-dependent transporter
OD600 nm
Time
AI-2 concentration
Time
C
LsrB
LsrC
LsrD
LsrA
LsrA
luxS
LuxS
AI-2
tqsA
LsrD
LsrB
LsrA
LsrC
LsrA
lsrK
lsrR
Plsr
lsrA
lsrC
lsrD
lsrB
lsrF
lsrG
LsrR
LsrG
P-AI-2
LsrK
LsrF
PTS-dependent transporter
OD600 nm
Time
AI-2 concentration
Time

Figure 2. Model for AI-2 secretion, uptake and signalling by the *lsr* system. (A) In low cell densities, i.e. lag phase, the extracellular concentration of AI-2 is low, and the *lsr* operon is repressed by LsrR. **(B)** In the exponential growth phase, AI-2 accumulates extracellularly, and initial uptake occurs through PTS-dependent transporters. Imported AI-2 is phosphorylated by LsrK to P-AI-2 which upon binding and removal of LsrR derepresses the *lsr* operon. **(C)** Activation of *lsr* operon leads to increased uptake by the LsrACDB-transporter-complex. A positive feedback loop occurs, and the extracellular concentration of AI-2 decreases rapidly. P-AI-2 is eventually degraded by LsrG and LsrF. Adapted and modified from Pereira *et al.* [37].

1.2 Jamming the signal: Quenching of quorum sensing

Communication is key, and maybe disrupting communication could be key to combat bacteria in present time as we gradually step into the ‘post-antibiotic era’, where many antibiotics are rendered useless due to microbial resistance. QQ has in the recent years attracted a lot of attention as a promising approach for controlling bacterial infections and generally limiting bacterial growth in undesired places. Until 2020, at least 57 molecules with QQ activity have been patented, but few are licensed and commercially available [16], [44].

The term ‘quorum quenching’ covers all the possible routes of disrupting QS, however, many studies distinguish between quorum quenching as the enzymatic deactivation of QS and ‘quorum sensing inhibition’ (QSI) as the chemical disruption of QS [45]. In this study, the term ‘quorum quenching’ describes both QQ and QSI.

In this section, different QQ strategies will be described and the scientific efforts within this field will be briefly reviewed.

1.2.1 Criteria for quorum quenching molecules

In order to remain effective, it has been proposed that QQ compounds should fulfill a few criteria. Most research on QQ has been focused on targeting AI-1-based QS, and therefore these criteria apply to this type of QS. In a comprehensive review on this topic, Kalia et al. 2013 state, based on the work of [46]–[48], that an effective AHL-QQ compound is: (1) a small molecule which efficiently reduces gene expression regulated by QS, (2) very specific for the targeted QS regulator with no unfavorable effect on either bacteria or host, (3) chemically stable with no risk of degradation by host metabolism, and (4) longer than native AHL chains [49]. All criteria except the last can be applied to AI-2-QQ, although there are some challenges in this context. The second criterion is crucial in preventing the emergence of resistant strains: When growth remains unaffected, there is no selection for development of resistant strains [17]. However, the ‘specificity for a QS regulator’ in this criterion remains a challenge in terms of AI-2-QQ, if the aim is to target the QS system of specific bacteria, e.g. a virulent pathogen in a human host. The above mentioned criteria apply for AI-1-QQ molecules, which have highly specific cognate receptors, and as AI-2 is an unspecific QS molecule recognized by many different receptors, AI-2-QQ will probably affect a wide range of bacteria in the environment. This could be a problem if the QQ molecules interfere with favorable microbiome species in and on humans [50]. In other cases where the aim is to minimize all bacterial growth, e.g. in anti-biofouling measures, this would merely be an advantage instead of a problem.

1.2.2 Quorum quenching strategies

In Gram-negative bacteria, there are three overall modes-of-action of QQ relating to the point of ‘attack’: The signal production, the signal molecule itself and the signal receptor [46].

Few studies have aimed at the signal production as a method of inhibiting QS, leaving the field relatively open for novel discoveries [16]. Nonetheless, researchers have discovered molecules inhibiting the production AI-2. For example, Gutierrez *et al.* 2013 found that transition state analogs of MTAN, the gene product of *pfs,* which is responsible for the conversion of a precursor of AI-2 as shown in Figure 1, effectively inhibits production of AI-2 without affecting bacterial growth [51].

More research has focused on neutralizing the QS signal itself. Still, most discoveries have revolved around enzymes and antibodies directed towards AHL-based QS [16], and as stated by Sikdar and Elias in 2020, ‘proficient enzymes able to neutralize AI-2 remain elusive’ [50]. However, Roy *et al*. managed to quench AI-2 signaling between co-cultures of *E. coli* and *S. typhimurium* by adding the native *E. coli* LsrK enzyme (described in Figure 2). Here, AI-2 is phosphorylated extracellularly by LsrK, and as P-AI-2 is negatively charged, transport into the cell is prevented [45], [52].

The most extensively studied QQ mechanisms are aimed at the signal receptor. Upon binding to the receptor, antagonists can e.g. block the active site of the receptor or modify the conformation of the receptor-signal complex. In the case of AI-2 QS, this would prevent uptake of signal molecules, rendering the bacteria ‘deafened’. As a part of several studies, scientists have synthesized AI-2 analogs which show QS-inhibiting abilities [45], [53]–[55].

1.3 Using biosensors to find quorum quenching compounds

In the pursuit of novel QQ molecules, researchers have taken different approaches. These include chemical techniques, computer-aided methods and virtual screening, nano- and microtechnological techniques, and bioassays [44]. The latter include the use of genetically engineered whole-cell biosensors (also known as bioreporters), where the screening process has proved to be easy and cost-effective to use [56]. Also, by constructing these biosensors using the tools and approaches of modern synthetic biology, one can easily adapt biosensors to sense and detect a wide array of desired elements (as described later in Section 1.4).

The common component of all biosensors is a biological element, which allows for the specific detection of a target analyte and transduces this event of detection into a readable signal. This signal is often one which can be easily converted into an electrical signal and fed to an electronic device for interpretation and data storage [57]. In cell-based biosensors, the biological element is the cell itself, and the transduction of the detection event is typically mediated by a reporter gene encoding a protein, which gives a colorimetric, luminescent or fluorescent signal. Whole-cell biosensors have been employed by the scientific community for a long time, and several biosensors detecting QQ compounds have been reported.

1.3.1 Examples of quorum quenching detecting biosensors

To date, several studies using cell-based biosensors for detection of QQ compounds have been published, where the great majority target inhibitors for AI-1 QS. These range from simple systems to more complex genetic circuits.

The easiest and most simple approach in QQ screening is to use natural indicator strains like *Chromobacterium violaceum* which produces a visible pigment called violacein upon induction by AI-1 QS [44]. In many other studies, plasmid-based biosensors with QS-regulated promoters fused to a reporter gene have been used. An example is the plasmid-based sensor developed by Hentzer et *al*., which contains the *Pseudomonas aeruginosa* QS-regulated promoter *lasB* fused to an unstable variant of the green fluorescent protein (GFP) [58]. The shorter half-life of the unstable GFP allows for continuous assessment of potential QQ activity of screened compounds, where QQ will be revealed by reduced fluorescence intensity. This sensor was later, 15 years after its publication, helpful in identifying the common carotenoid Zeaxanthin as an inhibitor of AI-1-based QS in *P. aeruginosa* [59].

A different and unique approach was taken by Rasmussen et *al*. when they in 2005 developed a unique suicide-based biosensors called QSIS (Quorum Sensing Inhibitor Selector) for identification of AI-1-QQ. Here, they fuse QS-controlled promoters, P_{luxI} or P_{lasB}, to genes encoding lethal proteins, *phlA* or *sacB*. Induction of these promoters by the cognate AI-1 will lead to cell death or growth-arrest. Hence, this biosensor will not grow unless a non-toxic QQ compound is present in necessarily high concentrations [17].

The QSIS strategy was later used by Weiland-Bräuer et *al*. to develop one of the more infrequent biosensors for identification of AI-2-QQ compounds, from which the present study has drawn certain inspiration. Here, they fused the AI-2 controlled promoter, P_{lsr} from *E. coli* K-12, to a killing gene, *ccdB*, which inactivates gyrase and leads to cell death. They employ this reporter circuit in *E. coli* DH5α as it lacks *luxS*, a gene necessary for production of AI-2 (to be able to control induction of P_{lsr}). Screening bacteria inhabiting the surface of marine eukaryotes with this biosensor, they managed to identify proteins with AI-2 interfering properties [60].

Generally, there has been extensive research into QQ of AI-1, and as a result, many biosensors aiming for detection of AI-1 quenching have been developed. Conversely, there are markedly fewer biosensors for detection of AI-2-QQ, and this field of research seems under-explored.

1.4 A synthetic biology approach via the BASIC DNA assembly system

The term ‘synthetic biology’ is widely used with different meanings. In the context of this study, it refers to a systematic approach of genetic modification inspired by other engineering fields. The central idea of this approach is to employ standardized genetic ‘parts’ which can be assembled in a modular fashion. The use of a synthetic biology inspired approach combined with the BASIC DNA assembly system, developed by Storch *et al*., allow for an easy and rapid interchange of genetic sequences (denoted parts) and tuneability [61]. This draws parallels to the BioBrick standard, the first of its kind, which has established standardized guidelines for parts. Here, similarly to the BASIC system, parts are flanked by standard prefix and suffix sequences, in a storage backbone, and these parts are readily cut and can be assembled with others using different assembly methods [62]. The ‘Registry of Standard Biological Parts’ is a collection of such genetic parts, and as of today, there are more than 20.000 documented genetic parts [63].

The BASIC system similarly rely on standardized prefix and suffix sequences. But, unique for its kind, it employs linker sequences used to assemble parts in the desired order. An assembly of multiple parts can be done simultaneously, and, for example, Storch *et al*. managed to assemble seven parts with 90% accuracy in one operation [61].

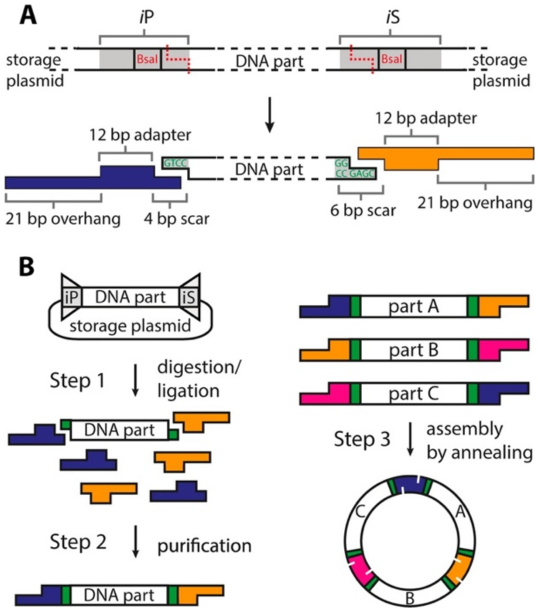
A
iP
iS
storage plasmid
BsaI
DNA part
BsaI
storage plasmid
12 bp adapter
12 bp adapter
GTCC
DNA part
GG
CC GAGC
21 bp overhang
4 bp scar
6 bp scar
21 bp overhang
B
iP
DNA part
iS
storage plasmid
part A
part B
part C
Step 1
digestion/
ligation
DNA part
Step 3
assembly
by annealing
C
A
B
Step 2
purification
DNA part

Figure 3 | BASIC standardization and workflow. (**A)** The BASIC DNA part is flanked by a prefix (iP) and a suffix (iS) sequence, each containing an inward facing BsaI site. Upon digestion with BsaI, a specific 4 bp overhang is generated to which DNA-linkers will ligate with its own 4 bp overhang. **(B)** The workflow of BASIC assembly. Step 1: Simultaneous digestion and ligation of linkers, separate for each part. Step 2: Purification, removal of unligated linkers. Step 3: Linker-adapted parts are mixed together and assembled into one construct. Figure adapted and modified from Storch et al. 2015.

1.4.1 The principles of BASIC

The very core elements of BASIC are (1) the standardized parts and (2) the DNA linkers.

1) All parts in a BASIC library are flanked by integrated prefix and suffix sequences (*i*P / *i*S, same for all parts) (Figure 3 A).
2) To assemble parts and to assemble them in the correct order, orthogonal DNA linker pairs are used (Figure 3 A-B). The 4 bp or 6 bp overhang is identical in all linkers, whereas the 21 bp overhang is complementary for each linker pair.

As shown in Figure 3B, the linkers are attached to parts simultaneously with the digestion of the BsaI sites. This is done in a reaction separate for each part, meaning each part contains a prefix and a suffix linker. In the final step, orthogonal linker pairs are assembled by annealing, hence generating the final constructs of parts where the order is determined by the choice of linkers.

1.4.2 Tuneability and adaptation is achieved by BASIC linkers

The BASIC system employs different linkers. **Neutral linkers** connects parts with a neutral sequence. **RBS linkers** include a ribosomal binding site (RBS) of different strengths, ranging from 1-3. The relative RBS strength of these linkers have been characterized via GFP expression. In relation to the strongest RBS linker (RBS3, 100% expression), RBS2 and RBS1 show relative expression levels of 56% and 5% respectively. This allows for tuneability of protein translation. **Methylated linkers** contain the BASIC prefix and suffix sequences. These are methylated to protect them from digestion of BsaI in the first step. However, upon transformation and replication *in vivo* of an assembled construct, this methylation disappears. By attaching methylated linkers to an assembly, the assembled construct constitutes a new "single" part which can be digested and linked to other parts. This is also how single parts are stored in a storage backbone: Here, methylated linkers with a BsaI site flank the single part whereas pairing linkers without a BsaI site are attached to the storage backbone. Hence, only the linkers attached to the part are cut, leaving the part 'ready' for assembly with other parts.

1.5 Aim of this study

This study seeks to develop a biosensor, which, firstly, detects compounds capable of quenching AI-2-based QS, and, secondly, reports these detection events with a two-signal output. Thirdly, the biosensor should be engineered in a way, and with methods, which allow for quick and easy adaption to other types of QS.

In order to fulfil the aims of the study, a circuit containing a genetic toggle switch (seen on Figure 4) was designed and constructed with a signal outcome depending on whether AI-2-based QS is active (not quenched) or inactive (quenched).

2 Materials and methods

2.1 Bacterial strains and plasmids used in this study

Strains used in this study include *E. coli* DH5α and *E. coli* MC4100. *E. coli* DH5α was used for all cloning purposes, genomic DNA extraction and as a host organism for test constructs and biosensor construct. *E. coli* MC4100 was used in the experiments described in Section 3.3.1 and 3.3.2. The separate genetics parts used in this study and their acquisition are described in Table 2 in Section 3. The plasmids, here denoted genetic constructs, used in this study is depicted in Figure 5 in Section 3.2. All plasmid extraction were performed using either NucleoSpin Plasmid (Macherey-Nagel, Ref 740499.250, Düren, Germany) or the BOMB protocol #5.3 v1.0 [64].

2.2 Growth medium, supplements and conditions

Luria-Bertani (LB) medium and M9 glucose medium were used in this study for all bacterial growth with the exception of under transformation of plasmids where SOC medium (Super Optimal broth with Catabolite repression) was used (Section 2.3.4). SOC medium consists of (dissolved in H_2O): 20 g/L tryptone, 5 g/L yeast extract, 0.5 g/l NaCl, adjusted to pH 7.0 with NaOH, and a final concentration of 20 mM glucose (added before use). LB medium consisted of (dissolved in H_2O) 10 g/L tryptone, 10 g/L NaCl and 5 g/L yeast extract. In this study, the M9 glucose medium used consists of (dissolved in H_2O) 1X M9 salts, 2 mM $MgSO_4$, 0,1 mM $CaCl_2$, 2 g/L glucose, 1 µg/mL thiamine, 1 µg/mL arginine supplemented with 1% 2X Yeast Extract Tryptone (YT) (all final concentrations). Where appropriate, ampicillin was added to a final concentration of 100 µg/mL. Unless otherwise stated, all strains were grown in 37 °C at 250 rpm in an incubation chamber.

A stock solution of 5-methyl-4-hydroxy-3-furanone (hereafter denoted sAI2) was made by dissolving sAI2 in H_2O to reach a final concentration of 1 M. This stock solution was stored in foil-covered tubes at -20 °C.

2.3 Cloning of genetic constructs

All cloning done is this study was done according to the principles of the BASIC DNA Assembly system invented by Storch *et al.* [61], following the protocols in chapter 14 of Chandaran and George, 2014 [65] with a few alterations (described Section 2.3.4 and 2.3.5).

The overall workflow is as follows (described in detail in the sections below). (1) Parts are adapted into the BASIC format with a prefix and a suffix sequence. (2) Parts are stored in storage backbones to build a library. Parts are cut out from storage backbones and simultaneously assembled into desired constructs and into the desired vector backbone. (3) For the 6-part construct (pJB30 and pJB33), the assembly was conducted in a two-step assembly process.

2.3.1 Adaptation of parts into BASIC format

The prefix and suffix sequences were attached to each part in different ways (prefix: 5'-TCTGGTGGGTCTCTGTCC-3' and suffix: 5'-CGATAGGTCTCCCGAGCC-3'). Part 3 (P_{tet}) was synthesized with the prefix and suffix (ordered from Twist Bioscence, San Francisco, USA). Part 4 (*sfGFP*), part 7 (*tetR*) and part 8 (*mRFP1*) were acquired from an in-house BASIC library and contained prefix and suffix before being used in this study. For part 1 (SEVA13-VB), part 2 (SEVA18-VB), part 5 (*λtl3*) and part 6 (P_{lsr}), prefix and suffix were incorporated by PCR (using Phusion High-Fidelity PCR Master Mix, Thermo Fisher Scientific, F531L) and template-specific primers with extensions coding for BASIC prefix and suffix. Common PCR program for all reactions were as follows. Initial denaturation: 98 °C, 30 seconds. Denaturation (25x): 98 °C, 10 seconds. Annealing (25x): 60 °C, 30 seconds. Extension (25x): 72 °C, time individual for each primer pair. Final extension 72 °C, 7 minutes. SEVA13-VB and SEVA18-VB were amplified with primers oJB31 and oJB32 (extension time of 2 min, 30 seconds) and purified with Nucleospin PCR clean up kit (Macherey-Nagel, Ref 740609.50, Düren, Germany). *λtl3* was amplified from pKD46 using primers oJB9 and oJB10 (extension time of 1 min) and purified like above. For P_{lsr}, genomic DNA from *E. coli* DH5α was extracted and purified using magnetic beads following the

BOMB protocol #7.1 v1.0 [64]. P_{sr} was amplified by PCR from the genomic DNA with primers oJB5 and oJB6 (extension time of 1 min), and it was purified as above.

2.3.2 Storage of parts

After incorporation of BASIC prefix and suffix, all parts were stored in the part library by inserting them in SEVA13-VB with the methylated linkers (described in Section 1.4.2) to flank the part for easy reuse. When storing SEVA13-VB and SEVA-18, these were flanked with methylated linkers and assembled with Part 8 (*mRFP1*). This enables reuse of the backbones for storing multi-part assemblies in them.

2.3.3 Assembly of constructs with more than 4 parts

Assembly of larger constructs (> 4 parts) was divided into two steps. In the first step, the first three and the last three parts were assembled separately and stored in SEVA13-VB with methylated linkers (composite part 1: P_{tet}, *sfGFP, λtl3*, composite part 2: P_{lsr}, *tetR, mRFP1*). Both composite parts were replicated *in vivo*, verified by colony PCR (cPCR) (described in Section 2.3.5) and extracted as well as purified (as described in Section 2.1). In the second step, treating the two composite parts like a normal part, they were assembled into SEVA13-VB and SEVA18-VB, which generated pJB30 and pJB33, respectively.

2.3.4 Transformation of *in vitro* assembled constructs

For transformation of *E. coli* DH5α with constructs assembled with BASIC, the 'Inoue Method for Preparation and Transformation of Competent *E. coli*' was followed in this study [66]. However, when plating transformed cells after recovery phase, 100 uL cell culture were plated on LB agar with antibiotic, and the remaining 800 uL was spun down (5000 x g, 5 min) before being plated on a separate but similar plate.

2.3.5 Assembly confirmation and sanger-sequencing

Upon transformation and subsequent overnight growth on plates, 4-10 colonies (half from each transformation plate) from each construct assembly were screened by colony-PCR (cPCR) using DreamTaq Green PCR Master Mix (2X) (Thermo Scientific, K1081) and with the general settings: Initial denaturation: 95 °C, 5:00 minutes. Denaturation (25x): 95 °C, 30 seconds. Annealing (25x): 57 °C, 30 seconds. Extension (25x): 72 °C, 1 min/kb. Final extension 72 °C, 7 minutes. Linker-specific primer pairs facing inward which amplify each separate part were used (overview of primers in Appendix 7.1). cPCR products were run in 1% agarose gel (150V, 30 min) and assemblies were verified based on presence and length of bands in the gel. 1 Kb Plus DNA Ladder from Invitrogen, Thermo Fisher Scientific (catalog number 10787018) was used as ladder (see Appendix 7.2 for example). All constructs were verified by cPCR, and pJB12, pJB17, pJB18, pJB25 and pJB30 were further verified by Sanger-sequencing. When sequencing the mentioned plasmids, each inserted construct were firstly amplified by PCR using Platinum SuperFi DNA Polymerase (Thermo Fisher Scientific, 12351010). with the following settings: Initial denaturation: 94 °C, 1:00 minute. Denaturation (35x): 94 °C, 10 seconds. Annealing (35x): 60 °C, 10 seconds. Extension (35x): 68 °C, 30 seconds/kb. Final extension 72 °C, 5 minutes. After purification of PCR reaction products using Nucleospin PCR clean up kit (Macherey-Nagel, Ref 740609.50, Düren, Germany), the sequencing reactions were prepared using the BigDye™ Terminator v3.1 Cycle Sequencing Kit (Thermo Fisher Scientific, 4337458) following manufacturer's instructions. Sequencing reactions were sent to the University Hospital of North Norway for final Sanger-sequencing.

2.4 Induction and biosensor assays

All testing of genetic constructs followed the same overall procedure described in this section. Addition of test substances is described separately for each experiment in Section 2.4.1 below.

Strains were inoculated in 5 mL medium and antibiotic (if appropriate) in 14 mL Falcon Round Bottom Polystyrene Tubes (Corning, #352059) with snap caps allowing gas exchange. Cell cultures were grown overnight in 37 °C at 250 rpm, and OD_{600} was measured in the morning. To be sure cells are exponentially growing when added to the assay, all cell cultures were diluted in 5 mL fresh medium to reach a new starting OD_{600} of ≈ 0.1. Cell cultures were again incubated under the same conditions and grown for approx. 1,5 hours until reaching an OD_{600} of ≈ 0.2. Cultures with higher OD_{600} than 0.2 were diluted until reaching OD_{600} ≈ 0.2. From here, 80 µL or 90 µL of culture were added to a 96 well plate with clear bottom (Corning 96-well Flat Clear Bottom, product number: 3340) along with 10 µL or 20 µL of inducer solution. The 96 well plate were covered with a film which allows gas exchange to decrease evaporation and prevent contamination (Breate-Easy, Diversified Biotech, Boston, USA). Red fluorescence (excitation: 580, emission: 615, gain: 100), green fluorescence (excitation: 480 and emission: 515, gain: 100) and OD_{600} was measured continuously every

15 minutes for 8 hours by a Synergy H1 Hybrid Multi-Mode Reader (BioTek, Agilent) in conditions of 37 °C and orbital shaking for 10 seconds every 15 minutes.

2.4.1 Addition of solutions to assays

In assays including *E. coli* MC4100 supernatant (Section 3.3.1), 80 μL of cell culture were added to each well along with 20 μL of supernatant from an exponentially growing (OD_{600} = 0.86) *E. coli* MC4100 culture in the same medium (LB medium or M9 glucose medium). For negative controls, sterile medium was added. In assays with *E. coli* MC4100 transformed with test constructs (Section 3.3.2), 100 μL of cell culture were added to each well. In assays including sAI2 (Section 3.3.3, 3.3.4 and 3.5), either 10 μL of 1M sAI2 or 5 μL of 1M sAI2 along with 5 μL dH_2O were added, reaching final concentrations of 100 mM sAI2 and 50 mM sAI2, respectively. For negative controls, 10 μL dH_2O was added. In assays including aTC (Section 3.5), 1 mL of cell culture was, prior to being transferred to wells, mixed in an Eppendorf tube with 0.5 μL of an 1 mg/mL aTC solution (solution contains aTC dissolved in 50% ethanol). 90 μL of this cell culture solution was transferred to the well and mixed with 10 μL of either 1M sAI2 or dH2o, reaching a final concentration of aTC of 0.96 μM.

2.4.2 Specific fluorescence calculations and statistics

Specific fluorescence is in this study defined as the fluorescence intensity of a cell culture with the fluorescence intensity of the medium used subtracted and then subsequently divided by OD_{600} of the particular cell culture. All cell cultures were measured in triplicates, and, for each time point, the standard error of the mean (SEM) was calculated and illustrated on the graph as fill areas. These are transparent in order to clearly see data in overlapping regions.

2.5 Data visualization and figure design

In this study, data visualization were created using RStudio [67]. With the exception of Figure 3 and Figure 14, all graphical elements were created by the author using Adobe Illustrator 2021 [68] or Adobe Photoshop 2021 [69]. The information which Figure 1, Figure 2 and Figure 3 is based on is referred to in the respective figure caption.

2.6 LB-sAI2 plates and fluorescent imaging

Similar to Weiland-Bräuer *et al.*, the LB-sAI2 plates were prepared mixing LB agar at 50°C with appropriate antibiotics and final concentrations of 50 mM sAI2. However, in the present study, the strains to be tested were spread evenly from an exponentially growing culture on the the LB-plates after the agar had solidified (Weiland-Bräuer *et al.* added 5 % (vol/vol) exponentially growing culture of the reporter strain while LB agar was fluid).

After overnight incubation at 37 °C, pictures of the plates were taken using a Kodak Image Station 4000MM Pro. Excitation and emission filters used were for green (λ_{Ex}: 485 nm, λ_{Em}: 535 nm) and red (λ_{Ex}: 570 nm, λ_{Em}: 600 nm) fluorescence. Exposure time for green fluorescence were 0.5 second and 1 second for red fluorescence.

3 Results

3.1 Genetic circuit of the biosensor and its mode of operation

One of the main purposes of the biosensor is to report quenching of AI-2-QS with a double-signal output where one signal implies that QS is quenched and the other signal the opposite, namely that QS is active. To achieve this, a genetic circuit was designed and assembled into a plasmid, yielding pJB30. This assembled construct encompasses six parts and a combination of linkers (Figure 4 for complete circuit, Table 2 for parts description). For the dual-signal output, two genes, *sfGFP* and *mRFP1*, encoding fluorescent proteins were included. The two proteins respectively exhibit green and red fluorescence, and they are therefore well suited for dual-imaging because of their differences in emission wavelengths. For the genetic switch, a P_{tet}-*tetR* system was employed. The AI-2-regulated promoter, P_{lsr}, functions as the 'sensing' entity of the circuit by transducing the induction (or the absence of induction) into gene expression of reporter genes and genetic switch genes.

The biosensor circuit works as follows: Firstly, AI-2 is supplied to the biosensor. If there is not a QQ compound present (Figure 4 A), QS will remain active. In this case, the supplied AI-2 will bind and remove LsrR from the P_{lsr} and initiate transcription of genes encoding a TetR repressor and a mRFP1 reporter protein. Here, TetR will bind to P_{tet} and prevent transcription of *sfGFP*, and, hence, the final output will be a red fluorescent signal. If a QQ compound is present (Figure 4 B), expression of TetR and mRFP1 will be inhibited by the native LsrR upon the binding of this to P_{lsr}. Here, the P_{tet} promoter will, behaving like a constitutive promoter, initiate transcription of *sfGFP* and eventually emit a green fluorescent signal as a final output signal. The *λtl3* terminator is positioned after *sfGFP* to prevent any transcription initiated by P_{tet} passing through to the P_{lsr}-controlled module.

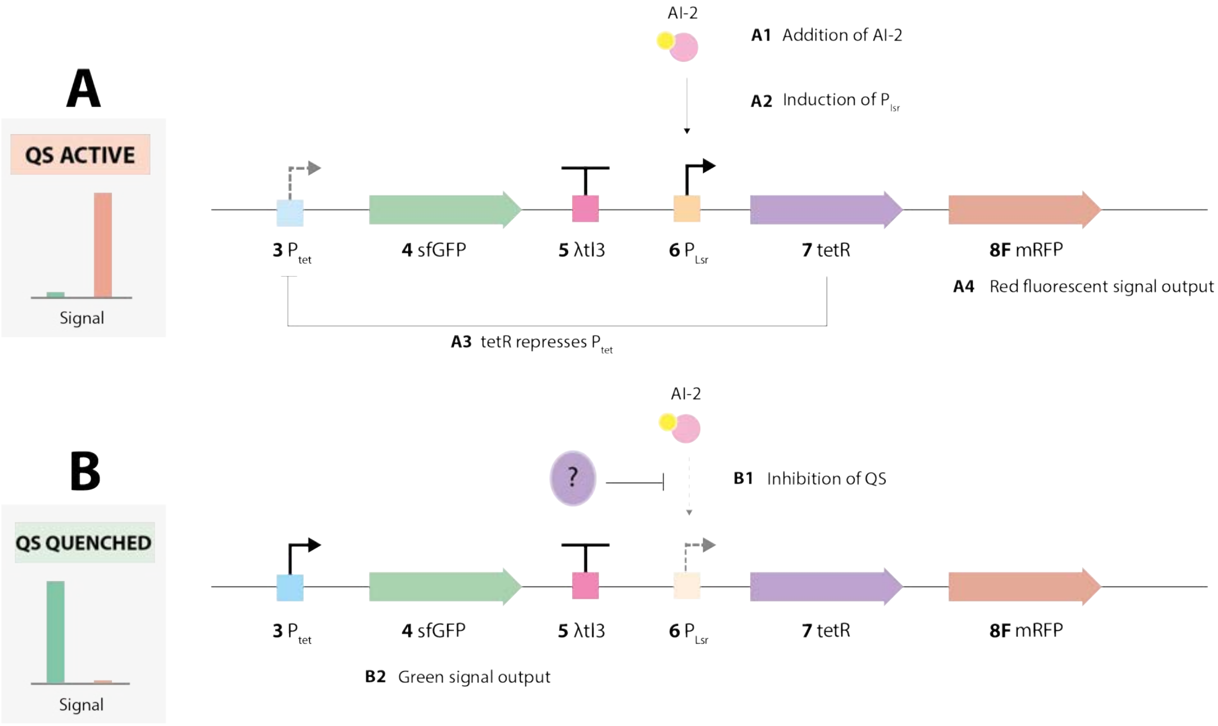
A
QS ACTIVE
Signal
AI-2
A1 Addition of AI-2
A2 Induction of P_lsr
3 P_tet
4 sfGFP
5 λtl3
6 P_Lsr
7 tetR
8F mRFP
A4 Red fluorescent signal output
A3 tetR represses P_tet
B
QS QUENCHED
Signal
AI-2
?
B1 Inhibition of QS
3 P_tet
4 sfGFP
5 λtl3
6 P_Lsr
7 tetR
8F mRFP
B2 Green signal output

Figure 4 | Genetic circuit of the biosensor and its operational principle. **(A)** Signal output when quorum sensing (QS) is active (i.e. not inhibited). **A1-A2.** Addition of autoinducer-2 (AI-2) induces the P_{lsr} promoter, which enables expression of downstream genes. **A3.** The expressed TetR repressor protein binds to and represses P_{tet} which blocks transcription of *sfGFP*. **A4.** Expression of *mRFP1* results in a red fluorescent signal output. **(B)** Signal output when quorum sensing is inhibited. **B1.** A given mechanism inhibits AI-2, and P_{lsr} remains uninduced. **B2.** Transcription of *sfGFP* is initiated through P_{tet}, generating a green fluorescent signal output. λtl3 terminator prevents further downstream transcription.

The host organism, hereafter referred to as 'chassis', of the biosensor is *E. coli* DH5α. This is mainly because of the fact that it was used successfully by Weiland-Bräuer *et al*. to harbor their QQ-bioreporter plasmid [60]. They used it because of its inability to synthesize both AI-1 and AI-2, due to the absence of *luxI* gene and a frameshift mutation in the *luxS* gene, respectively. Using DH5α prevents any self-induction of QS, making it possible to control it by exogenous addition of AI-2. Also, the chromosomal *lsr* operon (*lsrACDBFGE* and *lsrRK*) is present, and this is needed for transport, recognition and processing of AI-2 molecules. Furthermore, it is recommended by the creators of the BASIC DNA Assembly system that *E. coli* DH5α is used for storage of both individual parts and assembled constructs [61]. This enables easy and quick testing of constructs without the need for plasmid extraction and transformation of other chassis.

Table 2 | Overview of genetic parts used this study. (*) Standard European Vector Architecture [70].

Part	Function	Description	Acquisition	References
Part 1: SEVA13-VB	Plasmid backbone	Medium copy number backbone. Ori: *pBBR1,* resistance: *bla* (ampicillin-resistant). Part size: 3125 bp.	SEVA(*)	[70]
Part 2: SEVA18-VB	Plasmid backbone	High copy number backbone. Ori: *pUC,* resistance: *bla* (ampicillin-resistant). Part size: 2532 bp.	SEVA(*)	[70]
Part 3: P_{tet}	Promoter	Contains a *rrnB T1* terminator and two tetO sites (regulated by tetR) upstream of the actual *tet* promoter. Part size: 157 bp.	Synthesized from Twist Biosciences	[71]
Part 4: *sfGFP*	Reporter	Constitutively fluorescent green reporter protein, derived from *Aequorea victoria*, with enhancing folding abilities with regards to stability and maturation time. Ex λ: 485 nm, Em λ: 510 nm. Part size: 747 bp.	In-house stock	[72]
Part 5: *λtl3*	Terminator	Native transcription terminator from *Escherichia virus Lambda.* Part size: 332 bp.	PCR. Template: pKD46, Primers: oJB9, oJB10	[73]
Part 6: P_{lsr}	Promoter	Regulatory region of native *E. coli lsr*-operon. Repressed by LsrR upon binding. Repression is relieved when P-AI-2 binds to LsrR. Part size: 347 bp.	PCR. Template: *E. coli* DH5α. Primers: oJB5, oJB6.	[37], [60]
Part 7: *tetR*	Repressor	Binds to tetO site and represses transcription from P_{tet}. Binds also with high affinity to anhydrotetracycline which relieves repression of P_{tet}. Part size: 660 bp.	In-house stock	[74]
Part 8: *mRFP1*	Reporter	Monomeric red fluorescent protein, developed from DsRed (derived from *Discosoma sp*.). Ex λ: 584 nm, Em λ: 607 nm. Part size: 714 bp.	In-house stock	[75]
Part 9: P_{BAD}	Promoter	Arabinose-inducible promoter. Regulated by AraC: Repressed in absence of arabinose and presence of glucose. Induced in presence of arabinose. Part size: 424 bp	PCR. Template: pKD46, Primers: oJB7, oJB8	[76]

3.2 Building a library of parts and cloning genetic constructs

A main objective of the biosensor is to be modular and easily adaptable. To achieve modularity and to be able to assemble constructs in a parallel workflow, a library of genetic parts was built. These parts are separately described in Table 2. All parts were stored in SEVA13-VB (vector backbone) with methylated linkers reconstituting the BASIC-prefix (containing a BsaI cut site), meaning that they were to be easily cut out from the backbone and assembled with other parts or other backbones.

As outlined in Figure 5 several genetic constructs have been assembled using the BASIC DNA Assembly System by following the workflow described in Section 1.4. All constructs, with the exception of pJB33, have been cloned into the medium copy number plasmid SEVA13-VB.

The linkers constitute excellent primer binding sites, and this enables easy and quick verification of assemblies by PCR using primers amplifying each part. This is exemplified by the verification of pJB30, pJB12, pJB17 and pJB18 as shown in Appendix 7.2. All constructs were firstly confirmed by PCR and some were subsequently further verified by Sanger

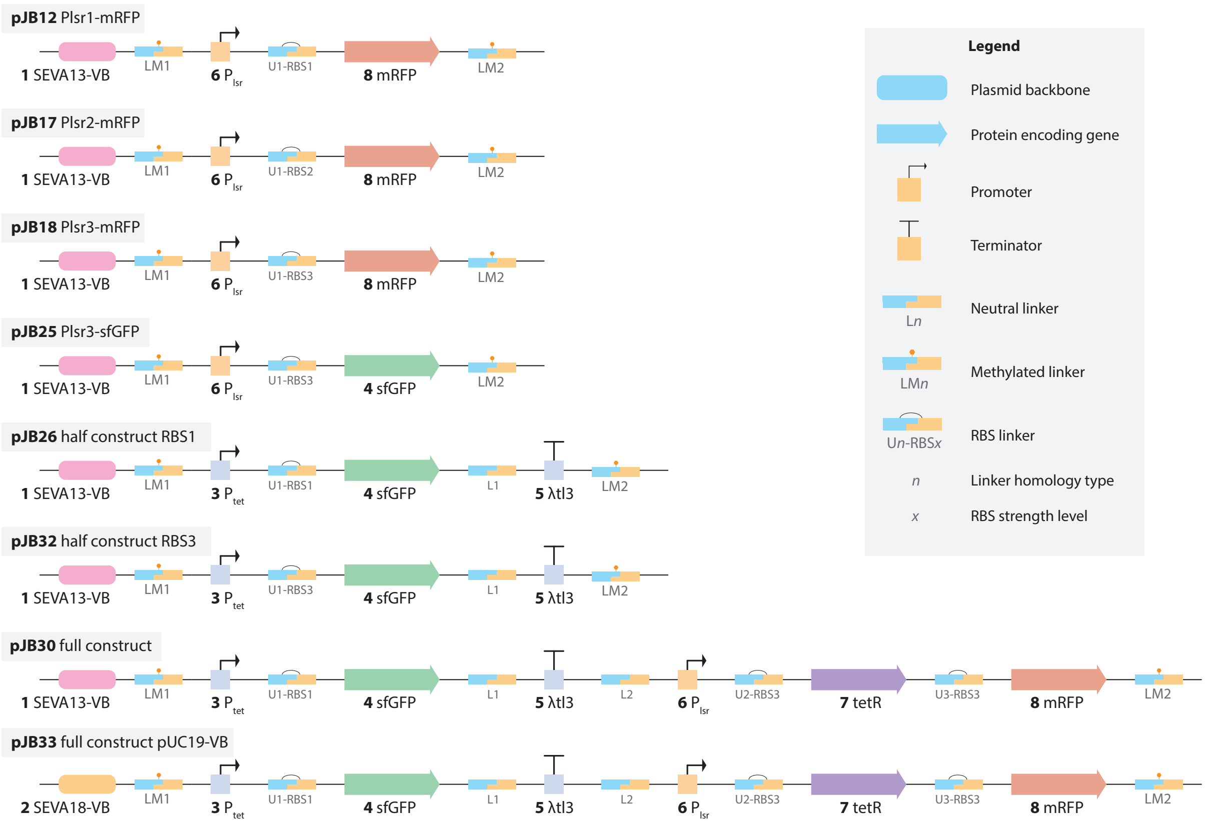
pJB12 Plsr1-mRFP
1 SEVA13-VB
LM1
6 Plsr
U1-RBS1
8 mRFP
LM2
pJB17 Plsr2-mRFP
1 SEVA13-VB
LM1
6 Plsr
U1-RBS2
8 mRFP
LM2
pJB18 Plsr3-mRFP
1 SEVA13-VB
LM1
6 Plsr
U1-RBS3
8 mRFP
LM2
pJB25 Plsr3-sfGFP
1 SEVA13-VB
LM1
6 Plsr
U1-RBS3
4 sfGFP
LM2
pJB26 half construct RBS1
1 SEVA13-VB
LM1
3 Ptet
U1-RBS1
4 sfGFP
L1
5 λtl3
LM2
pJB32 half construct RBS3
1 SEVA13-VB
LM1
3 Ptet
U1-RBS3
4 sfGFP
L1
5 λtl3
LM2
pJB30 full construct
1 SEVA13-VB
LM1
3 Ptet
U1-RBS1
4 sfGFP
L1
5 λtl3
L2
6 Plsr
U2-RBS3
7 tetR
U3-RBS3
8 mRFP
LM2
pJB33 full construct pUC19-VB
2 SEVA18-VB
LM1
3 Ptet
U1-RBS1
4 sfGFP
L1
5 λtl3
L2
6 Plsr
U2-RBS3
7 tetR
U3-RBS3
8 mRFP
LM2
Legend
Plasmid backbone
Protein encoding gene
Promoter
Terminator
Ln
Neutral linker
LMn
Methylated linker
Un-RBSx
RBS linker
n
Linker homology type
x
RBS strength level

Figure 5 | Overview of genetic constructs cloned in this study. The figure illustrates the order of the different parts from Table 2 and linkers. Note that the representation of the constructs in this figure is linear, opposed to the circular structure of the plasmids in their natural state.

sequencing. The reasoning for the design of each construct will be elaborated below in the relevant section.

3.3 Induction of ***P**_{lsr}*

It is crucial for the biosensor to be able to detect and respond to AI-2 via the P_{lsr} promoter. In order to optimize the expression from P_{lsr}, three test-constructs were assembled (pJB12, pJB17, pJB18). These constructs are identical with the exception of the RBS linker between P_{lsr} and *mRFP1,* which varies in the three RBS expression levels. The construct with the weakest RBS producing a readable signal significantly different from the control would be ideal, as this in theory would be least prone to leaky expression.

Three different strategies for induction of P_{lsr} were tested: (1) Induction by cell-free supernatant from AI-2-producing *E. coli* MC4100 strains growing exponentially, (2) induction by transforming MC4100 with plasmids containing test-constructs, and (3) induction using 'synthetic AI-2' 5-methyl-4-hydroxy-3-furanone (sAI2), which has been proposed to be effective form of the native AI-2 [60], [77]. All strategies were tested in both LB and M9 medium (see Section 2.2 for exact medium composition). M9 medium was included as it is a defined medium with almost no autofluorescence.

3.3.1 Strategy 1: Induction of P_{lsr} with supernatant from AI-2 producing cells

To test if P_{lsr} is induced by supernatant from AI-2-producing cells, cell-free supernatant from *E. coli MC4100* was added to the three test constructs as described in Section 2.4.1. This strain has both the genes responsible for AI-2 production (*luxS, pfs*) and genes for regulating AI-2 QS (*lsr* operon) according to the IMG database [78], [79]. Supernatant was extracted from MC4100 cultures in exponential growth phase ($OD_{600} \approx 0.7$-0.8) as this is where the extracellular concentration of AI-2 theoretically is highest (Figure 2). Controls received supernatant from exponentially growing *E. coli* DH5α which as previously described does not produce AI-2.

Figure 6 B-D includes red specific fluorescence measurements from testing the three test constructs, pJB12, pJB17 and pJB18. Here, it is apparent that the none of the test constructs are properly induced by supernatant from MC4100 when compared to the negative control (DH5α without plasmid). Not only does the specific fluorescence fluctuate notably, it is also very low (between 0 and 70 units) with no or very little increase over the course of the six

shown hours. There is, however, vague indications of an induction after six hours in Figure 6 D, where the specific fluorescence from pJB18 is slightly higher than the negative control. However, when comparing the induced pJB18 and the uninduced pJB18 (Figure 6 F), no differences in specific fluorescence were measured between these, revealing that any red fluorescence emitted due to the potential expression of mRFP1 from the construct has not been caused by an induction of P_{lsr}. No differences between test constructs and control were observed when using M9 medium instead of LB medium (Appendix 7.3).

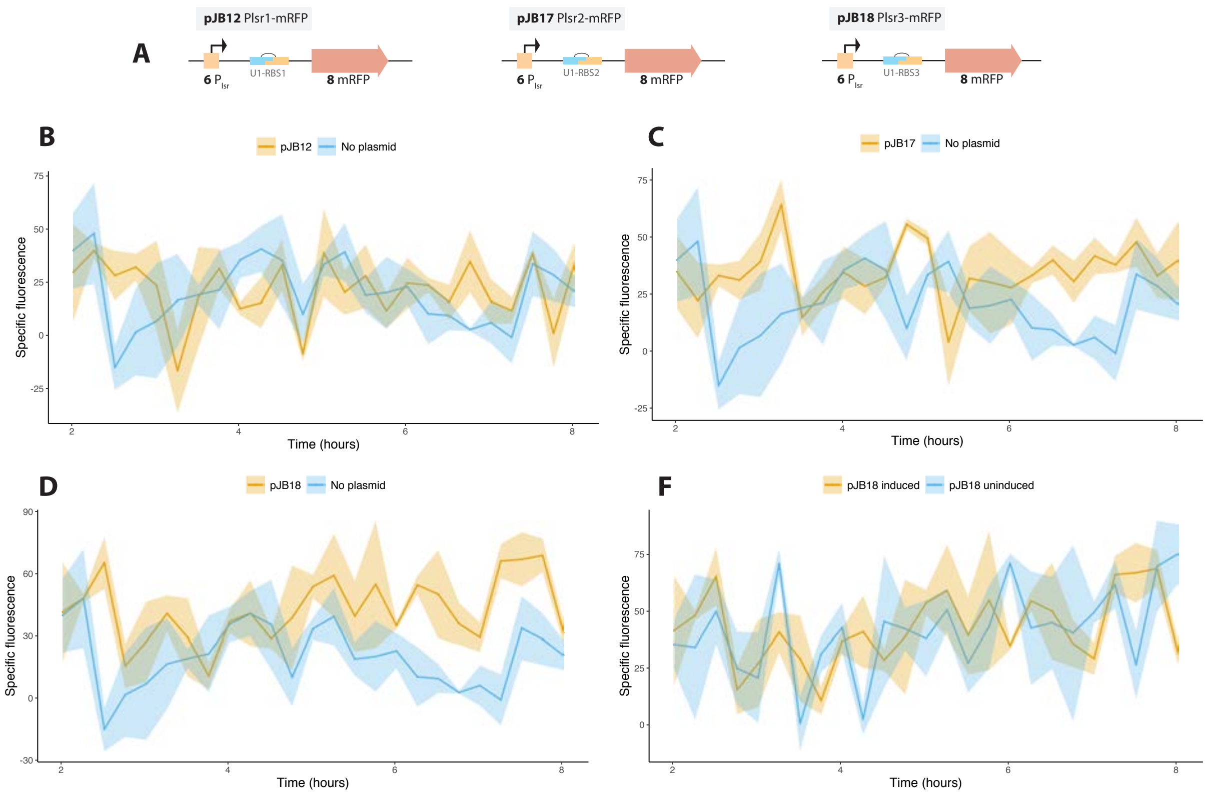

Figure 6 | Induction with MC4100 supernatant in LB medium. **(A)** Genetic overview of constructs tested in this experiment. **(B-F)** Test constructs in DH5α (pJB12, pJB17, pJB18, negative control without plasmid) were grown in culture tubes, and 80 µl culture were transferred upon reaching early exponential phase to a 96 well plate. Test constructs were supplied with 20 µl supernatant from *E. coli MC4100* in exponential growth phase, and controls (uninduced) were supplied with 20 uL LB medium. Fluorescence (excitation: 580 and emission: 615) and OD_{600} were monitored every 15 minutes for 8 hours. Graphs only depict 2-8 hours. Results are displayed as specific fluorescence (normalized with OD_{600} value and background fluorescence from medium subtracted). The displayed specific fluorescence values are the mean of three technical replicates, and the shaded area depicts the standard error of the mean.

3.3.2 Strategy 2: Induction of P_{lsr} by transformation of *E. coli* M4100 with sensor plasmid

To circumvent the potential problem of exogenous AI-2 not being transported into DH5α, *E. coli* MC4100 were transformed by electroporation with the test constructs. This strain produces AI-2, as described previously, and therefore, if the system works as intended, P_{lsr} should be induced, at least in the exponential growth phase. Furthermore, as MC4100 also carries the *lsr* operon, a biosensor with this chassis resembles the natural interaction between production, recognition and a potential inhibition of AI-2 QS (contrary to using DH5α with no AI-2 production as a chassis).

Figure 7 compares specific fluorescence from MC4100 containing pJB18, the test construct with the strong RBS linker, with MC4100 without plasmid in both LB medium and M9 glucose medium. Here, specific fluorescence levels are very low, just above and even below zero in the M9 medium, and it is apparent that there is no distinct difference between pJB18 and the control.

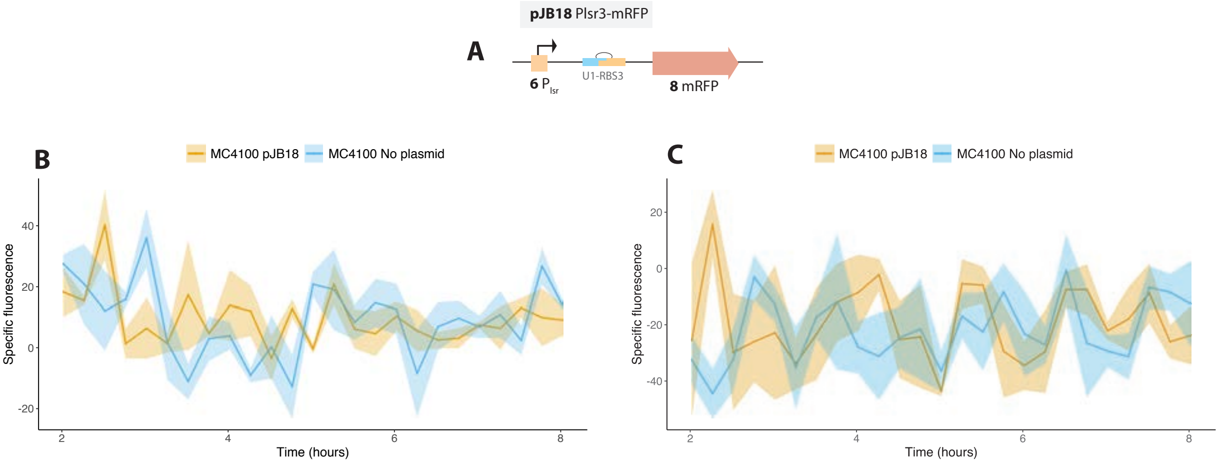

Figure 7 | Self-inducing pJB18 in *E. coli MC4100*. **(A)** Genetic overview of construct tested in this experiment. **(B-C)** The test construct in MC4100 and control (MC4100 without plasmid) were grown in culture tubes, and 100 µl culture were transferred upon reaching exponential phase to a 96 well plate. Fluorescence (excitation: 580 and emission: 615) and OD_{600} were monitored every 15 minutes for 8 hours. Graphs only depicts 2-8 hours. Results are displayed as specific fluorescence (normalized with OD_{600} value and background fluorescence from medium subtracted). The displayed specific fluorescence values are the mean of three technical replicates, and shaded area depict standard error of the mean. **(B)** Experiment conducted in LB medium. **(C)** Similar experiment conducted with M9 glucose medium instead of LB medium.

3.3.3 Strategy 3: Induction of P_{lsr} using a synthetic form of AI-2

The most controlled and precisely reproducible induction strategy would be to add known, precise amounts of an AI-2 QS inducer. Weiland-Bräuer *et al.* successfully induced P_{lsr} using sAI-2 (5-methyl-4-hydroxy-3-furanone). Here, they plated LB agar mixtures (0.8% agar) containing 5% (vol/vol) exponentially growing culture of the reporter strain and a final concentration of 50 mM sAI-2. In the present study, induction of P_{lsr} was tested with both 50 mM sAI-2 and 100 mM sAI-2 in liquid cultures.

Figure 8 B-D shows the attempts to induce the three test constructs using 50 mM sAI-2 in LB medium. The pattern here is very similar to the one observed using MC4100 supernatant (Section 3.3.1): The specific fluorescence from the test constructs are not higher than the

negative control (i.e. not induced), although there are vague indications of an induction with pJB18. However, the specific fluorescence measurements are unstable and very low, with levels going below zero. This depicted negative fluorescence is a result of normalization with cell density and the subtraction of red background fluorescence from sAI2. Also, comparing sAI-2-induced pJB18 and undinduced pJB18 indicates no distinct differences, meaning that the small amount of red fluorescence emitted by pJB18 has not been a result of an induction of P_{lsr}.

No improvements were observed when adding 100 mM sAI-2 (Appendix 7.4), or when growing cultures in M9 glucose medium (Appendix 7.5).

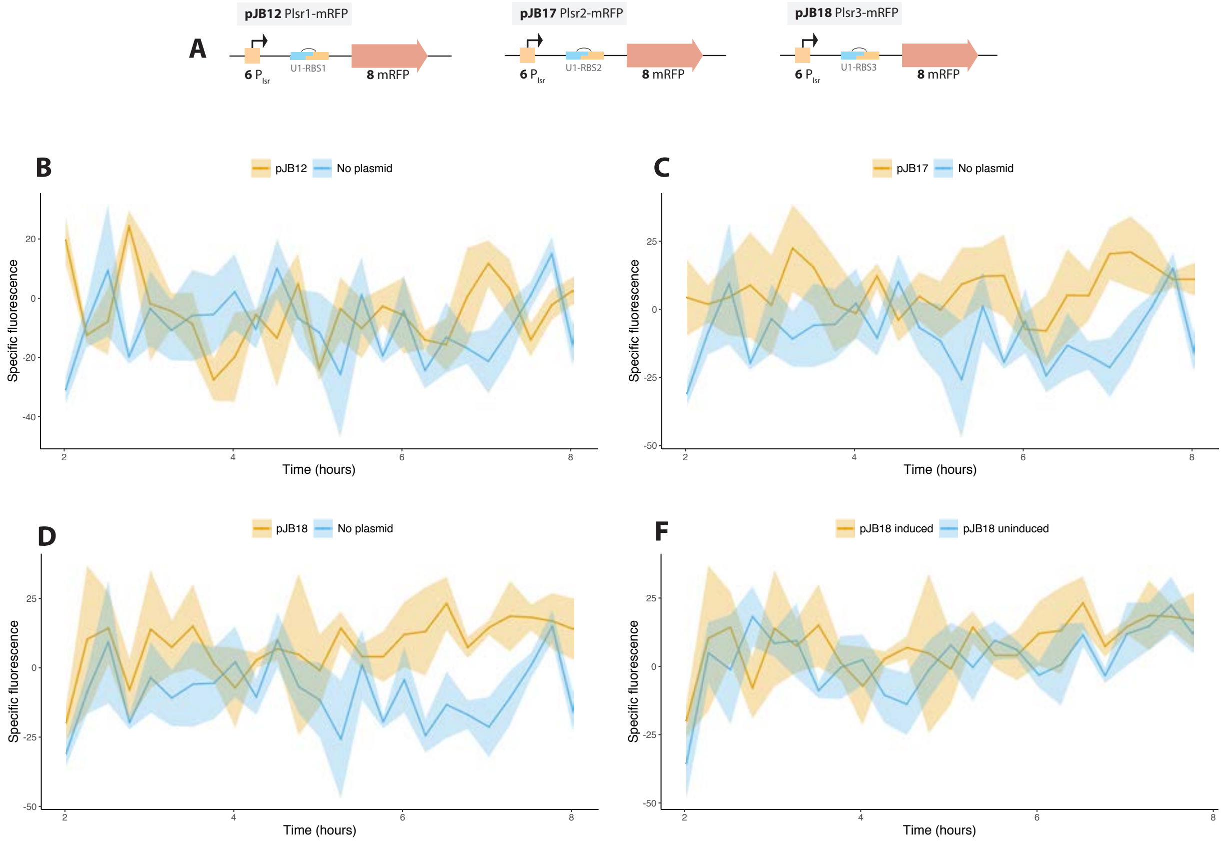

Figure 8 | Induction with 50 mM 5-methyl-4-hydroxy-3-furanone in LB medium. **(A)** Genetic overview of constructs tested in this experiment. **(B-F)** Test constructs in DH5α (pJB12, pJB17, pJB18, negative control without plasmid) were grown in culture tubes, and 90 µl culture were transferred upon reaching early exponential phase to a 96 well plate. Test constructs were supplied with 10 uL 5-methyl-4-hydroxy-3-furanone (sAI2) solution reaching a final concentration of 50 mM sAI2. Controls (uninduced) were supplied with H_2O. Fluorescence (excitation: 580 and emission: 615) and OD_{600} were monitored every 15 minutes for 8 hours. Graphs only depicts 2-8 hours. Results are displayed as specific fluorescence (normalized with OD_{600} value and background fluorescence from medium subtracted). The displayed specific fluorescence values are the mean of three technical replicates, and shaded area depict standard error of the mean.

3.3.4 Troubleshooting: Testing sfGFP as a reporter gene

Based on the results in Section 3.3.1-3.3.3, it appears that either the reporter gene, *mRFP*, does not generate enough fluorescence, or the P_{lsr} promoter is not induced properly.

Naturally, it could also be the case that both are not functioning as intended. To examine if the *mRFP1* reporter gene is the reason for the observed low specific fluorescence, a new construct, pJB25, was assembled. This contains the P_{lsr} promoter and a *sfGFP* reporter gene, linked together using the strongest RBS linker (RBS3).

Figure 9 B-C shows the specific green fluorescence emitted from pJB25 cultures induced with 50 mM sAI-2. Compared to when using *mRFP*, the *sfGFP* provides a more stable output with increasing values and a specific fluorescence of approximately 3000 units after eight hours. In Figure 9 B, it is apparent that pJB25 emits more fluorescence than the control after five hours, although, taking the error zones into account, the differences are not sizeable. Unlike with the mRFP-based test constructs, this fluorescence increases steadily with smaller fluctuations. However, as shown in Figure 9 C, there seems to be no difference between the induced pJB25 and the uninduced pJB25. It even look as if the uninduced culture emits slightly more green fluorescence than the induced culture. Hence, the increased fluorescence in pJB25 compared to the control with no plasmid is not caused by induction of P_{lsr}.

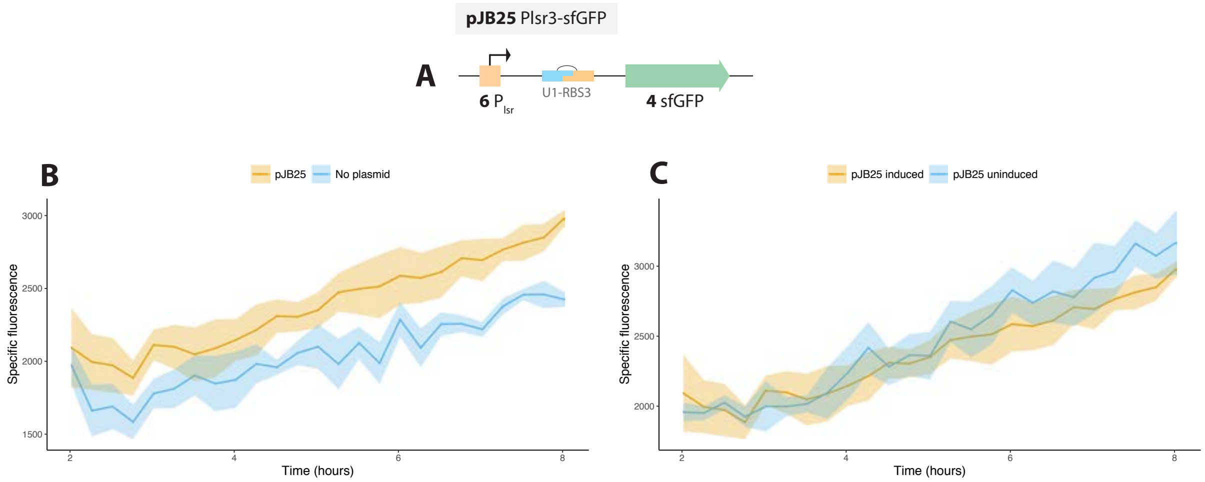

Figure 9 | Induction with 50 mM 5-methyl-4-hydroxy-3-furanone in LB medium. **(A)** Genetic overview of the construct tested in this experiment. **(B-C)** Test constructs in DH5α (pJB25, negative control without plasmid) were grown in culture tubes, and 90 µl culture were transferred upon reaching exponential phase to a 96 well plate. pJB25 were supplied with 10 uL 5-methyl-4-hydroxy-3-furanone (sAI2) solution reaching a final concentration of 50 mM sAI2. Controls (uninduced) were supplied with H_2O. Fluorescence (excitation: 480 and emission: 515) and OD_{600} were monitored every 15 minutes for 8 hours. Graphs only depict 2-8 hours. Results are displayed as specific fluorescence (normalized with OD_{600} value and background fluorescence from medium subtracted). The displayed specific fluorescence values are the mean of three technical replicates, and shaded area depict standard error of the mean.

3.3.5 Induction of P_{lsr} on LB-sAI2 plates

To mimic the biosensor assay used by Weiland-Bräuer *et al.*, pJB25 and pJB18 was tested in a similar-type LB agar plate-based assay [60]. This was done, as there could potentially be growth differences between cells in liquid medium and solid medium which could affect the way the cell takes up and interprets the sAI2. To test for this, the two test constructs pJB18

(P_{lsr}-*mRFP1*) and pJB25 (P_{lsr}-*sfGFP*) were spread evenly on LB agar plates with ampicillin and 50 mM sAI2 to form a thin mat of cells. Figure 10 shows both green and red fluorescent images of the test constructs after overnight incubation where a thin layer of cells were visible. Here, no visible fluorescence is emitted from either of the plates under both red and green fluorescent wavelengths, and this shows that P_{lsr} is not induced under these growth conditions. For comparison, an example of strong, green fluorescence can be seen in Appendix 7.6 where pJB32, which constitutively expresses sfGFP from P_{tet}, is grown similarly to pJB18 and pJB25.

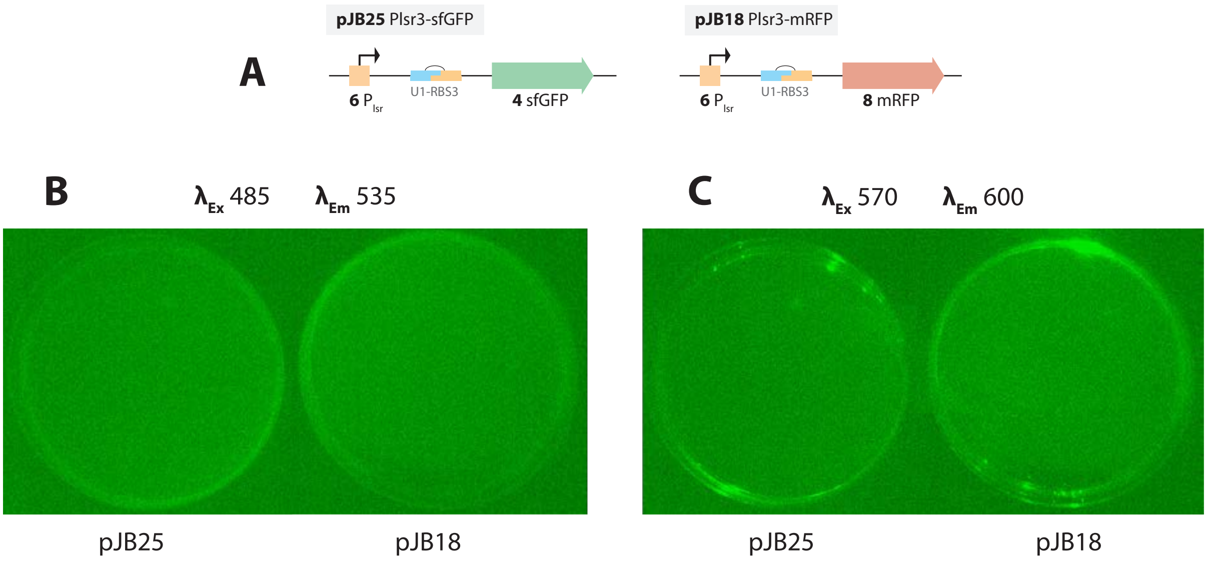

Figure 10 | P_{lsr} induction on LB agar plates containing 50 mM sAI-2. (A) Overview of the genetic construct in each strain tested. **(B)** Pictures of LB agar plates. Exponentially growing cultures of each strain were spread evenly on the plates in the evening and pictures were taken the following morning. LB agar plates contained ampicillin (100 µg/ml) to maintain plasmid stability.

3.4 Tuning the expression of *sfGFP* from P_{tet}

As described in Section 3.1, the composite part consisting of the first three genes of the biosensor (*Ptet-sfGFP- λtl3*) will generate a green fluorescent signal output when QS is inactive (i.e. quenched). To test if this functions as intended, pJB26 was assembled. This construct has a P_{tet} promoter linked to a *sfGFP* reporter gene with the weakest RBS linker (RBS1), followed by the *λtl3* terminator. Furthermore, pJB32, a construct with the same parts but with the strongest RBS linker (RBS3) between P_{tet} and *sfGFP* was assembled in order to verify the tuneability of the system. As the gene encoding the repressor of P_{tet}, *tetR,* is not present in any of the two constructs, P_{tet} should in theory function as a constitutive promoter.

Figure 11 B shows that the composite part works as intended, as the specific fluorescence generated by the construct is distinctively higher than the control. This is in spite of using the weakest RBS linker which results in a difference from the control by only a 1000 specific fluorescence units. In Figure 11 C, the picture is different with notably higher specific fluorescence from pJB32. This examplifies the tuneability of the BASIC system, as the substitution of a single linker sequence boosts the expression of sfGFP markedly: After eight hours, the specific flourescence of pJB32 is between five to six folds higher than that of pJB26.

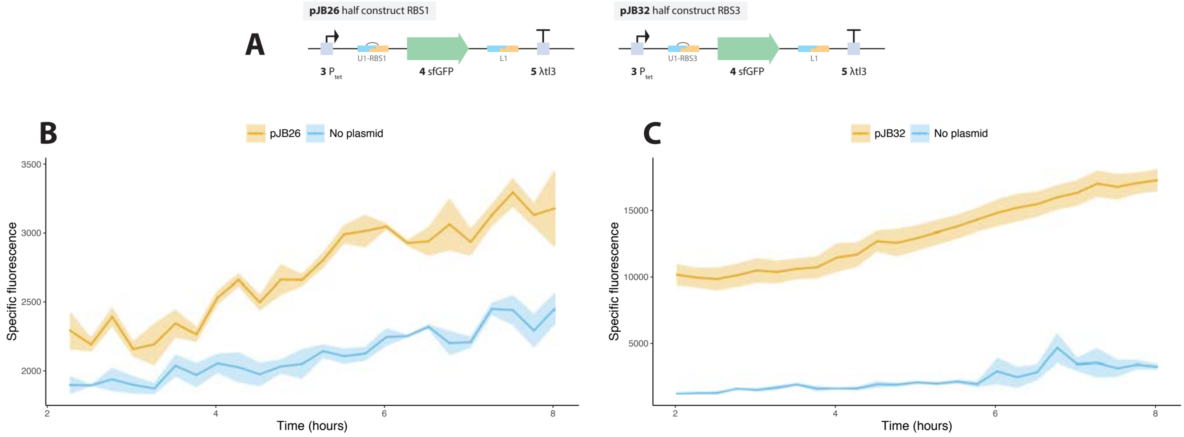

Figure 11 | Tuning the green signal output from *sfGFP*. **(A)** Genetic overview of the constructs tested in this experiment. **(B-C)** The test constructs and controls were grown in culture tubes, and 90 µl culture were transferred upon reaching early exponential phase to a 96 well plate and thereafter supplemented with 10 µl LB medium. Fluorescence (excitation: 480 and emission: 515) and OD_{600} were monitored every 15 minutes for 8 hours. Graphs only depict 2-8 hours. Results are displayed as specific fluorescence (normalized with OD_{600} value and background fluorescence from medium subtracted). The displayed specific fluorescence values are the mean of three technical replicates, and shaded area depict standard error

3.5 Simulating quorum quenching by artificially triggering the switch

The main idea of the genetic switch is to have two signal outputs: a green output for when QS in inactive and a red signal for when QS is active. When one signal is turned on, the other should be turned off. The above results show that the P_{lsr} promoter remain unaffected by the induction strategies, and there are indications of leaky expression of genes positioned downstream of P_{lsr} (see results in Figure 9).

If leaky expression is occurring through of P_{lsr}, *tetR* will be expressed and repress expression from P_{tet}, and, hence, the green signal output will be turned off. The repression happens when TetR binds to the two operator sequences in P_{tet} and blocks transcription. However, an addition of anhydrotetracycline (aTC) derepresses P_{tet} as aTC binds with high affinity to TetR, resulting in a conformational change rendering it unable to bind to the tetO regions [71], [74]. This opens up for two possibilities: Firstly, it is possible to simulate a scenario where QS is inactive (quenched) by adding aTC, as inhibition of TetR should have the same effect on P_{tet} as P_{lsr} being uninduced, and, ultimately, provide a green fluorescent signal. Secondly, if addition of aTC results in an increase in specific fluorescence, it would be a strong indicator that TetR is present, which likely would be caused by leaky expression through P_{lsr}.

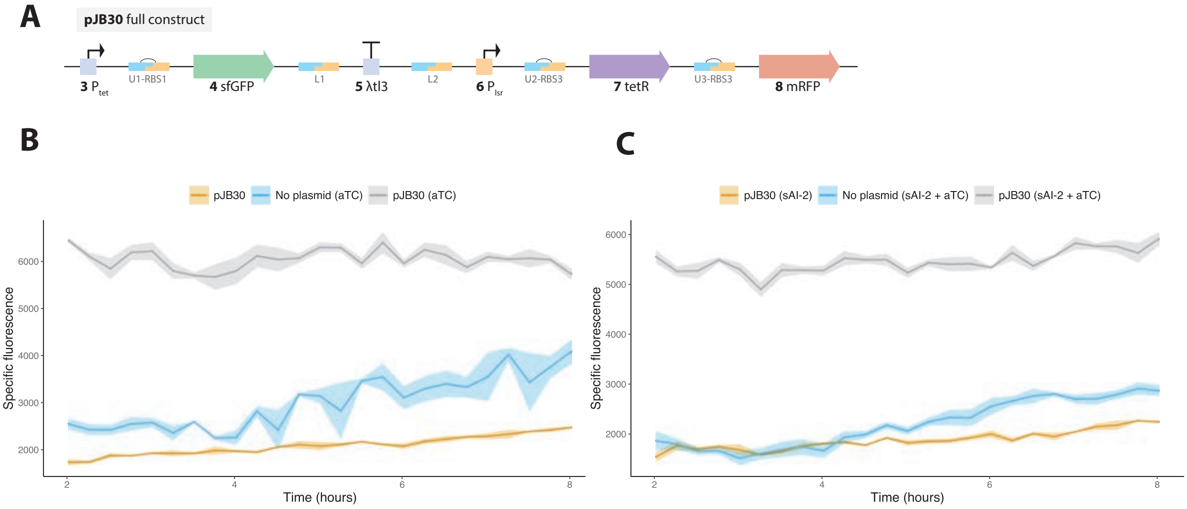

Figure 12 | Simulation of QQ: Artificially triggering the signal switch. **(A)** Genetic overview of the construct tested in this experiment. **(B-C)** The test constructs and controls were grown in culture tubes in LB and were transferred upon reaching early exponential phase to a 96 well plate. Thereafter, they were supplemented with either a final concentration of 100 mM 5-methyl-4-hydroxy-3-furanone (sAI2), both 100 mM sAI2 and 0.96 µM aTC, only 0.96 µM aTC or dH2O. Fluorescence (excitation: 480 and emission: 515) and OD_{600} were monitored every 15 minutes for 8 hours. Graphs only depicts 2-8 hours. Results are displayed as specific fluorescence (normalized with OD_{600} value and background fluorescence from medium subtracted). The displayed specific fluorescence values are the mean of three technical replicates, and shaded area depict standard error of the mean.

Figure 12 shows the specific fluorescence of the simulated QQ scenario. It is apparent that the specific fluorescence from pJB30 without aTC but both with sAI2 and without is low. Oddly, the specific fluorescence is even lower than the negative control strain without a plasmid. In contrast, the addition of aTC notably increases the specific fluorescence of pJB30, and it is obvious that sAI-2 does not affect the expression from P_{lsr} under these conditions. This large difference between the specific fluorescence measured in cultures with or without aTC (Figure 12 B) indicates that leaky expression of TetR is occurring. Furthermore, it shows the signal switch itself works, as the absence of TetR results in a stronger fluorescence response. Note that the linker between P_{tet} and *sfGFP* in pJB30 contains the weakest RBS (RBS1), and, thus, the signal output could be amplified greatly if this were interchanged with RBS3 as previously shown (Figure 11). The full biosensor construct was also cloned into a high copy number pUC-based vector backbone, generating pJB33, to examine if this would improve the output signal without changing the RBS linker. A similar pattern to the one was observed using pJB33, although the differences in specific fluorescence were smaller between cultures with or without aTC added (see Appendix 7.7).

3.6 Proof of concept biosensor

To assess if the genetic circuit is able to switch between signal outputs, a proof of concept (POC) plasmid was designed (Figure 13). The only difference from this circuit in this POC plasmid and the one in pJB30 is that the P_{lsr} promoter has been interchanged with the arabinose-inducible P_{BAD} promoter. Relying on the chromosomally expressed AraC of DH5a (*araC* is present as per [78]), P_{BAD}-mediated expression will be repressed in the absence of arabinose. P_{BAD} is also repressed in the presence of glucose [76]. Hence, the M9 glucose medium used in this study is not appropriate for this POC circuit, and another carbon source like glycerol should be utilized.

Growing cells with the POC plasmid in medium without arabinose or with glucose will simulate a quorum quenching scenario as P_{BAD} would be repressed and sfGFP would be expressed via the non-repressed P_{tet}. In contrary, medium with arabinose and without glucose would simulate a scenario where QS is active: Induction of P_{BAD} would drive expression of TetR and mRFP1 and repress P_{tet}. This relatively simple assay could establish whether or not the genetic circuit functions as intended. Furthermore, the possibility of transitioning from a QS-active state to a QS-quenched state could be assessed by adding glucose after induction of P_{BAD} has been confirmed by detecting red fluorescence from mRFP1.

An attempt was made to assemble this construct. However, when confirming the assembly by cPCR (Appendix 7.8), none of the eight colonies which were screened by cPCR contained a correctly sized insert (3325 bp, predicted *in silico*). All amplified inserts run in the gel had a size between 400 and 500 bp, and amplifying the P_{BAD} promoter *in silico* using the same primer set yields a product of 424 bp. Hence, the P_{BAD} was most likely not properly cut and released from its storage backbone, resulting in a failed assembly. Due to the limited time scope of this project, the assembly of this construct was not pursued.

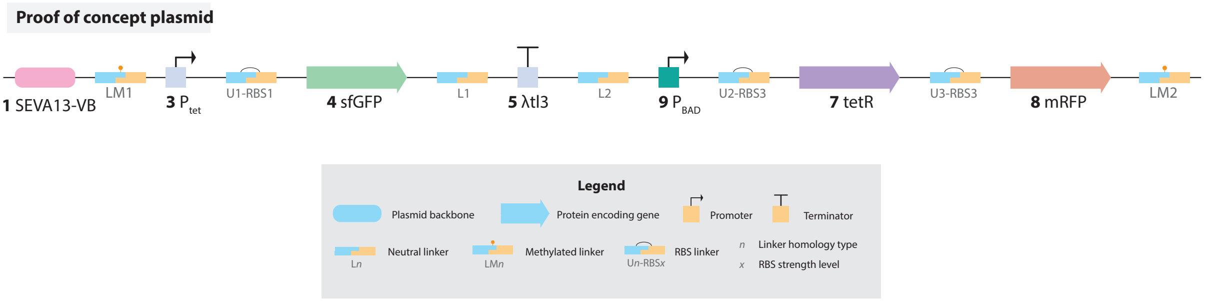
Proof of concept plasmid
1 SEVA13-VB
LM1
3 P tet
U1-RBS1
4 sfGFP
L1
5 λtl3
L2
9 P BAD
U2-RBS3
7 tetR
U3-RBS3
8 mRFP
LM2
Legend
Plasmid backbone
Protein encoding gene
Promoter
Terminator
Ln
Neutral linker
LMn
Methylated linker
Un-RBSx
RBS linker
n Linker homology type
x RBS strength level

Figure 13 | Genetic design of proof of concept circuit. Note that the representation of the construct in this figure is linear, opposed to the circular structure of the plasmid in their natural state.

4 Discussion

With the aim of designing a system for detection of QQ compounds, a cellular biosensor containing a plasmid-based circuit of six separate genetic parts was designed and constructed. By using the BASIC DNA Assembly System [61] to build a library of parts and to afterwards assemble these into several different constructs, a high degree of modularity and tuneability is achieved. The circuit employs a genetic switch, which should give a dual fluorescent output where only one output is turned on at a time. In more detail, a green fluorescent output should be visible in case of QQ, and a red fluorescent output should occur when QS is not quenched. In an attempt to simulate conditions where quorum sensing is quenched, the green fluorescent output works as intended. Also, this signal output is turned off in conditions where QS seems active. This is based on the assumption that leaky expression occurs through the QS-regulated promoter, P_{lsr}, which is unaffected by induction attempts. In contrast, the red fluorescent signal output does not seem to function. In this section, these findings will be discussed, and future prospects and possible improvements for each main element of the study will be proposed.

4.1 Second signal output decreases risk of false-positives

Reporter strains based on a single reporter gene fused to a QS-regulated promoter are not suitable for detection of QQ compounds. In this context, they are inherently prone to bias and false-positives, as argued by Defoirdt *et al.* in an opinion-article [80]. A 'QQ-detection event' using these reporters will be indicated by a decrease or absence of the QS-controlled phenotype. However, reporter phenotypes such as bioluminescence, β-galactosidase activity and fluorescent proteins are energy-costly and, thus, depend on the metabolic activity of the cell. Hence, compounds that are toxic to the cell but do not affect QS might be mistaken for a QQ compound. Furthermore, compounds can interfere with the reporter phenotype instead of its regulation (e.g. disrupt folding of GFP) [80]. To avoid these false-positives, control experiments verifying that compounds do not affect the reporter phenotype when unregulated by QS are needed. However, as shown by Defoirdt *et al*, many studies have not included such controls [80] despite being relatively straightforward. As described in Section 1.3.1, the suicide-based QQ biosensors (QSIS1-3) constructed by Rasmussen *et al*., and further developed by Weiland-Bräuer *et al*. to target quenching of AI-2 QS (based on QSIS1), compromise QS-controlled promoters fused to genes encoding lethal proteins (some variants include constitutively expressed reporter genes) [17], [60]. These setups avoid false-positive results from compounds affecting cellular growth and metabolism, as the biosensor only grows in the presence of a non-toxic QQ compound. Especially the QSIS1 biosensor has been employed in a wide range of studies for determination of QQ-activity [81]–[87].

As opposed to fusing a single reporter gene to a QS-controlled promoter, the dual signal of the pJB30 biosensor forms a more nuanced picture of the mechanisms occurring in the assay and decreases the risk of false-positives. If a compound with no QQ effects negatively affects cell metabolism to a degree where expression of fluorescent proteins are reduced greatly or even non-existing, both the positive (green fluorescent) or negative (red fluorescent) signal will in a similar fashion be reduced or even absent. Hence, the biosensor has an in-built control: at least one of the signal outputs should be of the same strength as in control assays without test-compounds. At the time of writing and of the writer's knowledge, a biosensor with a positive and negative signal output as in pJB30 has not been published before. However, some biosensors bear similarities: Although with a different structure in the genetic circuit compared to the present study, Bereza-Malcolm *et al.* also employed a dual-signal output using *gfp* and *mRFP1* to control for functionality and viability of a cadmium (Cd) detecting biosensor: In order to detect Cd, *cadR*, a Cd-dependent transcriptional regulator, and P_{cad}, a divergent operator which is inhibited by CadR in absence of Cd, were positioned upstream of *gfp* on a reporter plasmid. Furthermore, from the same plasmid, mRFP1 is expressed from a constitutive promoter. Hence, the output consists of a dual fluorescent output, where GFP is expressed in the presence of Cd. The constitutive expression of mRFP1 allows for controlling of proper biosensor functionality [88]

4.2 P_{lsr} remains unaffected by all three induction strategies

The results in Section 3.3 clearly show that none of the three induction strategies work as intended. Although induction with sAI-2 was, as mentioned, successfully used by Weiland-Bräuer *et al.*, and despite using the identical promoter region of the *lsr* operon [60], sAI-2 did not increase expression of either *mRFP1* or *sfGFP* in this study. In the mentioned study, the induced cells were grown on LB agar plates supplemented with sAI-2 instead of liquid cultures as in the present study. It is unknown whether or not this could play a pivotal role for induction of P_{lsr}. With regards to the induction strategies involving *E. coli* MC4100, these should theoretically be very viable as the strain has genes for both production and recognition of AI-2 molecules (Integrated Microbial Genomes (IMG) system [78]). MC4100 was for an example used as a positive control for AI-2 activity by Zan *et al*. Here, they measured AI-2 activity by induction of bioluminescence from the bioreporter *Vibro harveyi* TL-26 (unable to produce AI-2), and supernatant from MC4100 resulted in an approximately 27-fold change in bioluminescence compared to the negative control [89]. The same relative amount of supernatant was added to reporter strains as in this study.

The results in Figure 9 with pJB25 (*P_{lsr}-sfGFP*), and the fact that addition of aTC greatly increases expression from *P_{tet}* even in the absence of sAI-2, which implies presence of TetR (Figure 11), are both indicative of a leaky expression occurring through *P_{lsr}*. As expression from the promoter is controlled by LsrR, it is obviously crucial that the *lsrR* gene is present in the chromosome of the used chassis. Potentially, the expression of chromosomal *lsrR* could be faulty in the chassis used which could lead to lower levels of LsrR and weaker repression of *P_{lsr}*. Actually, the induction strategies relies on a functioning, native *lsr* operon, as LsrK is needed for phosphorylation of AI-2, and LsrACDB would increase uptake of AI-2. Also, as described in Section 1.1.2.3, the initial uptake of AI-2 happens via PTS-dependent transporters, which obviously is essential for induction strategy 1 and 3. The presence of an intact operon has not been verified as part of this work but could easily be verified by PCR and subsequent sequencing. However, as *P_{lsr}* was amplified (and sequence verified) from the same *E. coli* DH5α used as chassis for the biosensor and the test constructs, it is likely that especially the *lsr* operon is present.

4.2.1 Methods for induction of *P_{lsr}*

P_{lsr} has previously been induced using different methods, which potentially could be more suitable. In some studies, AI-2 has been synthesized *in vitro* in order to induce AI-2 QS: González *et al.* use purified LuxS and Pfs enzymes to synthesize AI-2 from *S*-adenosylhomocysteine, which they use to induce biofilm formation of *E. coli* [90]. Servinsky *et al.* and Tsao *et al*. follow the same *in vitro* synthesis method, and both induce an AI-2 regulated bioreporter via a signal amplification circuit (described later) [91], [92]. *In vitro* synthesis, when compared to supernatant from AI-2 producing cultures, has the advantage of being more precise and reproducible as you can add a known amount of AI-2.

As the AI-2 signal transduction process (phosphorylation of AI-2 and induction of *lsr* operon by removal of LsrR) is a relatively weak initiator of gene expression [91], scientists have in some studies amplified the signal through a two-step genetic circuit. Tsao *et al.* and Servinsky *et al.* both use two plasmids to augment the AI-2 signal: On one plasmid, the expression of the bacteriophage T7 polymerase (T7RPol) is controlled by P_{lsr}. The second plasmid expresses the gene of interest, either *dsRed* (Servinsky *et al.*) or *gfp, cat or lacZ* (Tsao *et al.*) under the control of a T7 promoter (*pT7*). The T7RPol strongly induces expression from *pT7* and thereby amplifies the AI-2 mediated expression [91], [92].

A different method for induction of P_{lsr} is to engineer 'supplier cells' by overexpressing *pfs* and *luxS* on a plasmid under control of an inducible promoter. Quan *et al.* used the expression vector pTrcHisB (IPTG inducible) to overexpress *pfs* and *luxS* and managed to induce expression of GFP under the control of P_{lsr} [93].

Another strategy could be to increase the chances of AI-2 detection. To increase the sensitivity of an AI-2-detecting biosensor, Stephens *et al*. overexpressed both LsrACDB and LsrK, which increases AI-2 uptake rate and phosphorylation of AI-2, respectively [94]. Furthermore, they deleted *lsrFG* from the chassis chromosome to prevent degradation of imported AI-2. These modifications resulted in a lower AI-2 detection level and increased reporter protein expression. However, this biosensor was created for the purpose of detecting AI-2 and not for inhibitors of AI-2. In the context of the present study, one could imagine that too many modifications of the genes responsible for AI-2 recognition and processing could result in a system, which does not resemble the natural AI-2 QS system and fails to detect actual QQ compounds.

Nevertheless, in future investigations, a positive control for verification of induction with AI-2 should ideally be included. The luminescent bioreporter, *V. harveyi* TL26, mentioned in Section 4.2, could be a potential candidate for this [95].

4.2.2 Different versions of P_{lsr} have previously been used successfully

As described in Section 1.1.2.4, P_{lsr} encompasses the regulatory region of the divergently transcribed *lsr* operon. In multiple studies, this region has been isolated and utilized for detection of AI-2 for several purposes. However, different lengths of P_{lsr} has been isolated, which in theory could affect the transcription efficiency from this promoter region. This study used the same primer binding sites as Weiland-Bräuer *et al.*, amplifying the exact same version of P_{lsr}. As shown in Figure 14, other scientists have generated either longer or shorter P_{lsr} with some overlapping into both *lsrR* and *lsrA* (according to this annotation). However, Tsao *et al.* has only amplified the exact region between *lsrR* and *lsrA* and fused this to a gene encoding T7 polymerase to generate pCT6. This plasmid has afterwards been used in a wide range of studies involving detection of AI-2 [42], [54], [55], [91], [94], [96]–[98], which indicates that this version of the *lsr* promoter functions, and, for future work on this biosensor, this promoter could be adapted. It is also noteworthy that these studies have amplified the AI-2 signal by the T7 expression system, as described in the previous section.

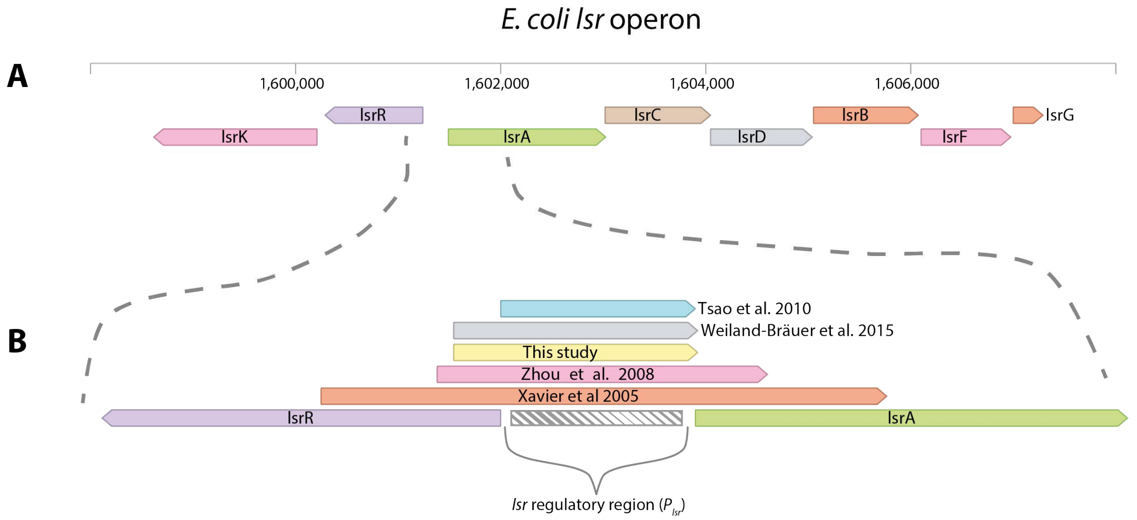

Figure 14 | Lengths of the lsr (P_{lsr}) regulatory region of selected studies. (A) Overview of *E. coli lsr* operon. **(B)** The genomic area around the *lsr* regulatory region (P_{lsr}) is singled out and an overview is shown of the different regions used by Tsao *et al.* [92], Weiland-Bräuer *et al.* [60], this study, Zhou *et al.* [99] and Xavier *et al.* [100]. Sequence and annotations were retrieved from Benchling (2021), https://benchling.com, and graphical elements for explanations are subsequently added.

4.3 mRFP1 provides little or no fluorescence

The specific fluorescence levels from mRFP1 seen in this study are insufficiently low, especially compared to those of sfGFP. If it is assumed that leaky expression is occurring through P_{lsr} constitutively, it is fair to conclude that *mRFP1* does not function properly as a reporter gene under the given circumstances, and that *sfGFP* seems far more ideal. This is to a higher degree more likely due to the brightness of each protein than to its maturation time. Balleza *et al*. compared *in vivo* maturation time in *E. coli* MG1655 of several fluorescent proteins. Here, they found that the maturation times of mRFP1 and sfGFP was 51.4 ± 4.0 and 39.1 ± 4.7 minutes, respectively (at this time point, 90% of each protein had matured) [101]. Given that the experiments runs for 8 hours, a notable amount of mRFP1 proteins should have had time to mature. Albeit expressed *in vitro* using the PUREsystem [102] and therefore likely different from expression in this study, Lentini *et al.* compared the fluorescence intensity for a wide range of fluorescent proteins, and they found that the ratio of fluorescence intensity from sfGFP to mRFP1 was 115.1 ± 6.9 [103]. Hence, there is a remarkable difference in fluorescence intensity from the two proteins. In the present study's test assays, the same plate-reader settings for gain was used for both red and green fluorescence measurement, and this could be a reason as to why the red fluorescence measurements fluctuate and appears absent. Furthermore, placing *mRFP1* under the control of a well-known inducible promoter and measuring fluorescence under the same assay conditions would determine if *mRFP1* is a suitable reporter gene.

Another possible reason as to why the fluorescence from mRFP1 is almost non-existing could be due to unintended mRNA folding: To initiate translation of *mRFP1*-mRNA, the RBS upstream of the 5'-UTR of *mRFP1* has to be freely accessible for the 16S rRNA of the small ribosomal subunit to bind and recruit other ribosomal subunits [104]. However, potential secondary structures occurring between the RBS of *mRFP1* and other mRNA can lead to reduced ribosome binding kinetics, and, hence, reduced expression. This was observed with DsRed-Express, a maturation-optimized variant of the predecessor of mRFP1, DsRed. Here, no fluorescence was recorded despite using a strong consensus RBS of *E. coli* in a P_{BAD}-induced expression vector. By changing seven bases (one amino acid change) of DsRed-Express to where high complementarity and secondary structures with the RBS were predicted, Pfleger *et al.* created $\mathrm{RFP}_{\mathrm{EC}}$ which were highly fluorescent in the P_{BAD}-vector with the same RBS [105]. Investigating the potential secondary structures relating to P_{lsr} and *mRFP1* in this study should be prioritized in future work.

There is a possibility that the two MC4100-based induction strategies work, but since the mRFP1 does not provide a clear signal, the induction may go unnoticed. Testing pJB25 (P_{lsr}-*sfGFP*) with either MC4100 supernatant or by transforming MC4100 with pJB25 could disclose whether or not these induction strategies can induce P_{lsr}.

Lentini *et al.* also found the ratio of fluorescence intensity between sfGFP and mCherry to be 49.9 ± 2.4, and as mCherry is more photostable than mRFP1 [106], changing mRFP1 with mCherry in this study's biosensor construct could improve its red fluorescent output. Other red fluorescent proteins are even brighter than mCherry: tdTomato [107], mRuby3 [108] and tdKatushka2 [109], [110] although these have longer maturation times than mCherry. Today, a wide range of red fluorescent proteins has been published [111] to choose from, and, in future, finding a well-functioning reporter gene is crucial for this biosensor.

4.4 One module of the genetic switch functions under a quorum quenching simulation

One state of the genetic switch, namely the state where QS is quenched with a green fluorescent output, seems to function. More precisely, sfGFP is expressed when TetR is blocked by aTC, and sfGFP is repressed when TetR is not blocked by aTC. Here, aTC resembles a QQ compound, although it interferes with TetR instead of AI-2-related processes. Further investigations into why the specific fluorescence of pJB30 with aTC added remains static and not increasing is needed. A possible explanation could be that aTC, although less toxic than the antibiotic tetracycline, possess some toxic properties [112], and pJB30 could be inhibited by the 450 ng/uL aTC used in the QQ-simulation assay. In a study by Dong *et al.*, they observed significant growth inhibition in *Clostridium acetobutylicum* when aTC concentrations exceeded 200 ng/mL (grown anaerobically in RCM medium, a rich medium optimal for cultivating *Clostridium*) [113]. Hence, in future work, the optimal aTC concentrations for this P_{tet}-TetR system and assay conditions which does not inhibit growth should be identified.

The green fluorescent signal is strong despite employing the weakest RBS linker, and this signal could easily be intensified by switching to a stronger RBS linker. The other state of the genetic switch, the 'QS-active' state with a red fluorescent output, only functioned in terms of leaky expression of TetR. Hence, further optimization is needed, and being able to induce P_{lsr}, let alone reduce leaky expression, is essential for this genetic switch to serve its purpose.

Tight regulation is crucial in order to get a clear signal output from the genetic switch, and this is also why the P_{tet}-*tetR* system was chosen. TetR binds efficiently with high specificity to the *tetO* sites of P_{tet} [74]. This is because, in the natural context of tetracycline resistance, overproduction of TetA, the tetracycline resistance protein, which is regulated by TetR, has been shown to cause large bacterial fitness reductions [74], [114]. To get an even clearer signal and to be able to detect a shift from one state to another, the turnover rate of TetR (and possibly the fluorescent proteins) should be increased: If shifting from QS-active to QS-quenched, TetR will remain active in the cytoplasm and continue to repress P_{tet} after induction of P_{lsr} has ceased. Hence, a possible QQ detection event would go unnoticed. A solution is to attach degradation tags to the proteins, which need a higher turnover rate. The most established method employs ssrA tags. These are ~11 amino acid peptide tags fused to the protein of interest, and they are recognized by ClpXP and ClpAP host proteases which target the attached protein for destruction [115], [116]. Furthermore, the degradation rate can be tuned by the identity of the c-terminal residues of the degradation tag [117]. Using either the LAA or LVA ssrA-tags (named after the last three amino acids of the tag), Purcell *et al* managed to engineer LacI repressors with half-lives in *E. coli* of just 8 and 13 minutes at 37 °C, respectively [116].

Such degradation tags were used in one of the earliest synthetic biology devices, made by Elowitz and Leibler in 2000, when constructing a synthetic oscillatory network consisting of three pairs of promoters and repressors. Here, the first promoter in the 'cascade' drives expression of the second promoters repressor and so forth [115]. These were assembled in the following order to construct the 'repressilator' (■ denotes a terminator sequence): P_{lac01}-*tetR* ■ λP_R-*lacI* ■ P_{tet01}- λ *cI*. Along with the repressilator, *E. coli* was transformed with a reporter plasmid with P_{tet01}-*gfp*. On a single-cell level, oscillations in GFP fluorescence were observed after induction with IPTG (which interferes with the LacI repression). To achieve these oscillations, different ssrA-tags were inserted at the 3' end of all repressors and *gfp* sequences, meaning that repressors and GFP had a half-life of less than 10 and 45 minutes, respectively. Temporal oscillations of GFP fluorescence of about 150 minutes were observed. Although oscillations are not expected in the genetic circuit of the present study, the same ability to shift in fluorescence as with the repressilator is a desired trait. This is, however, most relevant when employing the genetic circuit in a self-inducing strain with intact QS machinery (*lsr* operon and *luxS* gene in this case), as one would expect changes in the concentration of QS molecules in different growth phases.

4.4.1 Considerations on the proof of concept circuit

The proposed POC circuit in Figure 13 would serve as a good model circuit for testing, tuning and improving the genetic switch. However, the exact proposed POC circuit possibly needs modification itself as it relies on the chromosomal expression of AraC, the transcriptional regulator of P_{BAD}. As stated by R. Schleif, wild-type *in vivo* levels of AraC only needs a small excess over the number of regulatory binding sites on the chromosome [118]. Although the POC circuit is stored in a medium copy number plasmid which naturally lowers the need for AraC as compared to a high copy number plasmid, a plasmid-encoded AraC for the regulation of P_{BAD} could be necessary. Hence, inserting *araC* and an adjacent promoter on the plasmid with the POC circuit could be a future improvement. This promoter could ideally be the native *araC* promoter, P_c [119], or, for more controllability, an inducible promoter like T7. In the presence of arabinose, AraC functions as a transcription activator and promotes transcription from P_{BAD} [119], and therefore higher levels of AraC would likely ensure tight arabinose-dependent regulation [120].

4.5 Modularity via BASIC and alternative cloning strategy

As shown with the cloning performed in this study, the BASIC system is highly modular and allows for tuneability. An example of this is the considerable increase of green fluorescence shown in Figure 11 as a result of changing a single linker sequence, or the substitution of vector backbone (from SEVA13 to SEVA18) in the biosensor construct. A big part of the work conducted in this study was to establish the BASIC system and a library of genetic parts, and, from a methodical point of view, the inherent modularity of this system could have been utilized better with an alternative cloning strategy.

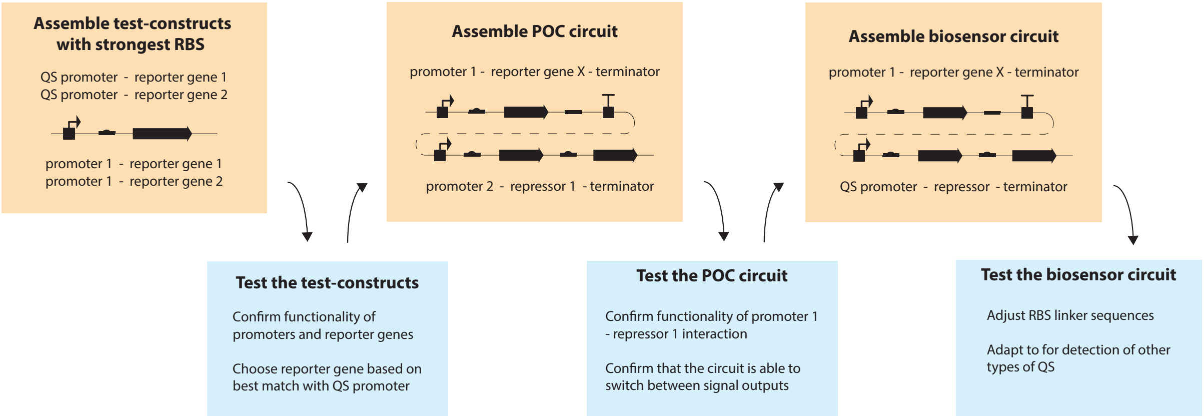
Assemble test-constructs with strongest RBS
QS promoter - reporter gene 1
QS promoter - reporter gene 2
promoter 1 - reporter gene 1
promoter 1 - reporter gene 2
Assemble POC circuit
promoter 1 - reporter gene X - terminator
promoter 2 - repressor 1 - terminator
Assemble biosensor circuit
promoter 1 - reporter gene X - terminator
QS promoter - repressor - terminator
Test the test-constructs
Confirm functionality of promoters and reporter genes
Choose reporter gene based on best match with QS promoter
Test the POC circuit
Confirm functionality of promoter 1 - repressor 1 interaction
Confirm that the circuit is able to switch between signal outputs
Test the biosensor circuit
Adjust RBS linker sequences
Adapt to for detection of other types of QS

Figure 15 | Proposed alternative cloning strategy. Abbreviations: RBS, ribosomal binding site. QS, quorum sensing. POC, proof of concept.

In the present study, the biosensor plasmid (pJB30) was assembled in parallel with the first three test-constructs which consists of P_{lsr}-*mRFP1* and a variety of RBS linkers (pJB12, pJB17, pJB18). However, both P_{lsr} and *mRFP1* appeared not be functioning as intended. Using these exact parts in the full biosensor plasmid could have been avoided with a cloning approach which divides the cloning into smaller steps. An alternative cloning strategy has been outlined in Figure 15. Here, the first step is to assemble short test-constructs of promoter and reporter genes to verify that the parts work as intended under the given assay circumstances. Furthermore, this would allow to assess which reporter gene is the best match with the QS promoter. In this study, P_{lsr} was used in combination with *mRFP1*, and because P_{lsr} is a weak initiator of gene expression [91], and *mRFP1* exhibit low brightness (Section 4.3), this was likely a poor match even if P_{lsr} had worked as intended. The next step is to assemble a proof of concept circuit where a known, inducible promoter is employed on the position of P_{lsr}. This would be done to assess if the genetic switch works, or, more specifically, how well the repressor represses its cognate promoter and whether or not the repressor is leaky expressed. Thirdly, the final biosensor construct should be assembled. Subsequently, the RBS linker sequences can be adjusted to finetune expression of e.g. repressor or reporter genes.

4.6 Optimization and future prospects

Several suggestions for improvements of the genetic circuit that constitutes the pJB30 biosensor has been covered. These can be divided into elements that are essential for the biosensor to function and possible optimizations, which can improve biosensor. The essential elements should be prioritized in the forthcoming future work.

A fundamental element of the biosensor which needs to function is the sensing entity. In order to detect QQ compounds, the P_{lsr} promoter should be able to detect AI-2 molecules in the first places. Several solutions have been suggested: Other induction strategies like *in vitro* synthesis of AI-2, supplier cells engineered to overproduce and export AI-2, an amplification of P_{lsr} induction using the T7 expression system, or testing other P_{lsr} lengths. Furthermore, a control strain or construct for AI-2 induction is needed for future QQ assays.

Another essential element for a biosensor with two signal outputs is to have two functioning reporter genes. Hence, either the correct conditions for *mRFP1* to function adequately should be identified. However, it may be more straightforward to change *mRFP1* with a stronger, more bright equivalent like *mCherry* or another reporter gene with similar excitation and emission properties (at least opposite of those of *sfGFP*).

A possible optimization is to engineer the repressor (and perhaps the reporter proteins) to have shorter half-lives in order to provide contemporary signals and to reveal shifts between the states of the genetic switch. This could be done by fusing degradation tags to the proteins expressed in the circuit. In addition, to increase sensitivity towards AI-2, the chromosomal genes encoding AI-2 degrading enzymes, *lsrFG*, could be deleted (e.g. by recombination-mediated knock out [73]).

As a more general optimization, construction of a proof of concept circuit with a tightly regulated and inducible promoter instead of the P_{lsr} promoter would serve not only as a model circuit for testing new changes of the circuit but also as a both positive and negative control for fluorescence in future assays.

5 Concluding remarks

In overall terms, a genetic circuit with a high degree of modularity and tuneability were designed and constructed, and this was employed in *E. coli* DH5α to generate a cell-based biosensor for detection of compounds with AI-2-quenching properties. However, only one of the two modules of the biosensor proved to be functioning as intended. The AI-2-sensing module consisting of P_{lsr}, *tetR* and *mRFP1*, which is expressed when QS is active, were likely non-functional due to leaky expression through P_{lsr} and lack of fluorescence from mRFP1. The other module consisting of P_{tet}, *sfGFP* and *λtl3* proved to function as intended, and the tuneability of expression of *sfGFP* was exemplified by the straightforward substitution of a small linker sequence. Furthermore, a simulation of QQ by addition of aTC which relieves TetR repression showed that the circuit is able to shift from one state to another.

Further research is needed into the AI-2-sensing module with special emphasis on regulation of P_{lsr} and the fluorescent signal expressed from this promoter.

6 References

[1] Y. H. Li and X. Tian, “Quorum sensing and bacterial social interactions in biofilms,” *Sensors*, vol. 12, no. 3. Multidisciplinary Digital Publishing Institute (MDPI), pp. 2519–2538, Mar. 2012, doi: 10.3390/s120302519.

[2] M. E. Davey and G. A. O’toole, “Microbial Biofilms: from Ecology to Molecular Genetics,” *Microbiol. Mol. Biol. Rev.*, vol. 64, no. 4, pp. 847–867, Dec. 2000, doi: 10.1128/mmbr.64.4.847-867.2000.

[3] H.-C. Flemming and J. Wingender, “The biofilm matrix,” *Nat. Publ. Gr.*, 2010, doi: 10.1038/nrmicro2415.

[4] C. M. Waters and B. L. Bassler, “Quorum Sensing: Cell-to-Cell Communication in Bacteria,” 2005, doi: 10.1146/annurev.cellbio.21.012704.131001.

[5] M. B. Miller and B. L. Bassler, “Quorum Sensing in Bacteria,” *Annu. Rev. Microbiol.*, vol. 55, no. 1, pp. 165–199, Oct. 2001, doi: 10.1146/annurev.micro.55.1.165.

[6] C. Fei, M. A. Ochsenkühn, A. A. Shibl, A. Isaac, C. Wang, and S. A. Amin, “Quorum sensing regulates ‘swim-or-stick’ lifestyle in the phycosphere,” *Environ. Microbiol.*, vol. 22, no. 11, pp. 4761–4778, Nov. 2020, doi: 10.1111/1462-2920.15228.

[7] K. Bivar Xavier, “Bacterial interspecies quorum sensing in the mammalian gut microbiota,” *Comptes Rendus - Biol.*, vol. 341, no. 5, pp. 297–299, 2018, doi: 10.1016/j.crvi.2018.03.006.

[8] P. Belda-Ferre *et al.*, “The oral metagenome in health and disease microbe-microbe and microbe-host interactions,” *ISME J.*, vol. 6, pp. 46–56, 2012, doi: 10.1038/ismej.2011.85.

[9] A. Schikora, S. T. Schenk, and A. Hartmann, “Beneficial effects of bacteria-plant communication based on quorum sensing molecules of the N-acyl homoserine lactone group,” *Plant Molecular Biology*, vol. 90, no. 6. pp. 605–612, 2016, doi: 10.1007/s11103-016-0457-8.

[10] M. Hadla and M. A. Halabi, “Effect of Quorum Sensing,” in *Comprehensive Analytical Chemistry*, vol. 81, Elsevier B.V., 2018, pp. 95–116.

[11] M. Zucca and D. Savoia, “The post-antibiotic era: Promising developments in the therapy of infectious diseases,” *Int. J. Biomed. Sci.*, vol. 6, no. 2, pp. 77–86, 2010.

[12] WHO World Health Organization, “Antibiotic resistance,” 2020. https://www.who.int/news-room/fact-sheets/detail/antibiotic-resistance (accessed Oct. 27, 2021).

[13] J. Bryan-Wilson, “No time to wait: Securing the Future From Drug-Resistant Infections,” *Artforum Int.*, vol. 54, no. 10, pp. 113–114, 2016.

[14] M. Guo, S. Gamby, Y. Zheng, and H. O. Sintim, “Small molecule inhibitors of AI-2 signaling in bacteria: State-of-the-art and future perspectives for anti-quorum sensing agents,” *Int. J. Mol. Sci.*, vol. 14, no. 9, pp. 17694–17728, 2013, doi: 10.3390/ijms140917694.

[15] X. Zhao, Z. Yu, and T. Ding, “Quorum-sensing regulation of antimicrobial resistance in bacteria,” *Microorganisms*, vol. 8, no. 3, pp. 1–21, 2020, doi: 10.3390/microorganisms8030425.

[16] S. Scutera, M. Zucca, and D. Savoia, “Novel approaches for the design and discovery of quorum-sensing inhibitors,” *Expert Opin. Drug Discov.*, vol. 9, no. 4, pp. 353–366, 2014, doi:

10.1517/17460441.2014.894974.

[17] T. B. Rasmussen *et al.*, “Screening for quorum-sensing inhibitors (QSI) by use of a novel genetic system, the QSI selector,” *J. Bacteriol.*, vol. 187, no. 5, pp. 1799–1814, 2005, doi: 10.1128/JB.187.5.1799-1814.2005.

[18] S. Mukherjee and B. L. Bassler, “Bacterial quorum sensing in complex and dynamically changing environments,” *Nat. Rev. Microbiol.*, vol. 17, no. 6, pp. 371–382, 2019, doi: 10.1038/s41579-019-0186-5.

[19] A. M. Folcik *et al.*, “Quorum Sensing Behavior in the Model Unicellular Eukaryote Chlamydomonas reinhardtii,” *iScience*, vol. 23, no. 11, p. 101714, Nov. 2020, doi: 10.1016/j.isci.2020.101714.

[20] C. Van Delden and B. H. Iglewski, “Cell-to-cell signaling and Pseudomonas aeruginosa infections,” *Emerg. Infect. Dis.*, vol. 4, no. 4, pp. 551–560, 1998, doi: 10.3201/eid0404.980405.

[21] B. K. Hammer and B. L. Bassler, “Quorum sensing controls biofilm formation in Vibrio cholerae,” *Mol. Microbiol.*, vol. 50, no. 1, pp. 101–104, 2003, doi: 10.1046/j.1365-2958.2003.03688.x.

[22] A. Clinton and K. P. Rumbaugh, “Interspecies and Interkingdom Signaling via Quorum Signals,” *Isr. J. Chem.*, vol. 56, no. 5, pp. 265–272, 2016, doi: 10.1002/ijch.201400132.

[23] C. D. Sifri, “Quorum sensing: Bacteria talk sense,” *Clin. Infect. Dis.*, vol. 47, no. 8, pp. 1070–1076, 2008, doi: 10.1086/592072.

[24] S. L. McKnight, B. H. Iglewski, and E. C. Pesci, “The Pseudomonas quinolone signal regulates rhl quorum sensing in Pseudomonas aeruginosa,” *J. Bacteriol.*, vol. 182, no. 10, pp. 2702–2708, 2000, doi: 10.1128/JB.182.10.2702-2708.2000.

[25] Y. Deng, J. Wu, F. Tao, and L. H. Zhang, “Listening to a new language: DSF-based quorum sensing in gram-negative bacteria,” *Chem. Rev.*, vol. 111, no. 1, pp. 160–179, 2011, doi: 10.1021/cr100354f.

[26] C. S. Kim *et al.*, “Characterization of Autoinducer-3 Structure and Biosynthesis in E. coli,” *ACS Cent. Sci.*, vol. 6, no. 2, pp. 197–206, 2020, doi: 10.1021/acscentsci.9b01076.

[27] D. Dhanasekaran, N. Thajuddin, M. Rashmi, T. L. Deepika, and M. Gunasekaran, “Screening of biofouling activity in marine bacterial isolate from ship hull,” *Int. J. Environ. Sci. Technol.*, vol. 6, no. 2, pp. 197–202, 2009, doi: 10.1007/BF03327622.

[28] P. V. Bramhachari, A. M. V. N. Prathyusha, G. M. Sheela, N. N. Rao Reddy, C. V. Berde, and N. M. Yugandhar, “Strategies for Disruption of Biofilm Formation Ability and Intricate Quorum Sensing Networks in Aquaculture Vibrio Pathogens,” in *Implication of Quorum Sensing and Biofilm Formation in Medicine, Agriculture and Food Industry*, Singapore: Springer Singapore, 2019, pp. 313–321.

[29] A. J. Bai and V. R. Rai, “Bacterial Quorum Sensing and Food Industry,” *Compr. Rev. Food Sci. Food Saf.*, vol. 10, no. 3, pp. 183–193, 2011, doi: 10.1111/j.1541-4337.2011.00150.x.

[30] G. Scarascia *et al.*, “Effect of quorum sensing on the ability of Desulfovibrio vulgaris to form biofilms and to biocorrode carbon steel in saline conditions,” *Appl. Environ. Microbiol.*, vol. 86, no. 1, pp. 1–14, 2020, doi: 10.1128/AEM.01664-19.

[31] N. E. Shepherd, R. S. Harrison, and D. P. Fairlie, “Targeting Quorum Sensing and Competence Stimulation for Antimicrobial Chemotherapy,” *Curr. Drug Targets*, vol. 13, no. 11, pp. 1348–1359,

2012, doi: 10.2174/138945012803530233.

[32] S. T. Rutherford and B. L. Bassler, “Bacterial quorum sensing: Its role in virulence and possibilities for its control,” *Cold Spring Harb. Perspect. Med.*, vol. 2, no. 11, pp. 1–25, 2012, doi: 10.1101/cshperspect.a012427.

[33] T. Defoirdt, N. Boon, P. Bossier, and W. Verstraete, “Disruption of bacterial quorum sensing: An unexplored strategy to fight infections in aquaculture,” *Aquaculture*, vol. 240, no. 1–4, pp. 69–88, 2004, doi: 10.1016/j.aquaculture.2004.06.031.

[34] B. L. Bassler, M. Wright, R. E. Showalter, and M. R. Silverman, “Intercellular signalling in Vibrio harveyi: sequence and function of genes regulating expression of luminescence,” *Mol. Microbiol.*, vol. 9, no. 4, pp. 773–786, 1993, doi: 10.1111/j.1365-2958.1993.tb01737.x.

[35] B. L. Bassler, E. P. Greenberg, and A. M. Stevens, “Cross-species induction of luminescence in the quorum-sensing bacterium Vibrio harveyi,” *J. Bacteriol.*, vol. 179, no. 12, pp. 4043–4045, 1997, doi: 10.1128/jb.179.12.4043-4045.1997.

[36] M. G. Surette, M. B. Miller, and B. L. Bassler, “Quorum sensing in Escherichia coli, Salmonella typhimurium, and Vibrio harveyi: A new family of genes responsible for autoinducer production,” *Proc. Natl. Acad. Sci. U. S. A.*, vol. 96, no. 4, pp. 1639–1644, 1999, doi: 10.1073/pnas.96.4.1639.

[37] C. S. Pereira, J. A. Thompson, and K. B. Xavier, “AI-2-mediated signalling in bacteria,” *FEMS Microbiol. Rev.*, vol. 37, no. 2, pp. 156–181, 2013, doi: 10.1111/j.1574-6976.2012.00345.x.

[38] R. E. Rettner and M. H. Saier, “The autoinducer-2 exporter superfamily,” *J. Mol. Microbiol. Biotechnol.*, vol. 18, no. 4, pp. 195–205, 2010, doi: 10.1159/000316420.

[39] T. Xue, L. Zhao, H. Sun, X. Zhou, and B. Sun, “LsrR-binding site recognition and regulatory characteristics in Escherichia coli AI-2 quorum sensing,” *Cell Res.*, vol. 19, no. 11, pp. 1258–1268, 2009, doi: 10.1038/cr.2009.91.

[40] Y. Wang, B. Liu, D. Grenier, and L. Yi, “Regulatory mechanisms of the LuxS/AI-2 system and bacterial resistance,” *Antimicrobial Agents and Chemotherapy*, vol. 63, no. 10. 2019, doi: 10.1128/AAC.01186-19.

[41] M. Herzberg, I. K. Kaye, W. Peti, and T. K. Wood, “YdgG (TqsA) controls biofilm formation in Escherichia coli K-12 through autoinducer 2 transport,” *J. Bacteriol.*, vol. 188, no. 2, pp. 587–598, 2006, doi: 10.1128/JB.188.2.587-598.2006.

[42] J. Zhao, C. Quan, L. Jin, and M. Chen, “Production, detection and application perspectives of quorum sensing autoinducer-2 in bacteria,” *J. Biotechnol.*, vol. 268, no. August 2017, pp. 53–60, 2018, doi: 10.1016/j.jbiotec.2018.01.009.

[43] M. J. Federle, “Autoinducer-2-Based Chemical Communication in Bacteria: Complexities of Interspecies Signaling,” in *Bacterial Sensing and Signaling*, vol. 23, no. 1, Basel: KARGER, 2009, pp. 18–32.

[44] L. Lu *et al.*, “Screening Strategies for Quorum Sensing Inhibitors in Combating Bacterial Infection,” *J. Pharm. Anal.*, 2021, doi: 10.1016/j.jpha.2021.03.009.

[45] C. Grandclément, M. Tannières, S. Moréra, Y. Dessaux, and D. Faure, “Quorum quenching: Role in

nature and applied developments," *FEMS Microbiol. Rev.*, vol. 40, no. 1, pp. 86–116, 2015, doi: 10.1093/femsre/fuv038.

[46] T. B. Rasmussen and M. Givskov, "Quorum-sensing inhibitors as anti-pathogenic drugs," *Int. J. Med. Microbiol.*, vol. 296, no. 2–3, pp. 149–161, 2006, doi: 10.1016/j.ijmm.2006.02.005.

[47] M. Hentzer and M. Givskov, "Pharmacological inhibition of quorum sensing for the treatment of chronic bacterial infections," *J. Clin. Invest.*, vol. 112, no. 9, pp. 1300–1307, 2003, doi: 10.1172/JCI20074.

[48] D. A. Vattem, K. Mihalik, S. H. Crixell, and R. J. C. McLean, "Dietary phytochemicals as quorum sensing inhibitors," *Fitoterapia*, vol. 78, no. 4, pp. 302–310, 2007, doi: 10.1016/j.fitote.2007.03.009.

[49] V. C. Kalia, "Quorum sensing inhibitors: An overview," *Biotechnol. Adv.*, vol. 31, no. 2, pp. 224–245, 2013, doi: 10.1016/j.biotechadv.2012.10.004.

[50] R. Sikdar and M. Elias, "Quorum quenching enzymes and their effects on virulence, biofilm, and microbiomes: a review of recent advances," *Expert Rev. Anti. Infect. Ther.*, vol. 18, no. 12, pp. 1221–1233, 2020, doi: 10.1080/14787210.2020.1794815.

[51] J. A. Gutierrez, T. Crowder, A. Rinaldo-Matthis, M. C. Ho, S. C. Almo, and V. L. Schramm, "Transition state analogs of 5′-methylthioadenosine nucleosidase disrupt quorum sensing," *Nat. Chem. Biol.*, vol. 5, no. 4, pp. 251–257, 2009, doi: 10.1038/nchembio.153.

[52] V. Roy, R. Fernandes, C. Tsao, and W. E. Bentley, "Cross Species Quorum Quenching Using a Native AI-2 Processing Enzyme," *ACS Chem. Biol.*, vol. 5, no. 2, pp. 223–232, Feb. 2010, doi: 10.1021/cb9002738.

[53] C. A. Lowery, J. Park, G. F. Kaufmann, and K. D. Janda, "An unexpected switch in the modulation of AI-2-based quorum sensing discovered through synthetic 4,5-dihydroxy-2,3-pentanedione analogues," *J. Am. Chem. Soc.*, vol. 130, no. 29, pp. 9200–9201, 2008, doi: 10.1021/ja802353j.

[54] S. Gamby *et al.*, "Altering the communication networks of multispecies microbial systems using a diverse toolbox of AI-2 analogues," *ACS Chem. Biol.*, vol. 7, no. 6, pp. 1023–1030, 2012, doi: 10.1021/cb200524y.

[55] V. Roy, J. A. I. Smith, J. Wang, J. E. Stewart, W. E. Bentley, and H. O. Sintim, "Synthetic analogs tailor native AI-2 signaling across bacterial species," *J. Am. Chem. Soc.*, vol. 132, no. 32, pp. 11141–11150, 2010, doi: 10.1021/ja102587w.

[56] C. Miller and J. Gilmore, "Detection of quorum-sensing molecules for pathogenic molecules using cell-based and cell-free biosensors," *Antibiotics*, vol. 9, no. 5, 2020, doi: 10.3390/antibiotics9050259.

[57] R. B. Cathcart, *The Science and Applications of Synthetic and Systems Biology*, vol. 2, no. 1. Washington, D.C.: National Academies Press, 2011.

[58] M. Hentzer *et al.*, "Inhibition of quorum sensing in Pseudomonas aeruginosa biofilm bacteria by a halogenated furanone compound," *Microbiology*, vol. 148, no. 1, pp. 87–102, 2002, doi: 10.1099/00221287-148-1-87.

[59] B. Gökalsın, B. Aksoydan, B. Erman, and N. C. Sesal, "Reducing Virulence and Biofilm of Pseudomonas aeruginosa by Potential Quorum Sensing Inhibitor Carotenoid: Zeaxanthin," *Microb. Ecol.*, vol. 74, no. 2, pp. 466–473, 2017, doi: 10.1007/s00248-017-0949-3.

[60] N. Weiland-Bräuer, N. Pinnow, and R. A. Schmitz, “Novel reporter for identification of interference with Acyl homoserine lactone and autoinducer-2 quorum sensing,” *Appl. Environ. Microbiol.*, vol. 81, no. 4, pp. 1477–1489, 2015, doi: 10.1128/AEM.03290-14.

[61] M. Storch *et al.*, “BASIC: A New Biopart Assembly Standard for Idempotent Cloning Provides Accurate, Single-Tier DNA Assembly for Synthetic Biology,” *ACS Synth. Biol.*, vol. 4, no. 7, pp. 781–787, 2015, doi: 10.1021/sb500356d.

[62] G. Røkke, E. Korvald, J. Pahr, O. Øyås, and R. Lale, “BioBrick assembly standards and techniques and associated software tools,” *Methods Mol. Biol.*, vol. 1116, pp. 1–24, 2014, doi: 10.1007/978-1-62703-764-8_1.

[63] “https://igem.org/Registry,” 2021. https://igem.org/Registry (accessed Nov. 28, 2021).

[64] P. Oberacker *et al.*, “Bio-On-Magnetic-Beads (BOMB): Open platform for high-throughput nucleic acid extraction and manipulation,” *PLoS Biol.*, vol. 17, no. 1, pp. 1–16, 2019, doi: 10.1371/journal.pbio.3000107.

[65] S. Chandaran and K. W. George, *DNA Cloning and Assembly, Methods and Protocols (BASIC in Chapter 14)*, vol. 1116. 2014.

[66] J. Sambrook and D. W. Russell, “The Inoue Method for Preparation and Transformation of Competent E. Coli : ‘Ultra-Competent’ Cells,” *Cold Spring Harb. Protoc.*, vol. 2006, no. 1, p. pdb.prot3944, Jun. 2006, doi: 10.1101/pdb.prot3944.

[67] R Core Team, “R: A Language and Environment for Statistical Computing.” Vienna, Austria, 2020, [Online]. Available: https://www.r-project.org/.

[68] Adobe Inc., “Adobe Illustrator.” 2021, [Online]. Available: https://www.adobe.com/products/illustrator.

[69] Adobe Inc., “Adobe Photoshop CC.” 2021, [Online]. Available: https://www.adobe.com/products/photoshop.

[70] R. Silva-Rocha *et al.*, “The Standard European Vector Architecture (SEVA): A coherent platform for the analysis and deployment of complex prokaryotic phenotypes,” *Nucleic Acids Res.*, vol. 41, no. D1, pp. 666–675, 2013, doi: 10.1093/nar/gks1119.

[71] P. Carroll, D. G. Niranjala Muttucumaru, and T. Parish, “Use of a tetracycline-inducible system for conditional expression in Mycobacterium tuberculosis and Mycobacterium smegmatis,” *Appl. Environ. Microbiol.*, vol. 71, no. 6, pp. 3077–3084, 2005, doi: 10.1128/AEM.71.6.3077-3084.2005.

[72] J. D. Pédelacq, S. Cabantous, T. Tran, T. C. Terwilliger, and G. S. Waldo, “Engineering and characterization of a superfolder green fluorescent protein,” *Nat. Biotechnol.*, vol. 24, no. 1, pp. 79–88, 2006, doi: 10.1038/nbt1172.

[73] K. A. Datsenko and B. L. Wanner, “One-step inactivation of chromosomal genes in Escherichia coli K-12 using PCR products,” *Proc. Natl. Acad. Sci. U. S. A.*, vol. 97, no. 12, pp. 6640–6645, 2000, doi: 10.1073/pnas.120163297.

[74] C. Georgi, J. Buerger, W. Hillen, and C. Berens, “Promoter strength driving TetR determines the regulatory properties of tet-controlled expression systems,” *PLoS One*, vol. 7, no. 7, 2012, doi: 10.1371/journal.pone.0041620.

[75] R. E. Campbell *et al.*, “A monomeric red fluorescent protein,” *Proc. Natl. Acad. Sci. U. S. A.*, vol. 99, no. 12, pp. 7877–7882, 2002, doi: 10.1073/pnas.082243699.

[76] L. M. Guzman, D. Belin, M. J. Carson, and J. Beckwith, “Tight regulation, modulation, and high-level expression by vectors containing the arabinose P(BAD) promoter,” *J. Bacteriol.*, vol. 177, no. 14, pp. 4121–4130, 1995, doi: 10.1128/jb.177.14.4121-4130.1995.

[77] K. Winzer *et al.*, “LuxS: Its role in central metabolism and the in vitro synthesis of 4-hydroxy-5-methyl-3(2H)-furanone,” *Microbiology*, vol. 148, no. 4, pp. 909–922, 2002, doi: 10.1099/00221287-148-4-909.

[78] I. M. A. Chen *et al.*, “The IMG/M data management and analysis system v.6.0: New tools and advanced capabilities,” *Nucleic Acids Res.*, vol. 49, no. D1, pp. D751–D763, 2021, doi: 10.1093/nar/gkaa939.

[79] S. Mukherjee *et al.*, “Genomes OnLine Database (GOLD) v.8: Overview and updates,” *Nucleic Acids Res.*, vol. 49, no. D1, pp. D723–D733, 2021, doi: 10.1093/nar/gkaa983.

[80] T. Defoirdt, G. Brackman, and T. Coenye, “Quorum sensing inhibitors: How strong is the evidence?,” *Trends Microbiol.*, vol. 21, no. 12, pp. 619–624, 2013, doi: 10.1016/j.tim.2013.09.006.

[81] K. Saurav *et al.*, “In search of alternative antibiotic drugs: Quorum-quenching activity in sponges and their bacterial isolates,” *Front. Microbiol.*, vol. 7, no. APR, pp. 1–18, 2016, doi: 10.3389/fmicb.2016.00416.

[82] M. E. Skindersoe *et al.*, “Effects of antibiotics on quorum sensing in Pseudomonas aeruginosa,” *Antimicrob. Agents Chemother.*, vol. 52, no. 10, pp. 3648–3663, 2008, doi: 10.1128/AAC.01230-07.

[83] T. H. Jakobsen *et al.*, “Food as a source for quorum sensing inhibitors: Iberin from horseradish revealed as a quorum sensing inhibitor of Pseudomonas aeruginosa,” *Appl. Environ. Microbiol.*, vol. 78, no. 7, pp. 2410–2421, 2012, doi: 10.1128/AEM.05992-11.

[84] A. S. Andersen *et al.*, “Quorum-sensing-regulated virulence factors in Pseudomonas aeruginosa are toxic to Lucilia sericata maggots,” *Microbiology*, vol. 156, no. 2, pp. 400–407, 2010, doi: 10.1099/mic.0.032730-0.

[85] D. Hançer Aydemir, G. Çifci, V. Aviyente, and G. Boşgelmez-Tinaz, “Quorum-sensing inhibitor potential of trans-anethole aganist Pseudomonas aeruginosa,” *J. Appl. Microbiol.*, vol. 125, no. 3, pp. 731–739, 2018, doi: 10.1111/jam.13892.

[86] F. Kaplan *et al.*, “Bacterial attraction and quorum sensing inhibition in caenorhabditis elegans exudates,” *J. Chem. Ecol.*, vol. 35, no. 8, pp. 878–892, 2009, doi: 10.1007/s10886-009-9670-0.

[87] A. B. Sawant, C. H. Gill, and R. S. Nirwan, “Synthesis and biological activities of some flavones,” *Indian J. Heterocycl. Chem.*, vol. 22, no. 1, pp. 61–66, 2012.

[88] L. Bereza-Malcolm, S. Aracic, R. Kannan, G. Mann, and A. E. Franks, “Functional characterization of Gram-negative bacteria from different genera as multiplex cadmium biosensors,” *Biosens. Bioelectron.*, vol. 94, no. December 2016, pp. 380–387, 2017, doi: 10.1016/j.bios.2017.03.029.

[89] J. Zan, C. Fuqua, and R. T. Hill, “Diversity and functional analysis of luxS genes in vibrios from marine sponges Mycale laxissima and Ircinia strobilina,” *ISME J.*, vol. 5, no. 9, pp. 1505–1516, 2011, doi: 10.1038/ismej.2011.31.

[90] A. F. González Barrios, R. Zuo, Y. Hashimoto, L. Yang, W. E. Bentley, and T. K. Wood, “Autoinducer

2 controls biofilm formation in Escherichia coli through a novel motility quorum-sensing regulator (MqsR, B3022)," *J. Bacteriol.*, vol. 188, no. 1, pp. 305–316, 2006, doi: 10.1128/JB.188.1.305-316.2006.

[91] M. D. Servinsky *et al.*, "Directed assembly of a bacterial quorum," *ISME J.*, vol. 10, no. 1, pp. 158–169, 2016, doi: 10.1038/ismej.2015.89.

[92] C. Y. Tsao, S. Hooshangi, H. C. Wu, J. J. Valdes, and W. E. Bentley, "Autonomous induction of recombinant proteins by minimally rewiring native quorum sensing regulon of E. coli," *Metab. Eng.*, vol. 12, no. 3, pp. 291–297, 2010, doi: 10.1016/j.ymben.2010.01.002.

[93] Y. Quan *et al.*, "Regulation of bacteria population behaviors by AI-2 'consumer cells' and 'supplier cells,'" *BMC Microbiol.*, vol. 17, no. 1, pp. 1–9, 2017, doi: 10.1186/s12866-017-1107-2.

[94] K. Stephens *et al.*, "Engineering Escherichia coli for enhanced sensitivity to the autoinducer-2 quorum sensing signal," *Biotechnol. Prog.*, vol. 35, no. 6, pp. 1–6, 2019, doi: 10.1002/btpr.2881.

[95] T. Long *et al.*, "Quantifying the integration of quorum-sensing signals with single-cell resolution," *PLoS Biol.*, vol. 7, no. 3, pp. 0640–0649, 2009, doi: 10.1371/journal.pbio.1000068.

[96] M. D. Servinsky, P. C. Allen, C.-Y. Tsao, C. M. Byrd, C. J. Sund, and W. E. Bentley, "Construction of a cell-based sensor for the detection of autoinducer-2," *Sens. Agric. Food Qual. Saf. IV*, vol. 8369, no. May 2012, pp. 83690V-83690V–9, 2012, doi: 10.1117/12.920590.

[97] M. K. Rhoads *et al.*, "Incorporating LsrK AI-2 quorum quenching capability in a functionalized biopolymer capsule," *Biotechnol. Bioeng.*, vol. 115, no. 2, pp. 278–289, 2018, doi: 10.1002/bit.26397.

[98] A. Zargar, D. N. Quan, and W. E. Bentley, "Enhancing Intercellular Coordination: Rewiring Quorum Sensing Networks for Increased Protein Expression through Autonomous Induction," *ACS Synth. Biol.*, vol. 5, no. 9, pp. 923–928, 2016, doi: 10.1021/acssynbio.5b00261.

[99] X. Zhou, X. Meng, and B. Sun, "An EAL domain protein and cyclic AMP contribute to the interaction between the two quorum sensing systems in Escherichia coli," *Cell Res.*, vol. 18, no. 9, pp. 937–948, 2008, doi: 10.1038/cr.2008.67.

[100] K. B. Xavier and B. L. Bassler, "Interference with AI-2-mediated bacterial cell-cell communication," *Nature*, vol. 437, no. 7059, pp. 750–753, 2005, doi: 10.1038/nature03960.

[101] E. Balleza, J. M. Kim, and P. Cluzel, "Systematic characterization of maturation time of fluorescent proteins in living cells," *Nat. Methods*, vol. 15, no. 1, pp. 47–51, 2018, doi: 10.1038/nmeth.4509.

[102] Y. Kuruma and T. Ueda, "The PURE system for the cell-free synthesis of membrane proteins," *Nat. Protoc.*, vol. 10, no. 9, pp. 1328–1344, 2015, doi: 10.1038/nprot.2015.082.

[103] R. Lentini *et al.*, "Fluorescent proteins and in vitro genetic organization for cell-free synthetic biology," *ACS Synth. Biol.*, vol. 2, no. 9, pp. 482–489, 2013, doi: 10.1021/sb400003y.

[104] T. Nieuwkoop, N. J. Claassens, and J. van der Oost, "Improved protein production and codon optimization analyses in Escherichia coli by bicistronic design," *Microb. Biotechnol.*, vol. 12, no. 1, pp. 173–179, 2019, doi: 10.1111/1751-7915.13332.

[105] B. F. Pfleger, N. J. Fawzi, and J. D. Keasling, "Optimization of DsRed production in escherichia coli: Effect of ribosome binding site sequestration on translation efficiency," *Biotechnol. Bioeng.*, vol. 92, no. 5, pp. 553–558, 2005, doi: 10.1002/bit.20630.

[106] N. C. Shaner, P. A. Steinbach, and R. Y. Tsien, “A guide to choosing fluorescent proteins,” *Nat. Methods*, vol. 2, no. 12, pp. 905–909, 2005, doi: 10.1038/nmeth819.

[107] N. C. Shaner, R. E. Campbell, P. A. Steinbach, B. N. G. Giepmans, A. E. Palmer, and R. Y. Tsien, “Improved monomeric red, orange and yellow fluorescent proteins derived from Discosoma sp. red fluorescent protein,” *Nat. Biotechnol.*, vol. 22, no. 12, pp. 1567–1572, 2004, doi: 10.1038/nbt1037.

[108] B. T. Bajar *et al.*, “Improving brightness and photostability of green and red fluorescent proteins for live cell imaging and FRET reporting,” *Sci. Rep.*, vol. 6, no. January, pp. 1–12, 2016, doi: 10.1038/srep20889.

[109] D. Shcherbo *et al.*, “Bright far-red fluorescent protein for whole-body imaging,” *Nat. Methods*, vol. 4, no. 9, pp. 741–746, 2007, doi: 10.1038/nmeth1083.

[110] K. D. Piatkevich and V. V Verkhusha, “Advances in engineering of fluorescent proteins and photoactivatable proteins with red emission,” *Curr. Opin. Chem. Biol.*, vol. 14, no. 1, pp. 23–29, Feb. 2010, doi: 10.1016/j.cbpa.2009.10.011.

[111] T. J. Lambert, “FPbase: a community-editable fluorescent protein database,” *Nat. Methods*, vol. 16, no. 4, pp. 277–278, 2019, doi: 10.1038/s41592-019-0352-8.

[112] M. Gossen and H. Bujard, “Anhydrotetracycline, a novel effector for tetracycline controlled gene expression systems in eukaryotic cells,” *Nucleic Acids Res.*, vol. 21, no. 18, pp. 4411–4412, 1993, doi: 10.1093/nar/21.18.4411.

[113] H. Dong, W. Tao, Y. Zhang, and Y. Li, “Development of an anhydrotetracycline-inducible gene expression system for solvent-producing Clostridium acetobutylicum: A useful tool for strain engineering,” *Metab. Eng.*, vol. 14, no. 1, pp. 59–67, 2012, doi: 10.1016/j.ymben.2011.10.004.

[114] T. N. M. Nguyen, Q. G. Phan, L. P. Duong, K. P. Bertrand, and R. E. Lenski, “Effects of carriage and expression of the Tn10 tetracycline-resistance operon on the fitness of Escherichia coli K12,” *Mol. Biol. Evol.*, vol. 6, no. 3, pp. 213–225, 1989, doi: 10.1093/oxfordjournals.molbev.a040545.

[115] Elowitz, “A synthetic oscillatory network repressilator,” *Nature*, vol. 403, pp. 335–338, 2000.

[116] O. Purcell, C. S. Grierson, M. D. Bernardo, and N. J. Savery, “Temperature dependence of ssrA-tag mediated protein degradation,” *J. Biol. Eng.*, vol. 6, pp. 13–15, 2012, doi: 10.1186/1754-1611-6-10.

[117] K. E. McGinness, T. A. Baker, and R. T. Sauer, “Engineering Controllable Protein Degradation,” *Mol. Cell*, vol. 22, no. 5, pp. 701–707, 2006, doi: 10.1016/j.molcel.2006.04.027.

[118] R. Schleif, “AraC protein, regulation of the l-arabinose operon in Escherichia coli, and the light switch mechanism of AraC action,” *FEMS Microbiol. Rev.*, vol. 34, no. 5, pp. 779–796, 2010, doi: 10.1111/j.1574-6976.2010.00226.x.

[119] R. Schleif, “Regulation of the L-arabinose operon of Escherichia coli,” *Trends Genet.*, vol. 16, no. 12, pp. 559–565, 2000, doi: 10.1016/S0168-9525(00)02153-3.

[120] G. L. Rosano and E. A. Ceccarelli, “Recombinant protein expression in Escherichia coli: Advances and challenges,” *Front. Microbiol.*, vol. 5, no. APR, pp. 1–17, 2014, doi: 10.3389/fmicb.2014.00172.

7 Appendix

7.1 Primers used in this study

Table 3 | Primers used in this study.

Primer	Sequence (5’-3’)	Relevant description
oJB5	tctggtgggtctctgtcccgcgacctgttcttctt	Primer for amplification and incorporation of BASIC prefix to Part 6: P_{lsr}. Primer adapted and modified from [60]
oJB6	cgataggtctcccgagcccatatttcccccgttcagtt	Primer for amplification and incorporation of BASIC suffix to Part 6: P_{lsr}. Primer adapted and modified from [60]
oJB7	tctggtgggtctctgtcccatactcccgccattcagag	Primer for amplification and incorporation of BASIC prefix to Part 9: P_{BAD}
oJB8	cgataggtctcccgagccaacctccttagagctcgaattc	Primer for amplification and incorporation of BASIC suffix to Part 9: P_{BAD}
oJB9	tctggtgggtctctgtccctggctgaaattggttttcg	Primer for amplification and incorporation of BASIC prefix to Part 5: λtl3
oJB10	cgataggtctcccgagccccatacccatggattcttcg	Primer for amplification and incorporation of BASIC suffix to Part 5: λtl3
oJB15	cgtggaaacactattatctggtggg	Forward primer for verification of BASIC assembly. Binds to LM1
oJB16	ccgaagttacaccagattggactg	Reverse primer for verification of BASIC assembly. Binds to LM1
oJB17	cccaccagataatagtgtttccacg	Forward primer for verification of BASIC assembly. Binds to LM2
oJB18	ccgaagttacaccagattggactg	Reverse primer for verification of BASIC assembly. Binds to LM2
oJB19	ctattggctgagataagggtagc	Forward primer for verification of BASIC assembly. Binds to U2-RBSx
oJB20	gctacccttatctcagccaatag	Reverse primer for verification of BASIC assembly. Binds to U2-RBSx
oJB21	ctcgtggtctgacggtaaaatc	Forward primer for verification of BASIC assembly. Binds to U3-RBSx
oJB22	gattttaccgtcagaccacgag	Reverse primer for verification of BASIC assembly. Binds to U3-RBSx
oJB23	caccgtctcaggtaagtatcag	Forward primer for verification of BASIC assembly. Binds to U1-RBSx
oJB24	ctgatacttacctgagacggtg	Reverse primer for verification of BASIC assembly. Binds to U1-RBSx
oJB25	gacactccgagacagtcagagggta	Forward primer for verification of BASIC assembly. Binds to L1
oJB26	taccctctgactgtctcggagtgtc	Reverse primer for verification of BASIC assembly. Binds to L1
oJB29	gtgtgaaaagtcagtatccagtcgtgtagttc	Forward primer for verification of BASIC assembly. Binds to L2
oJB30	gaactacacgactggatactgacttttcacac	Reverse primer for verification of BASIC assembly. Binds to L2
oJB31	tctggtgggtctctgtccactagtcttggactcctgttg	For incorporation of BASIC prefix to part 1: SEVA13-VB and part 2: SEVA18-VB
oJB32	cgataggtctcccgagccttaattaaaggcatcaaataaaacgaaaggc	For incorporation of BASIC suffix to part 1: SEVA13-VB and part 2: SEVA18-VB

7.2 Example of verification of assembly by PCR

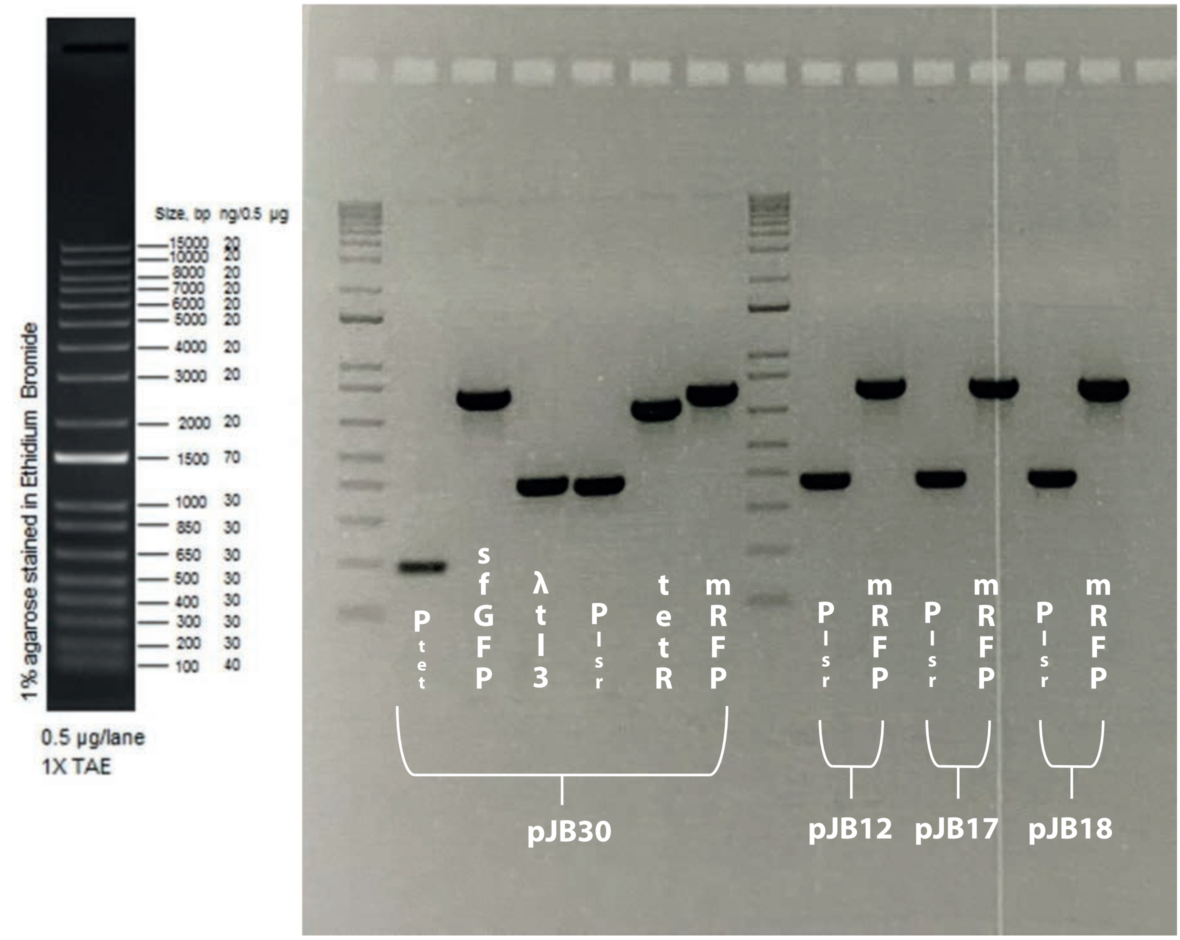
Size, bp ng/0.5 µg
15000 20
10000 20
8000 20
7000 20
6000 20
5000 20
4000 20
3000 20
2000 20
1500 70
1000 30
850 30
650 30
500 30
400 30
300 30
200 30
100 40
1% agarose stained in Ethidium Bromide
0.5 µg/lane
1X TAE
Ptet
sfGFP
λtl3
Plsr
tetR
mRFP
Plsr
mRFP
Plsr
mRFP
Plsr
mRFP
pJB30
pJB12
pJB17
pJB18

Figure 16 | PCR verification of biosensor and test constructs. Example of part-wise PCR verification using primers binding to linkers for amplification of each part. All bands are from separate reactions with an inward-facing primer pair binding to the two linkers flanking the part of interest. Part sizes can be found in Table 2. DNA ladder used is 1 Kb Plus DNA Ladder from Invitrogen, Thermo Fisher Scientific (catalog number 10787018).

7.3 Induction with MC4100 supernatant in LB medium

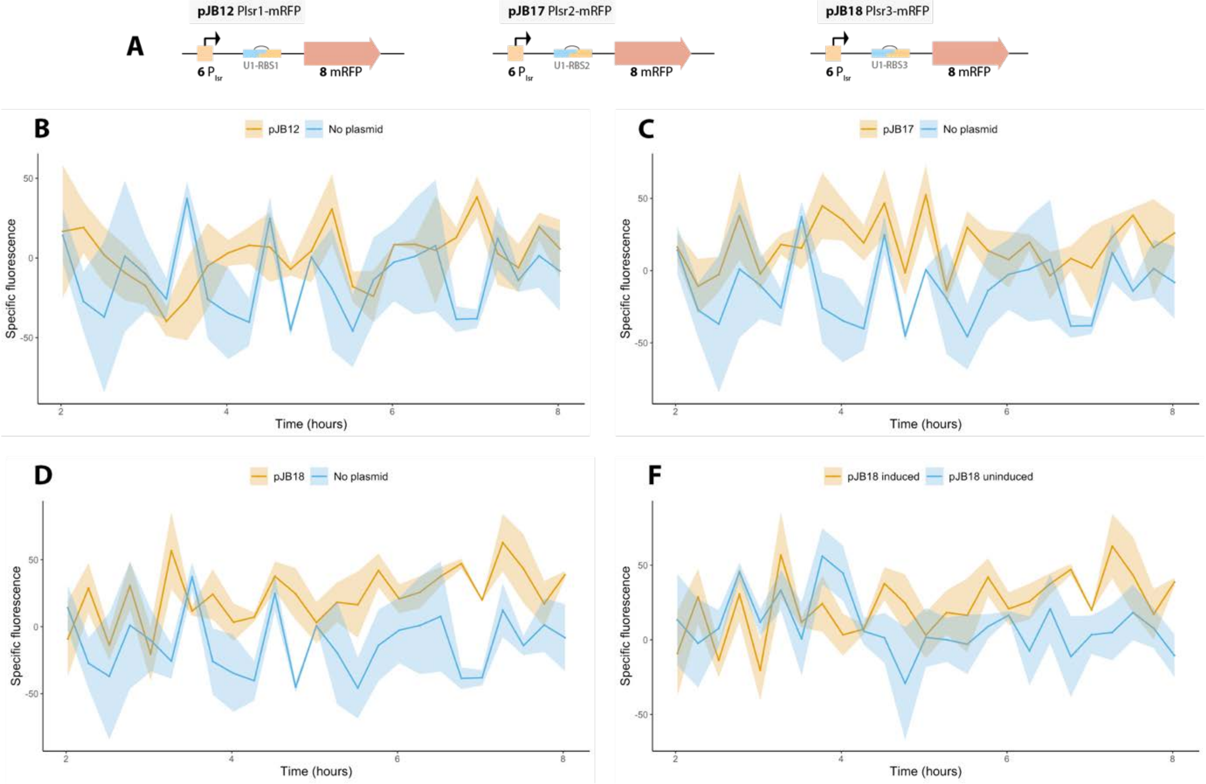

Figure 17 | Induction with MC4100 supernatant in LB medium. **(A)** Genetic overview of constructs tested in this experiment. **(B-F)** Test constructs in DH5α (pJB12, pJB17, pJB18, negative control without plasmid) were grown in culture tubes, and 80 µl culture were transferred upon reaching early exponential phase to a 96 well plate. Test constructs were supplied with 20 µl supernatant from *E. coli MC4100* in exponential growth phase, and controls (uninduced) were supplied with 20 uL LB medium. Fluorescence (excitation: 580 and emission: 615) and OD_{600} were monitored every 15 minutes for 8 hours. Graphs only depicts 2-8 hours. Results are displayed as specific fluorescence (normalized with OD_{600} value and background fluorescence from medium subtracted). The displayed specific fluorescence values are the mean of three technical replicates, and shaded area depict standard error of the mean.

7.4 Induction with 100 mM sAI-2 in LB medium

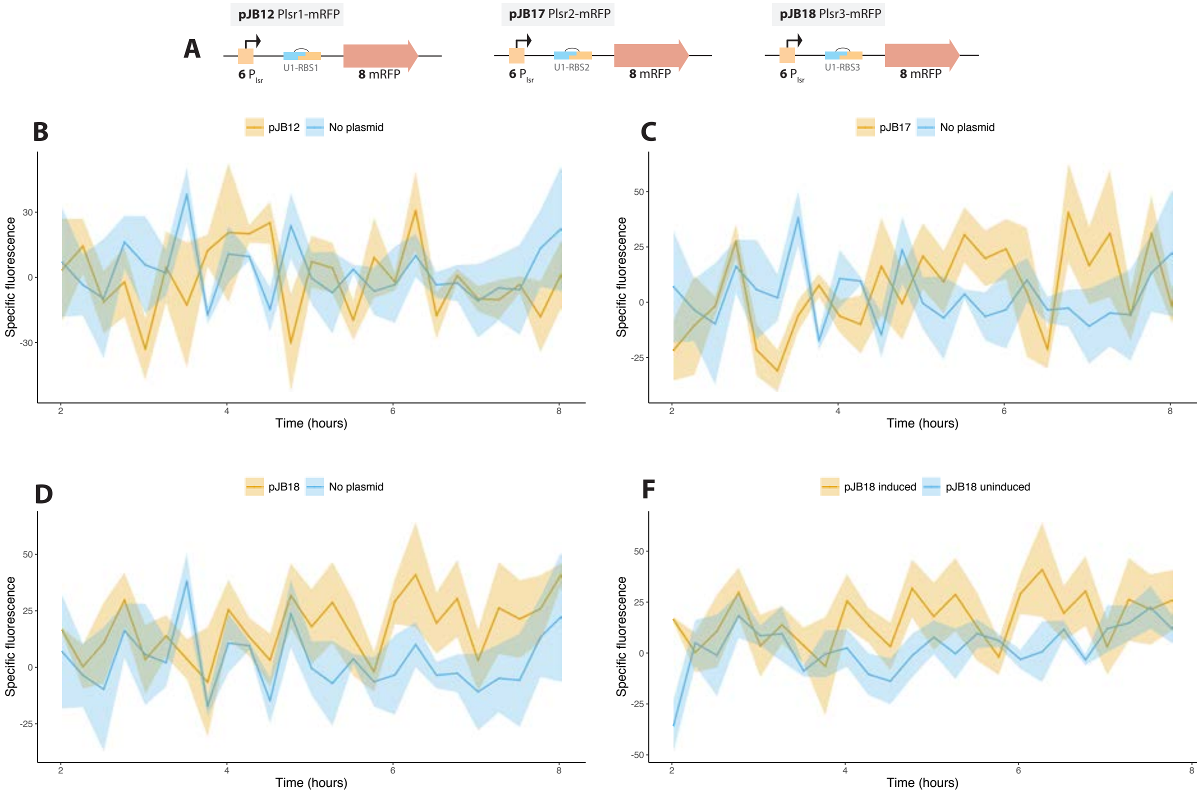

Figure 18. | Induction with 100 mM 5-methyl-4-hydroxy-3-furanone in LB medium. **(A)** Genetic overview of constructs tested in this experiment. **(B-F)** Test constructs in DH5α (pJB12, pJB17, pJB18, negative control without plasmid) were grown in culture tubes, and 90 µl culture were transferred upon reaching exponential phase to a 96 well plate. Test constructs were supplied with 10 uL 5-methyl-4-hydroxy-3-furanone (sAI2) solution reaching a final concentration of 100 mM sAI2. Controls (uninduced) were supplied with H_2O. Fluorescence (excitation: 580 and emission: 615) and OD_{600} were monitored every 15 minutes for 8 hours. Graphs only depicts 2-8 hours. Results are displayed as specific fluorescence (normalized with OD_{600} value and background fluorescence from medium subtracted). The displayed specific fluorescence values are the mean of three technical replicates, and shaded area depict standard error of the mean.

7.5 Induction with 50 mM sAI-2 in M9 medium

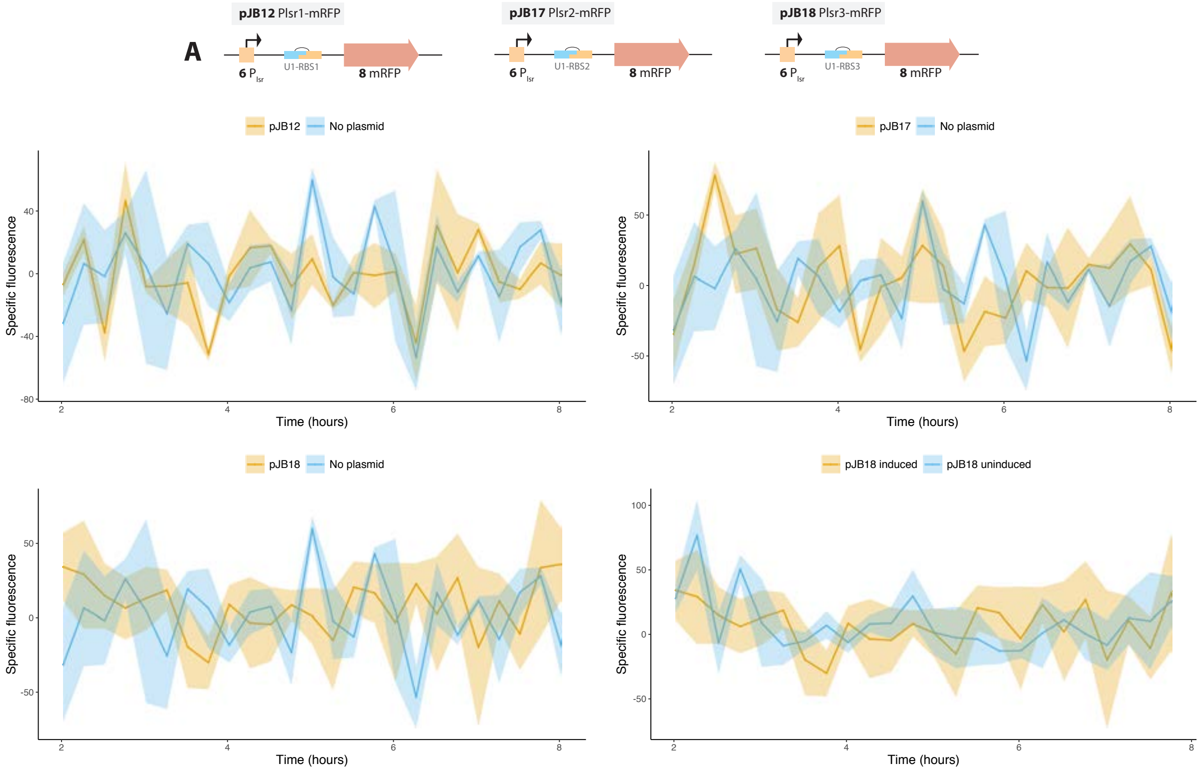

Figure 19. | Induction with 50 mM 5-methyl-4-hydroxy-3-furanone in M9 medium. **(A)** Genetic overview of constructs tested in this experiment. **(B-F)** Test constructs in DH5α (pJB12, pJB17, pJB18, negative control without plasmid) were grown in culture tubes, and 90 µL culture were transferred upon reaching early exponential phase to a 96 well plate. Test constructs were supplied with 10 µL 5-methyl-4-hydroxy-3-furanone (sAI2) solution reaching a final concentration of 50 mM sAI2. Controls (uninduced) were supplied with 10 µL H_2O. Fluorescence (excitation: 580 and emission: 615) and OD_{600} were monitored every 15 minutes for 8 hours. Graphs only depicts 2-8 hours. Results are displayed as specific fluorescence (normalized with OD_{600} value and background fluorescence from medium subtracted). The displayed specific fluorescence values are the mean of three technical replicates, and shaded area depict standard error of the mean.

7.6 Green fluorescence from pJB32 on LB agar plate

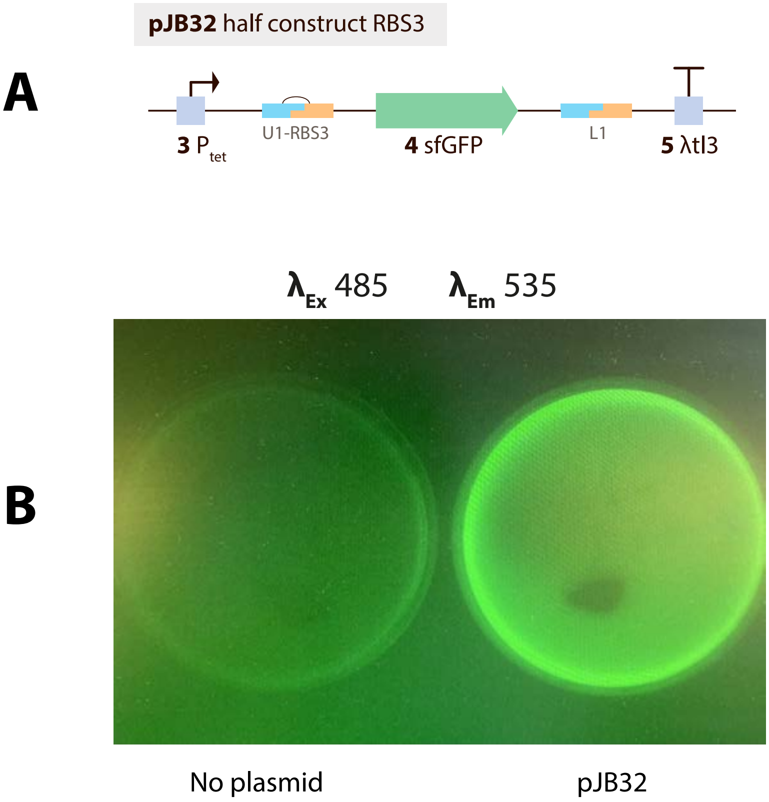
A
pJB32 half construct RBS3
3 P tet
U1-RBS3
4 sfGFP
L1
5 λtl3
B
λEx 485
λEm 535
No plasmid
pJB32

Figure 20 | Fluorescent image of LB agar plates with negative control and pJB32. (A) Overview of pJB32 genetic composition. **(B)** Pictures of LB agar plates. Exponentially growing cultures of each strain were spread evenly on the plates in the evening and pictures were taken the following morning. The LB agar plate which pJB32 were spread on also contained ampicillin (100 µg/mL) to maintain plasmid stability. This is an cropped image taken with a cell phone of the screen image generated by the Kodak Image Station 4000 MM Pro.

7.7 QQ simulation: Testing biosensor construct in high copy number vector backbone

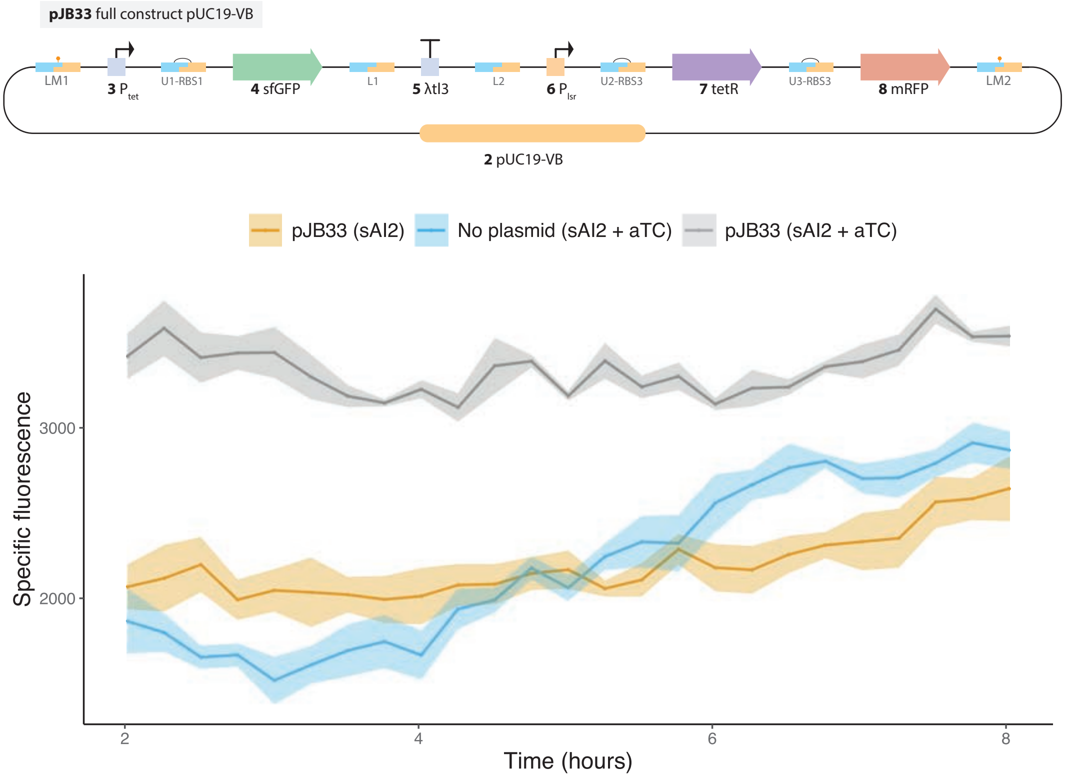

Figure 21 | Simulation of QQ: Testing the signal switch in high copy number backbone. **(A)** Genetic overview of the construct tested in this experiment. **(B-C)** The test constructs and controls were grown in culture tubes in LB, and 90 µl culture were transferred upon reaching early exponential phase to a 96 well plate (if stated anhydrotetracycline (aTC) was also added). Thereafter, they were supplemented with 5-methyl-4-hydroxy-3-furanone (sAI2) reaching a final concentration of 100 mM. Fluorescence (excitation: 480 and emission: 515) and OD_{600} were monitored every 15 minutes for 8 hours. Graphs only depicts 2-8 hours. Results are displayed as specific fluorescence (normalized with OD_{600} value and background fluorescence from medium subtracted). The displayed specific fluorescence values are the mean of three technical replicates, and shaded area depict standard error of the mean.

7.8 Colony PCR of proof of concept circuit assembly attempt

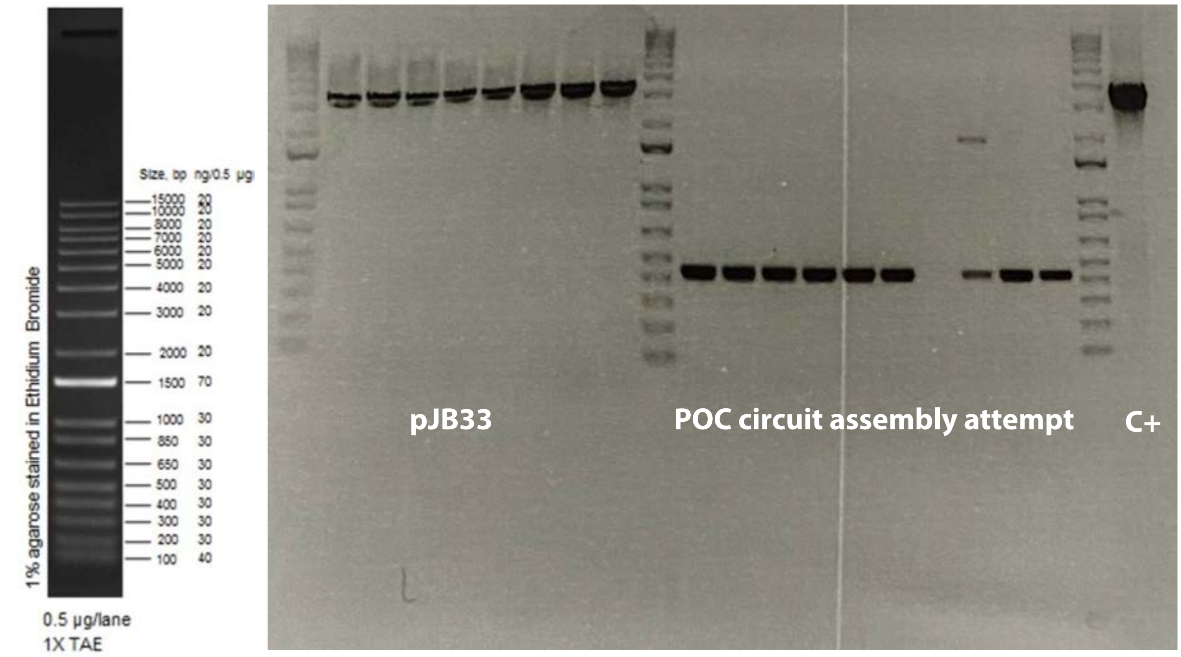
Size, bp ng/0.5 µg
15000 20
10000 20
8000 20
7000 20
6000 20
5000 20
4000 20
3000 20
2000 20
1500 70
1000 30
850 30
650 30
500 30
400 30
300 30
200 30
100 40
1% agarose stained in Ethidium Bromide
0.5 µg/lane
1X TAE
pJB33
POC circuit assembly attempt
C+

Figure 22 | Colony PCR of POC assembly attempt. The eight bands above pJB30 are the products 8 colony PCR (cPCR) reactions of pJB33 transformants (excluding the vector backbone) using insert-specific primers. Predicted size is 3110 bp. The 10 bands in the middle are the products of 10 cPCR reactions of the proof-of-concept construct transformatns using insert-specific primers. Predicted size was 3325 bp. The rightmost band is an control PCR reaction of the pJB30 biosensor construct using the same insert-specific primers and settings as the other bands (predicted size 3110 bp). DNA ladder used is 1 Kb Plus DNA Ladder from Invitrogen, Thermo Fisher Scientific (catalog number 10787018).